THE EFFECT OF DISPERSION ON PLANT EMBRYO DEVELOPMENT

A Dissertation
Presented to
The Academic Faculty

By

Nazmul Huda Al Mamun

In Partial Fulfillment
Of the Requirements for the Degree
Doctor of Philosophy in Mechanical Engineering

Georgia Institute of Technology

May 2015

THE EFFECT OF DISPERSION ON PLANT EMBRYO DEVELOPMENT

Approved by:

Dr. Cyrus K. Aidun, Advisor
School of Mechanical Engineering
Georgia Institute of Technology

Dr. Janet K. Allen
School of Industrial and Systems Engineering
University of Oklahoma

Dr. Ulrika Egertsdotter, Co-Advisor
School of Mechanical Engineering
Georgia Institute of Technology

Dr. David Clapham
Department of Forest Genetics
Swedish University of Agricultural Sciences

Dr. S. Mostafa Ghiaasiaan
School of Mechanical Engineering
Georgia Institute of Technology

Date Approved: February 16, 2015

To My parents, Mohona, Faizan, Zarifa, Maieasha, Naiar, Makeen, Ibrahim,
my parents-in-law

ACKNOWLEDGEMENTS

I would like to show my gratefulness to my advisors Dr. Aidun and Dr. Egertsdotter for their guidance, encouragement, valuable suggestions, and scientific advices. Dr. Aidun's guidance on this project beginning from the bioreactor design to the mathematical modeling and Dr. Egertsdotter's engagement and support in all sorts of questions on the biology part of this research was of immense help in understanding embryo development through somatic embryogenesis.

I am greatly indebted to Dr. Clapham for his valuable advice and remarks on the manuscripts prepared for submission to the journals. I express my gratitude to Dr. Allen and Dr. Ghiaasiaan for reviewing this work and suggestions on mathematical modeling on nutrient concentration distributions. I am grateful to Dr. Shifa for her generosity to advise me on statistical analyses in this dissertation.

Thanks go to my labmates at Georgia Tech and Umeå Plant Science Center. Their support and cooperation were of inestimable value to me to carry on this project.

I want to thank the Kempe Foundation in Sweden for their generous support that provides me an opportunity to have hands on experience on somatic embryogenesis.

TABLE OF CONTENTS

LIST OF TABLES

LIST OF FIGURES

LIST OF SYMBOLS

a_v	Interface area $(\alpha - \gamma)$ to volume ratio; $[cm^{-1}]$
A_α	Nutrient A in α
A_γ	Nutrient A in γ
$A_\alpha P_T$	Nutrient A and transport protein complex
$[A_\alpha P_T]$	Concentration of protein-nutrient complex at $\Sigma(t)$; $[cm^{-2}]$
$C_{A\alpha}$	Molar concentration of a nutrient species A in $\alpha - phase$ (extracellular phase); $[mol/cm^3]$
$\langle C_{A\alpha} \rangle$	Superficial concentration of nutrient A in α; $[mol/cm^3]$
$\langle C_{A\alpha} \rangle^*$	Intrinsic concentration of nutrient A in α; $[mol/cm^3]$
$\tilde{C}_{A\alpha}$	Special deviation of concentration $C_{A\alpha}$ in the averaging volume; $[mol/cm^3]$
$C_{A\gamma}$	Molar concentration of a nutrient species A in $\gamma - phase$ (intracellular phase); $[mol/cm^3]$
$\langle C_{A\gamma} \rangle$	Superficial concentration of nutrient A in γ; $[mol/cm^3]$
$\langle C_{A\gamma} \rangle^*$	Intrinsic concentration of nutrient A in γ; $[mol/cm^3]$
D_{AM}	Diffusion coefficient of A in the medium; $[cm^2/s]$
$D_{A\alpha}$	Diffusion coefficient of A in $\alpha - phase$; $[cm^2/s]$
$\overline{\overline{D}}_{A\alpha,eff}$	Effective diffusion coefficient tensor of A in the two-phase model; $[cm^2/s]$
$D_{A\gamma}$	Diffusion coefficient of A in $\gamma - phase$; $[cm^2/s]$
$D(\bar{q})$	Sum of the lengths of all embryos in a length interval, δ
$\bar{J}_{\alpha\Sigma}$	Diffusion flux from α to $\Sigma(t)$ at the interface $\Sigma\_(t)$ in $\forall$; $[mol/cm^2 \cdot s]$
$\bar{J}_{\Sigma\gamma}$	Diffusion flux from $\Sigma(t)$ to γ at the interface $\Sigma\_(t)$ in $\forall$; $[mol/cm^2 \cdot s]$
$\bar{J}_M$	Diffusion flux from the medium at the medium-PEMs cluster interface; $[mol/cm^2 \cdot s]$
$\bar{J}_{PEM}$	Diffusion flux to the cluster at the medium-PEMs cluster interface; $[mol/cm^2 \cdot s]$
K_m	Half-saturation constant as in the Michaelis-Menten enzyme kinetics; $[mol/cm^3]$
k_1	Forward reaction rate coefficient for the 2nd order reaction;

	$[cm^3/mol \cdot s]$
k_{-1}	Reverse reaction rate coefficient for the 1st order reaction; $[1/s]$
k_2	Forward reaction rate coefficient for the 1st order reaction; $[1/s]$
k_{-2}	Reverse reaction rate coefficient for the 2nd order reaction; $[cm^3/mol \cdot s]$
	[The unit of reaction rate coefficient for a reaction of order (a+b) is $mol^{1-(a+b)} \cdot L^{(a+b)-1} \cdot s^{-1}$]
l_α	Characteristic length of $\alpha - phase$; $[cm]$
n	Number of mature embryos in a length interval, δ
n'	Number of mature embryos per g FW (Fresh weight)
$\hat{n}$	Unit normal pointing outward on S from $phase\ \alpha$
P_0	Concentration of transport proteins at $\Sigma(t)$; $[mol/cm^2]$
P_T	Free transport proteins in the cell membrane for facilitated diffusion
$[P_T]$	Concentration of free transport proteins at $\Sigma(t)$; $[cm^{-2}]$
q_i	Length of an embryo *i*
$\bar{q}$	Average length of somatic embryos in a length interval, δ
r_0	Radius of a cell which is considered as a sphere; $[cm]$
$r_\forall$	Radius of the averaging volume; $[cm]$
r^*	Characteristic length of diffusion-reaction process; $[cm]$
R	Characteristic length (radius) of a hemispherical PEMs cluster; $[cm]$
S	Surface bounding the averaging volume, $\forall$; $[cm^2]$
S_α	Portion of the surface area S which is in $phase\ \alpha$; $[cm^2]$
t^*	Characteristic time; $[sec]$
$\forall$	Averaging volume; $[cm^3]$
$\forall_\alpha(t)$	Volume occupied by $phase\ \alpha$ in $\forall$; $[cm^3]$
$\forall_\gamma(t)$	Volume occupied by $phase\ \gamma$ in $\forall$; $[cm^3]$
$\bar{w}_\Sigma$	Surface velocity of $\Sigma(t)$; $[cm/s]$
vvm	Volume of air per unit volume of liquid medium per min

Greek symbols

$\beta_1, \beta_2, \beta_3, \beta_4, \beta_5$	Ratios associated to the reaction rate coefficients
μ_A	Maximum specific nutrient, A, utilization rate; $[mol/cm^3 \cdot s]$

$\Sigma(t)$	Interface between the α and $\gamma - phases$; $[cm^2]$
$\Sigma_-(t)$	Surface of $\Sigma(t)$ on the side of α; $[cm^2]$
$\Sigma_+(t)$	Surface of $\Sigma(t)$ on the side of γ; $[cm^2]$
$\hat{\xi}$	Unit normal pointing outward on $\Sigma(t)$ from $phase\ \alpha$ to $phase\ \gamma$
ϵ_α	Volume fraction of $\alpha - phase$
$\varphi(\bar{q})$	Normalized distribution function; $[mm^{-1} or\ cm^{-1}]$
ϕ_{max}	Maximum uptake rate of nutrient by the cell; $[mol/cm^2 \cdot s]$
$\mathcal{K}$	Initial concentration of nutrient in the medium; $[mol/cm^3]$

SUMMARY

The focus of this research is to gain insight into the role of dispersion for synchronized development and yield of mature embryos on solid and in liquid culture medium. It is hypothesized that dispersion and synchronous development of embryos will result in high yield of plants. The increase in yield would be helpful in practical implementation of somatic embryogenesis for large-scale clonal propagation of plants and agricultural goods. This doctoral research investigates the yield and the synchronized development of mature embryos, if immature embryos in aggregates of proembryogenic masses (PEMs) have access to same nutritional environment. In order to explore this, a dispersion mechanism was automated and used to provide the same nutritional environment to all PEMs. The effectiveness of the dispersion system was investigated by culturing the PEMs of Norway spruce (*Picea abies*) on solid medium and in a well-functioning liquid culture system, i.e., bioreactor that could be used for large-scale clonal propagation of plants. Distribution of nutrient concentrations at different locations in an aggregate of PEMs during the culture period was studied using a mathematical model.

Results have indicated that dispersion of aggregates of PEMs of Norway spruce has a favorable effect on the rate of proliferation of PEMs and subsequent development of mature somatic embryos. Compared to non-dispersed aggregates of PEMs with dispersed aggregates of PEMs, embryo development increased two folds on solid medium and three to five folds in liquid medium in bioreactors in this study. Bioreactor culture has shown significantly higher yield of mature embryos compared to that on solid culture.

The effect of dispersion on synchronized development of mature embryos appears to be cell line dependent. Dispersion has improved synchronization of embryo development in one of two cell lines used in liquid medium experiments and two of four cell lines examined on solid medium. Cell line 11:12:02 has shown more synchronized development of embryos in dispersed PEMs in both medium. To further investigate the details to understand the association between development of mature embryos and nutrient uptake by cells and tissues, a nutrient diffusion model was developed using the volume averaging technique. It estimated the concentration distributions of nutrients, e.g. sugars, in a PEMs cluster on solid medium over a period of culture. The Michaelis-Menten enzyme kinetics was used in the model for uptake of nutrients by cells and tissues. Enzymatic assaying of soluble sugars was performed to determine concentrations of sugars (glucose, fructose, and sucrose) at different locations in tissue clusters. In both experiments and model simulation, sharp decline in concentrations of sucrose and fructose was observed in the first 12 hours after inoculation in glucose-containing ½ LP gel medium. A significant match between predicted and experimental outputs was observed over the culture period. Both experiments and simulation of the model showed a rapid uptake of glucose from the medium and saturation of PEMs cluster within 12 hours. Hence in a PEMs cluster there was no scarcity of nutrients that would inhibit growth and development of somatic embryos. Though dispersion resulted in a significant increase in development of mature somatic embryos, it might not play the decisive role in synchronized development of embryos. It seems that the major factor in synchronization is the initial developmental stage of immature embryos in a culture and genetic characteristics.

CHAPTER 1

INTRODUCTION

Somatic embryogenesis is an *in vitro* process in which a somatic plant cell, or a group of somatic plant cells, is induced to form a somatic embryo (Filonova et al., 1999). At the earliest developmental stage of somatic embryos, the immature embryos multiply on proliferation medium. The masses composed of immature somatic embryos are referred to as proembryogenic masses (PEMs). In Norway spruce, PEMs can only be established from the somatic cells in the zygotic embryos (von Arnold et al., 2005). Somatic embryogenesis process offers many advantages in terms of embryo preservation, formation of mature embryos, automation of the process, etc. Somatic embryos can be preserved cryogenically in liquid nitrogen for many years, which allows testing of particular genotype before implementing in large-scale production. Somatic embryogenesis (SE) offers a unique propagation method as development of somatic embryos closely resembles that of zygotic embryos, with functioning shoot and root apices and removes the problems associated with rooting of cuttings (Fereol et al., 2005). Therefore it produces better quality plants, and makes the clonal propagation technique cost-effective by reducing the loss of embryos during maturation. Also, this process can be automated for industrial scale implementation. For this reason, different types of bioreactors (e.g., mechanically agitated bioreactors, pneumatically agitated bioreactors, temporary immersion bioreactors, etc.) are developed to carry out somatic embryogenesis for clonal propagation (reviewed by Moorhouse et al., 1996; Honda et al., 2001; Honda and Kobayashi, 2004).

1.1 Motivation and Objectives

Cells in the PEMs are likely to receive different levels of nutrients from the nutrient medium due to their locations in the aggregates with reference to the surface in contact with the medium. This could affect the growth of somatic embryos resulting in asynchronous development of embryos. By synchronization, it is referred to the simultaneous development of somatic embryos cultured on solid and/or in liquid nutrient medium. Synchronized development of embryos is important in making the harvest of mature embryos more efficient, resulting in higher yields of plants. Synchronized development of embryos allows more embryos to be harvested at the same time and thus has an overall positive effect on the yield of plants. Synchronization considerably increases the effectiveness of automated harvest systems for somatic embryos, making large-scale clonal propagation of plants and agricultural goods efficient.

The objective of this thesis is to investigate the yield and the synchronized development of mature somatic embryos, if the PEMs of Norway spruce are provided equal growth conditions through dispersion.

In order to meet the objectives, different bioreactor technologies applied to plant cell cultures have been studied extensively to design an efficient bioreactor for plant cell culture as discussed in Chapter 2. A dispersion mechanism that is automated to provide equal nutritional environment to all the tissues in aggregates of PEMs is also discussed in this chapter. The performance of the bioreactor and the effectiveness of the dispersion of PEMs are investigated in Chapter 3. A further investigation of the dispersion is carried

out in Chapter 4 where an automated system is designed and integrated with the bioreactors so that the equal growth conditions can still be provided during the proliferation phase of the PEMs. A mathematical model is developed in order to understand the effect of nutrient distributions in the cell aggregates for synchronized growth of somatic embryos as explained in Chapter 5. Experiments are performed on ½ LP solidified medium supplemented with glucose to validate the predicted results. This is also discussed in Chapter 5. Chapter 6 presents the conclusions drawn and the contributions made in these investigations, and finally Chapter 7 suggests further investigation of this work that would be of great interest. Types and use of different bioreactors, and a detailed derivation of the mathematical model of nutrient distributions in a PEMs aggregate are provided in the appendices.

This research may give a better understanding of the effect of providing the same nutritional environment to all PEMs on enhancement and synchronization of embryo growth and development on solid and in liquid medium. This may point out the ways of developing an efficient and productive culture system for somatic embryogenesis which will then be able to have a favorable impact on large-scale production of elite plants.

1.2 Review of Literatures

1.2.1 Clonal propagation techniques

Production of clonal propagules from selected superior genotypes has been playing a vital role in large-scale production of high value plants for forestry, agricultural applications, biofuel production, ornamental purposes, and molecular pharming within

the pharmaceutical sector. Optimal growth and yield from plantations can only be obtained when genetically identical (clonal) plants are utilized. Clonal propagations have many advantages, such as,

(i) *Uniform crop production*: uniform crop makes harvesting and further processing of raw materials easier.

(ii) *Cost effectiveness*: it is overall more cost effective to deal with a uniform crop throughout the processes from planting to harvesting. A uniform planting stock of which the growth requirements are previously known and the genotype has been optimally matched to the environment, is more cost effective to maintain and also may result in higher gain from the breeding program.

(iii) *Quality raw materials*: clonal propagation gives an opportunity to have transgenic modifications of plants and thus assists the improvements of the quality of raw materials (Merkle and Dean, 2000).

Clonal propagation techniques vary with plant species. For many ornamental (Rout et al., 2006) and medicinal (Rout et al., 2000) plant species, cutting and meristem culture or axillary bud/shoot culture have been the common methods of clonal propagation. However, cutting has several limitations, such as resulting in no growth or plagiotropic growth while used in several woody plant species (e.g. coffee, cotton, mango and all trees), and a limited number of cuttings is possible from the same plant. Even meristem or bud/shoot culture is not an effective method to provide normal growth of clonal plants of agricultural species (Sun, 2010). On the other hand, somatic

embryogenesis has shown potential in clonal propagation of many ornamental, medicinal, and agricultural plant species; for instance, coffee (Barry-Etienne et al., 2002), cotton (Rathore et al., 2006), maize (Che et al., 2006), mango (Krishna and Singh, 2007), oil palm (Morcillo et al., 2006), sugarcane (Lakshmanan et al., 2006), and all soft wood trees, such as, Loblolly pine, Radiata pine, White spruces, and Douglas fir (Thorpe et al., 2006), and hard wood trees, for example, Eucalyptus (Pinto et al., 2004). For large-scale clonal propagation of woody plants, somatic embryogenesis is the only method currently being used (Thorpe et al., 2006).

1.2.2 Process of somatic embryo development

Somatic embryogenesis is defined as a clonal propagation technique which results in the formation of somatic embryos from somatic cells. Somatic cells generate embryogenic cells that undergo a series of morphological and biochemical changes to form somatic embryos (Quiroz-Figueroa et al., 2006). Embryogenic cells are rich in cytoplasm (Komamine et al., 1990), and are capable of forming somatic embryos without further exogenous addition of growth regulators to the culture medium (De Jong et al., 1993). Komamine et al. (2005) observed the morphological changes of carrot cells in suspension culture during somatic embryogenesis. In auxin-containing medium, continuous division of cells results in the formation of isodiametric cell masses (Schmidt et al., 1997). Guzzo et al. (1994) found that there were some enlarged cells that were detached from the surface of the cell masses in the medium. These cells were competent to generate embryogenic cells. However it is yet to be known of any specific gene that reliably plays a role in converting somatic cells into embryogenic cells (Schmidt et al.,

1997). Komamine et al. (2005) observed that embryogenic carrot cell aggregates formed from competent single cells through morphological and biochemical changes in presence of auxin. The culture medium was then changed to auxin free medium in which the embryogenic cell clusters proliferated through multiplication and without any differentiation. Certain parts of cell aggregates divided rapidly and formed globular embryos. In the final stage of carrot cell somatic embryogenesis, the globular embryos took the heart and torpedo shapes and finally developed plantlets. If the cells were cultured in auxin-free medium initially, the cells might have lost totipotency. They would become elongated and not be able to divide and differentiate (Komamine et al., 2005).

Somatic embryogenesis of a conifer species (Norway spruce) was first established by Hakman and von Arnold in 1985 (Hakman and von Arnold, 1985). This process passes through several steps, such as proliferation (multiplication), embryo differentiation, maturation, and germination (Figure 1.1). Proliferation is the process in which multiplication of cells occurs in proembryogenic masses (PEMs) by repeated division in response to growth regulators (Figure 1.1(a)). In absence of plant growth regulators, somatic cells differentiate and formation of immature somatic embryos from cell aggregates takes place (Figure 1.1(b)). Maturation of somatic embryos takes place in response to maturation medium. Only the polarized immature embryos are matured during this developmental phase. A polarized immature embryo consists of meristematic cells in the ‘head’ region, and highly vacuolated tubular cells in the suspensor region (Figure 1.1(c)). An embryo gets matured from the head region and the suspensor region disappears. From histological study it has been observed that the true somatic embryos

have both shoot and root meristems with vascular tissues shown in Figure 1.1(d) (Deo et al., 2009). At the germination stage, the root develops and elongates.

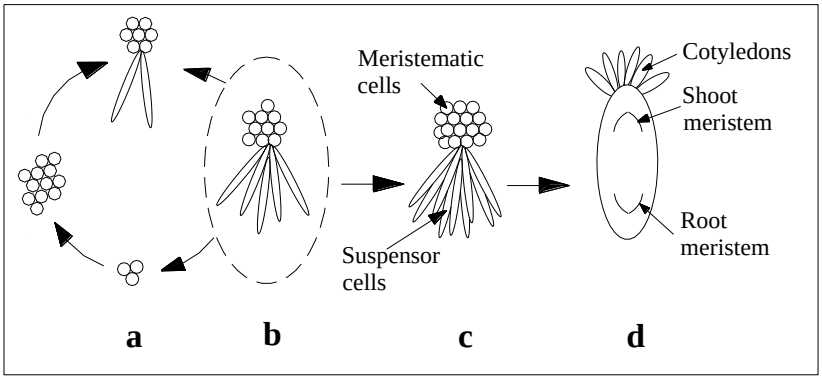

Figure 1.1 Somatic embryo developmental stages in soft wood trees. (a) Multiplication of cells is taking place and different cellular structures corresponding to different developmental stages of an immature embryo are present. (b) Only the more differentiated, polarized structures proceed to the maturation phase. (c) A maturing somatic embryo, having polarized structure, is composed of meristematic cells and oblong vacuolated cells known as suspensor cells. (d) A mature somatic embryo shows the initial cotyledons. A properly matured embryo has distinctive meristems that give rise to shoot and root. (Sun, 2010)

1.2.3 Challenges of somatic embryogenesis in liquid culture medium

Consistent success of somatic embryogenesis is yet to be observed in most conifer species (Merkle and Dean, 2000). Researchers have been continuing to provide significant efforts in improving the technique of somatic embryogenesis for different plant species. Traditionally somatic embryogenesis is carried out on solid medium. It requires intensive manual handling in selecting, separating, and sorting of embryos

during maturation and germination phases. Lack of automation causes the culture process to be expensive for mass production of plants. Introduction of suspension culture in liquid medium can be considered an advancement in this effort. However, the liquid medium requires a continuous agitation for the culture of somatic embryos to distribute the nutrients evenly in the culture medium (Sun, 2010). Since agitation is directly associated with the development of hydrodynamic stress, it plays as a limiting factor in liquid culture (Suehara et al., 1998).

Hyperhydricity (Debergh et al., 1992) is a major bottleneck of liquid cell culture systems. It results in watery tissues, deficiency in organization of vascular bundles that connect the shoot and root meristems in embryos, and reduced cell to cell adhesion (reviewed by Gaspar et al., 1995). In plants, morphological abnormalities, with varying amount in different species, include shorter internodes in the stems, and brittle, translucent, and wrinkled leaves (Debergh et al., 1981; Kevers et al., 1984; Gaspar et al., 1987; Paques and Boxus, 1987; Ziv, 1991; Gaspar, 1991 & 1995). Using temporary immersion bioreactors reduces the possibility of these malformations since the explants are not immersed in nutrient medium constantly throughout the culture period.

Polarization, resulting in an embryonic region (meristematic cells region) and a unidirectional development of suspensor region (Figure 1.1(c)) in a maturing embryo, is a prerequisite of proper embryo development (Sun, 2010). Somatic embryos developed on solid proliferating medium are more polarized than in liquid proliferating medium (Egertsdotter and von Arnold, 1998) because of formation of suspensor cells in random

directions in liquid medium. Egertsdotter and von Arnold (1998) observed the size fraction of cell cultures of Norway spruce smaller than 200 µm formed well-developed embryos having polarized structures in liquid suspension cultures.

Coagulation to form cell aggregates is another severe issue in liquid culture systems. Agitation does not prevent the formation of aggregates of somatic embryos. This reduces the system's productivity and efficiency. Several mechanical and pneumatic techniques have been developed to prevent the formation of agglomerates of PEMs, such as, continuous agitation on a shaker table, stirring and circulating the fluid, or aerating the suspension cultures (Margaritis and Wallace, 1984; Takayama, 1991; Scragg, 1992; Doran, 1993; Takayama and Akita, 1994). These techniques either subject the cells to severe shearing forces and cause cell damage, or have proven to be insufficient to disperse the aggregates (Chattopadhyay et al., 2004).

In somatic embryogenesis, the synchronous development of embryos may result in high yield of plants. The cells inside PEMs aggregates may get lesser access to nutrients from culture medium in comparison to cells at the surface of the clusters resulting in different development of somatic embryos. Tonon et al. (2001) studied the synchronous development of *Fraxinus angustifolia*, though not a conifer species, in liquid suspension culture in Erlenmeyer flask. They established two sets of cell cultures, (i) fractionation of cells and cell aggregates on a size basis (160-500, 500-1000, 1000-2000, & >2000 µm) and observed asynchronously developed mature embryos regardless of size classes; and (ii) fractionation by density gradient centrifugation in Ficoll solution

of cell and cell aggregates (10-12%, 12-14%, 14-16%, 16-18%, & >18% Ficoll layer) and observed that no embryos were formed in the lightest three fractions , but the heaviest two fractions provided simultaneous growth of mature embryos with satisfactory yield.

Though it is important to keep embryos dispersed in liquid while maximizing the rate of growth as well as probability of germination and successful plant formation, embryos cannot grow in isolation (Egertsdotter and von Arnold, 1995). The cultured cells release the conditioning factors to the surrounding medium. This medium has influences on the growth of embryos. Egertsdotter et al. (1993) and Egertsdotter and von Arnold (1995, 1998) observed that not only the mechanical stresses from agitation but also the stress-related proteins released into the Norway spruce culture medium affect the development of somatic embryos from proliferation to maturation. The morphology of somatic embryos and the number of suspension cells produced affect the release of the conditioning factors.

In spite of having these issues, the liquid culture system is getting more popularity because it can easily be automated, and intensive manual handling can be avoided during maturation and germination; hence the costs may be reduced. Bioreactor technology is the first step in this automation process. Bioreactor is used to create an environment with controlled temperature, pH, and liquid agitation for embryogenic or organogenic culture by providing nutrients and air to explants. It can be used for somatic embryogenesis, production of biomass, metabolites, and enzymes (Appendix A), and for biotransformation of exogenously added metabolites.

1.2.4 Bioreactor design

Bioreactors are closed, sterile systems for clonal propagation of organogenic propagules or somatic embryos. The internal environment of bioreactors is typically controlled to different extents depending on the model of a bioreactor and plant material. Circulation, mixing, aeration, cell suspension, temperature, pH, and dissolved oxygen are a few physical and chemical parameters that are associated with the environment inside bioreactors. Different plant species and propagation materials have different requirements that will dictate the specific settings for the internal environment of bioreactors and determine the most appropriate bioreactor model to be used.

The growth and development of plant cells *in vitro* mostly depend on liquid medium circulation, mixing, and aeration for distribution of oxygen and nutrients (Illing et al., 1999; Curtis, 2005). So the effective design of a bioreactor must ensure this growth favorable environment. The bioreactor design is technically challenged by the properties of suspension culture, such as viscosity, shear sensitivity of cells, tendency of cell aggregation, and foam formation (Doran, 1999). Especially the shear sensitivity of cells play a significant role, because the plant cells are low shear tolerant (Mandels, 1972). This leads to several novel designs of bioreactors which have become successful in micropropagation. The main difference between these bioreactors is the means of operation. Details of bioreactors are provided in Chapter 2. In this research, a temporary immersion bioreactor is designed where mechanical and pneumatic agitations are avoided.

CHAPTER 2

DESIGN OF A TEMPORARY IMMERSION BIOREACTOR FOR CLONAL PROPAGATION OF PLANTS

The bioreactors used for clonal propagation can be divided into two broad categories, (i) mechanically operated bioreactors and (ii) pneumatically operated bioreactors (Mamun et al., 2015). Stirred tank, rotating drum, and spin-filter bioreactors fall into the first category. The second category bioreactors are comprised of bubble column bioreactors, airlift bioreactors, and temporary immersion bioreactors. There are other types of bioreactors, such as diffusion bioreactors, magnetically stabilized fluidized bed bioreactors, immobilized plant cell reactors, disposable bioreactors, flow bioreactors, ultrasonic nutrient mist bioreactors, membrane bioreactors, etc. (Table in Appendix A), which differ in operation in a non-conventional manner.

In stirred tank bioreactors, agitation has been achieved by flat blade, marine, cell-lift, disk turbine impellers, magnetic stirrer, spindle with aeration tube, reciprocating plate, and rotating wall vessel to facilitate liquid circulation, mixing, and distribution of O_2 and nutrients. In order to reduce shear damage of the cells caused by mechanical agitation in stirred tank bioreactors, airlift and bubble column bioreactors are investigated for micropropagation of several plant cells. However cultures in these bioreactors may suffer from hyperhydricity and hamper the development. Temporary immersion of cells could be a possible solution and used to culture different plant species.

Because of the vast area of research, there are a large number of publications focusing on bioreactors for clonal propagation. Hence the focus is on different types of bioreactors designed for plant biomass, metabolites, and enzymes production in micropropagation process, and somatic embryogenesis, and their advantages and limitations for plant proliferation.

2.1 Different Designs of Bioreactors

2.1.1 Mechanically Operated Bioreactors

2.1.1.1 Stirred tank bioreactor

A conventional stirred tank bioreactor consists of an impeller or agitator along with different ports for aeration, medium addition or removal, etc. Design of an agitator is becoming a real challenge to the researchers to maintain maximum cell viability. Stirred tank bioreactor has high volumetric mass transfer coefficients, and is enabled to maintain homogeneous nutrition environment in the culture medium through agitation (Huang and McDonald, 2009). However its high specific power input (P/V- power per unit volume), high energy dissipation rate, turbulence around the agitator, and shear damage of cells, tissues and embryos lead to consider other mechanisms of operating a bioreactor (Huang and McDonald, 2009).

Stirred tank bioreactors have been playing a significant role for several decades for clonal propagation. Such a bioreactor system was used by Jay et al. (1992) to study the effect of dissolved oxygen on carrot somatic embryogenesis (*Daucus carota L.*). Culture medium in a glass vessel bioreactor (3 l, working volume was 1.7 l) was stirred

by an impeller consisting of four blades as shown in Figure 1 (a). The process temperature was maintained 27 ºC with a water jacket. The bioreactor was connected with oxygen/nitrogen gas chamber, air compressor, and electronically controlled valve, and equipped with oxygen and pH probes. Dissolved oxygen concentration in the medium was maintained either at 100% (by supplying pure oxygen) or at 10% (by supplying pure nitrogen). Higher growth rate of cells during proliferation was observed in the culture medium having 100% concentration of dissolved oxygen because of low cytochrome oxydase activity (Atwell and Greenway, 1987; Jay et al., 1992). Similar trend was observed in somatic embryo production. This might be due to rapid synthesis of ethylene and acetaldehyde in hypoxic condition (Jackson et al., 1985; Small et al., 1989; Jay et al., 1992). Both ethylene (Tisserat and Murashige, 1977) and acetaldehyde (Perata and Alpi, 1991) showed inhibition characteristics of embryo production (embryogenesis) of carrot cells (Jay et al. 1992). Similar stirred tank bioreactor system was used by Jay et al. (1994) to investigate the effect of pH of culture medium on carrot cells' growth. HCl (1N) and KCl (1N) were used to maintain the media pH of 4.3 and KOH (1N) was used for pH of 5.8. In absence of 2,4-dichlorophenoxyacetic acid (2,4-D), more embryos were produced in the media of pH of 4.3 compared to that of pH of 5.8. However plantlet formation occurred more in the later. This may be associated with lower uptake rate of ammonium (NH_4^+) and sugar by the embryos in the more acidic medium (pH= 4.3). Jay et al. (1994) noted that the inability to release protons by the embryos limited the nutrients uptake, as observed by Schubert et al. (1990) in case of root culture of field beans (*Vicia faba*).

Depending on requirement and applications, researchers have developed several different designs of stirred tank bioreactors. A few examples are shown in Figure 2.1. Their features and purpose are explained in Appendix A.

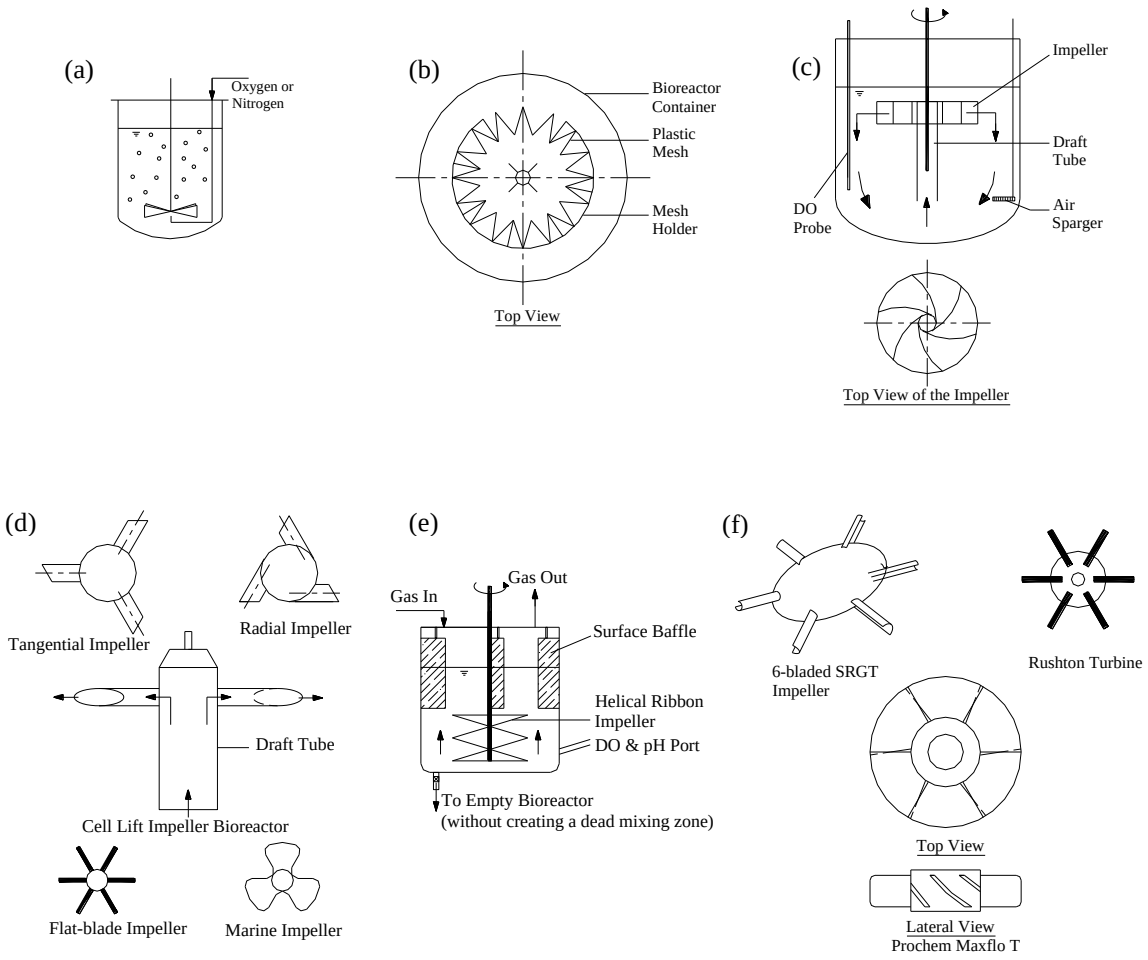

Figure 2.1 Different designs of stirred tank bioreactor; rotation of impeller in the bioreactor provides agitation to the liquid medium that helps to maintain homogeneity of nutrient and O_2 in the medium, (a) schematic of a conventional stirred tank bioreactor (Jay et al., 1992), (b) stirred tank bioreactor with plastic mesh for immobilization of hairy roots (Cardillo et al., 2010), (c) centrifugal impeller stirred tank bioreactor that provides an axial inlet and radial outlet of medium causing better mixing, low shear, and higher liquid lift (Wang & Zhong, 1996), (d) cell lift impeller bioreactor in which cells along with medium are lifted through the draft tube of the impeller and result in either tangential or radial exit of cells; conventional flat bed and marine impellers were also used for comparison (Treat et al., 1989), (e) bioreactor with double helical ribbon impeller that pumps liquid upward when rotates counter clockwise (Jolicoeur et al., 1992), (f) Rushton turbine and Scaba (SRGT) impellers (Amanullah et al., 1998); in Scaba impeller six curved parabolic blades were used and its rotation resulted in radial flow of fluid in the bioreactor.

2.1.1.2 Rotating drum bioreactor

Rotating drum bioreactor is being used in plant cell culture as an alternate of stirred tank bioreactor to achieve higher mass transfer and cell viability. In a comparative study between stirred tank and rotating drum bioreactors, Tanaka et al. (1983) observed a lower cell growth of *Vinca rosea* in stirred tank bioreactor, equipped with baffles, air sparger , and flat six-blade impeller, agitated at a rpm of lower than 115 or higher than 170. This could possibly be due to insufficient transfer of O_2 to the cells at a lower rpm, or damage of the cells because of hydrodynamic shear at a higher rpm. The study showed that rotating drum bioreactor performed more efficiently to supply oxygen to the cultures than stirred tank bioreactor under highly viscous and low hydrodynamic shear conditions. The drum, made of polycarbonate, consisted of air supply and vent ports and an oxygen sensor as shown in Figure 2.2. The experiment was conducted in three sizes of drum, 1 l, 2.4 l, and 4 l. The two types of bioreactors were compared under a constant air flow rate of 1.0 vvm to maintain the same k_La value (volumetric oxygen transfer coefficient) in both cases.

Fung and Mitchell (1995) studied the performance of baffles in rotating drum bioreactor while performing SSF (solid-state fermentation: fermentation on moist solid substrate in absence of or near absence of free liquid (Pandey, 1992; Domínguez et al., 2001)) of *Rhizopus oligosporus*. They observed about 58% rise of oxygen uptake rate in a baffled reactor over a non-baffled one based on the weight of initial dry substrate. A stainless steel drum of 10.9 m long and 0.56 m in diameter had four evenly spaced baffles of width 0.17 m (ratio of baffle width to drum diameter was 1:3.29) were placed along

the length of the drum. Air entered and left at two ends of the drum at a rate of 24 l/min. During operation, they noticed a higher temperature of the culture in the baffled bioreactor that might possibly be due to rapid metabolic heat generation because of better aeration in the system and concluded that number and shape of the baffles, along with rotational speed, and aeration rate might play a significant role to optimize culture process in rotating drum bioreactor.

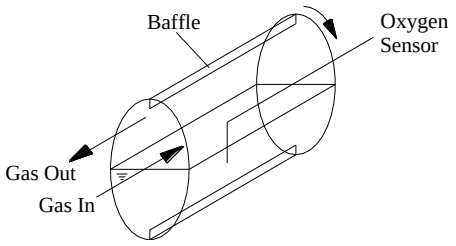

Figure 2.2 Rotating Drum Bioreactor constructed with a vessel having baffles inside contains the culture and the medium at the bottom. Rotation of the vessel facilitates mass transfer under low shear condition (Tanaka et al., 1983).

2.1.2 Pneumatically Operated Bioreactors

2.1.2.1 Bubble column bioreactor

Bubble column is one of the early inventions among pneumatically operated bioreactors. A conventional bubble column bioreactor, shown in Figure 2.3(a), consists of a cylindrical vessel having an air sparger at the bottom. Because of its high heat and mass

transfer rates, plug free operations, and low operating and maintenance cost (Kantarci et al. 2005), bubble column bioreactor has been playing an important role in large scale production of high value plants and metabolites.

Arcuri et al. (1983) produced thienamycin using a continuously operated bubble column bioreactor as shown in Figure 2.3(b). *Streptomyces cattleya* cells were immobilized by attaching them with celite particles. A cylinder, referred to as a solid-liquid disengagement cylinder, was placed inside the reactor to separate celite-cell aggregates from the medium during continuous operation.

Instead of using a vertical side wall bubble column reactor, Fujimura et al. (1984) studied continuous production of L-arginine from *Serratia marcescens cells* in a cone shaped bioreactor (jacketed), shown in Figure 2.3(c), using immobilized cell culture procedure. The shape of the bioreactor could possibly eliminate the dead zone and provide better mixing of nutrients and mass transfer to the cells. About $3x10^{10}$ cells were entrapped per ml of carrageenan gel beads. Oxygen played a key role for the growth of *S. marcescens* cells. Concentration of L-arginine in the medium increased with increase in oxygen concentration. Since the gel behaved as a diffusion-barrier, higher concentration of dissolved oxygen in the medium provided sufficient oxygen diffusion for growth of the cells. El-sayed and Rehm (1987) investigated the performance of a conventional bubble column bioreactor having a straight vertical vessel and a conical shaped bubble bioreactor through continuous production of penicillin by *Penicillium chrysogenum* cells entrapped in Ca-alginate beads for immobilization. They observed that at a certain air

flow rate, conventional bubble column bioreactor lost fluidization partially because of swelling of the beads due to cell growth. However it was not an issue for the conical bubble reactor; instead, lower mechanical abrasion at the wall among rotating beads and better distribution of nutrients and oxygen were achieved.

A bubble column bioreactor with cylindrical loofa sponges was used by Ogbonna et al. (2001), shown in Figure 2.3(d), to produce ethanol from sugar beet juice (as a substrate) by *Saccharomyces cerevisiae*. The function of loofa sponges was to immobilize the cells. They proposed external loop (bubble column) bioreactor which could immobilize the cells uniformly on loofa sponges at different sections and produce ethanol efficiently in a large scale.

Use of bubble column bioreactor for large scale clonal propagation of plant was investigated by Akita et al. (1994) using a 500 l bioreactor. The shoots of *Stevia rebaudiana* were used in this experiment. A porous disc of 300 mm diameter was attached at the bottom of the bioreactor as a gas sparger. There were four fluorescent lamps, with an approximate intensity of 1000 lux each, inside the bioreactor. Inoculum size was 460 g (Fresh weight) in 300 l of sterilized culture medium. Compressed air was sparged into the medium at a rate of 15 l/min. Shoots grew very well having a final weight of approximately 64.6 kg (Fresh weight), though damage occurred by air bubbles just above the gas sparger, and gradual decrease in growth was observed away from fluorescent lamps.

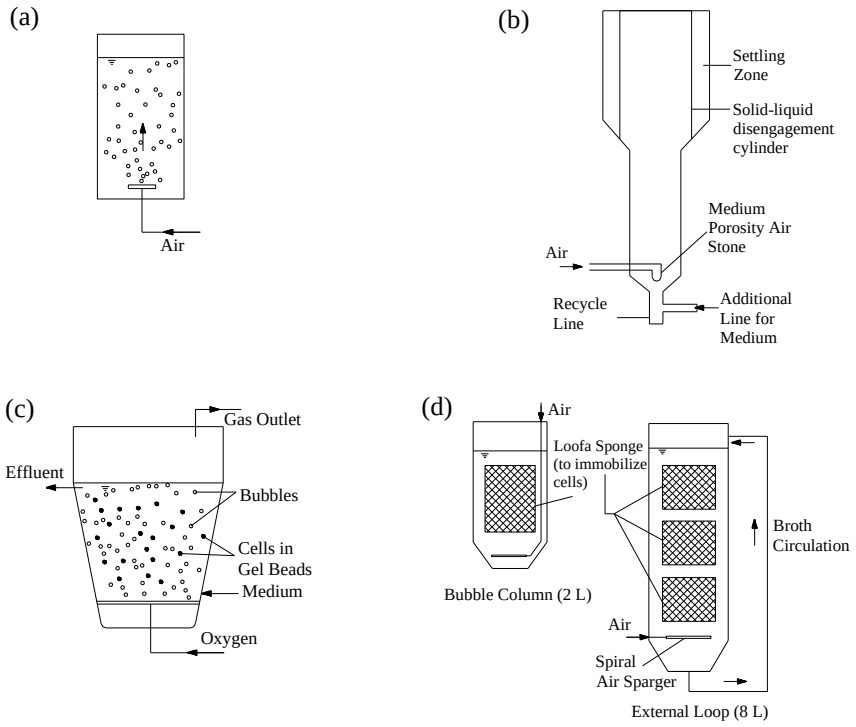

Figure 2.3 Bubble Column Bioreactor, (a) schematic of a conventional bubble column bioreactor having an air sparger at the bottom that generates air bubbles and provides agitation in the medium, (b) Arcuri et al. (1983) has used a settling zone for cell aggregates in the bubble column bioreactor for continuous operation (bubble formation and medium perfusion), (c) cone shaped reactor working similar to conventional bubble column bioreactor reduces the possibility of dead zones (Fujimura et al., 1984), (d) bioreactor with cells immobilized on loofa sponges sparging air from the bottom and having medium circulation through an external loop (Ogbonna et al. 2001).

2.1.2.2 Airlift bioreactor

Airlift bioreactor is introduced for plant cell culture to provide a low hydrodynamic shear environment. It reduces the loss of cell viability compared to stirred tank bioreactor and eliminates the dead zones that cause inefficient mixing in the bubble

column bioreactor. An airlift bioreactor is operated by sparging gas (or air) in liquid medium placed underneath a draft tube of the bioreactor. This causes a pressure difference between inside and outside of the draft tube and results in a fluid circulation in the bioreactor.

A conventional airlift bioreactor consists of a sparger, a bioreactor vessel, a solid vertical side draft tube, known as riser and placed inside the bioreactor vessel, and several ports as needed. Researchers have made modifications of this initial design in order to improve the bioreactor performance, such as mixing, shear rate, growth rate of cells, biomass yield, and oxygen transfer rate (Smart and Fowler, 1984; Fu et al., 2003; Chen et al., 2010). Smart and Fowler (1984) investigated the efficiency of a simple air lift bioreactor in terms of aeration rate, mixing, growth rate of cells, and biomass yield in the suspension culture of *Catharanthus roseus*. The bioreactor consisted of a vessel (5 l LKB Ultraferm fermenter) and a 94 mm diameter draft tube placed above an air sparger ring, shown in Figure 2.4(a), having 17 holes of 0.533 mm in diameter each. The relation between aeration and agitation was established in terms of superficial gas velocity (V_s) and mixing time (t_m) as follows,

$$t_m = 0.032 \frac{H}{\sqrt{V_s}} \left(\frac{D}{d}\right)^2 \quad (1)$$

where, *H* and *D* are the height and diameter of a fermenter respectively, and *d* is the diameter of the draft tube. The system geometry and ratios of *H/D* and *d/D* played a significant role in mixing. Growth rate of plant cells cultured in this experiment reduced

with aeration over a certain rate. Design of the draft tube was modified in an experiment performed by Townsley et al. (1983) where they used a conical shaped draft tube above the air sparger ring in a larger vessel, shown in Figure 2.4(b), for the suspension culture of selected *Tripterygium wilfordii* for the production of tripdiolide. The cone shaped draft tube was used to provide sufficient circulation at the bottom of the vessel. The plant cells were pushed up by air through the draft tube, and with decrease in cross-sectional area of the draft tube along the flow path, the velocity of cells and medium increased. Hence the cells started falling at a higher velocity outside the draft tube. This way an efficient mixing was achieved during the culture process. A small magnetic stirrer was used in this system along with the draft tube. Air was recycled in this experiment by controlling the level of oxygen in the air. Increased biomass yield as well astripdiolide production were observed.

A comparative study of bioreactor performance among stirred tank, bubble column, conventional airlift bioreactors and a bioreactor with mesh/net draft tube, shown in Figure 2.4(c), was carried out by Chen et al. (2010) for the production of chitinolytic enzymes from suspension culture of *Paenibacillus taichungensis*. Under same operating conditions of the volume of culture medium, aeration rate, and inoculated culture, the net draft tube bioreactor showed a little improvement in chitinolytic enzyme yield (~ 2.94%) and productivity (~ 4.26%) over the conventional airlift bioreactor. The enzyme activity and the cultivation time were same in both cases. However this newly designed bioreactor showed much better performance over bubble column reactor, but the stirred tank bioreactor had same productivity as that of the net draft tube airlift bioreactor.

In order to investigate the improvement of productivity, Sajc et al. (1995) developed an external loop airlift bioreactor for production and continuous extraction of extracellular metabolites (anthraquinones) by immobilized culture of *Frangula alnus* Mill. plant cells (Figure 2.4(d)). The results showed much higher production of anthraquinones compared to shake flask culture of immobilized cells. Solvents, such as silicone oil and n-hexadecane, were used in different runs to facilitate extraction of metabolites. Frequent replacement of the solvent with the fresh one showed higher yields of anthraquinones, because with time the solvent became saturated with the products.

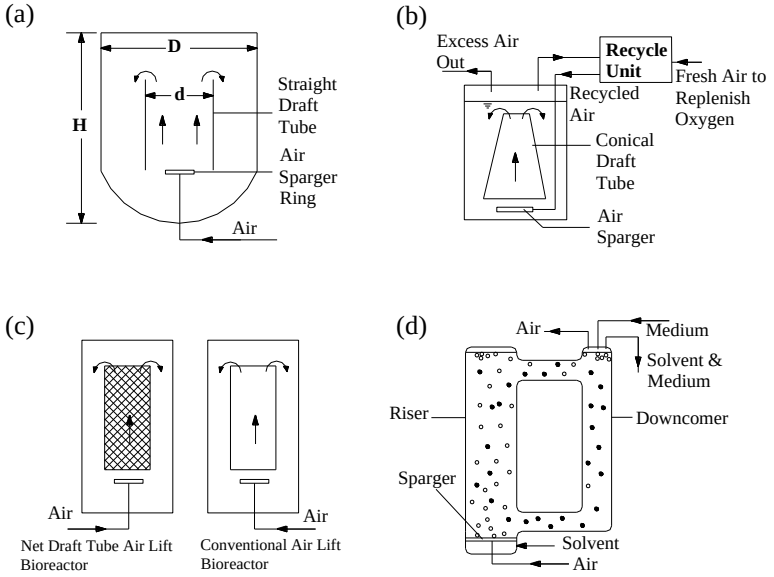

Figure 2.4 Various designs of airlift bioreactors in which the air or gas is sparged underneath the draft tube of the bioreactor; this causes a pressure difference between inside and outside of the draft tube and results in a fluid circulation in the bioreactor (a-c: internal loop, d: external loop), (a) Smart and Fowler (1984), (b) Townsley et al. (1983), (c) Chen et al. (2010), and (d) Sajc et al. (1995).

2.1.2.3 Temporary Immersion Bioreactor

The advantage of temporary immersion over suspension culture is that the explants in the temporary immersion bioreactor are not immersed permanently in liquid medium and, therefore, eliminates hyperhydricity that may be caused by excessive accumulation of water in the tissues. Hyperhydricity may cause cell damage due to depletion of O_2, formation of reactive oxygen species (ROS), and oxidative stress induction in the cells (Ziv, 2005). All temporary immersion systems so far been developed have been working on similar technology, i.e., the explants are kept away from the medium, and the medium is stored in a separate (usually lower) compartment in the same vessel where the explants are placed, or in a separate reservoir(s). The medium is then pushed by air to immerse the explants to provide nutrients and at the same time to refresh the gas composition in the headspace. After a period of immersion, the liquid medium returns to the reservoir either by gravity or suction. This process may take place once or more in 24 h period with an air pump, solenoid valve, timer, etc.

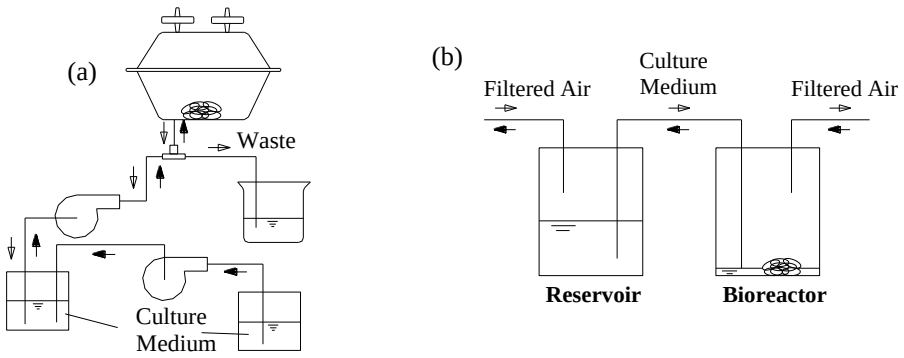

Figure 2.5 Temporary Immersion Bioreactor in which the culture and the medium remain in separate containers or in different compartments in the same container so that the culture does not immerse in the medium continuously; instead the medium is pumped to the culture container/compartment, culture is soaked with the medium, and then the medium is drained out; (a) Tisserat and Vandercook (1985) and (b) Escalona et al. (1999).

An automated temporary immersion culture system, shown in Figure 2.5(a), of plant propagules was developed and tested with orchid tips, aster shoot tips, cow tree shoot tips, date palm, and carrot callus by Tisserat and Vandercook (1985). An elevated (30 to 45 cm above the plane on which the rest of the system was placed) polystyrene container of 320 mm long, 175 mm wide, and 165 mm high was used as a culture chamber. Sometimes a plastic tray with 10 to 28 wells was used inside the chamber for the purpose of containing the plantlets or callus on it. The culture chamber was connected through silicone tubings with pumps, 3-way valve (stainless steel), and reservoirs of culture media. Air filters were used to avoid contamination. The system was operated with computer and electronic circuitry to ensure an automated consistent supply of

nutrients periodically to the explants during the culture process. The culture medium was replenished when necessary.

Alvard et al. (1993) investigated six different culture conditions for banana meristem. The explants were cultured on semi-solid and in liquid media with complete immersion, partial immersion, temporary immersion (20 min in 2 h), continuous air bubbling at 20 l/h, and cellulose culture support having the bases of explants in contact with the medium. The most promising outcome came from the temporary immersion technique in which multiplication rate was the highest without hyperhydricity. Shoots used as initial material for this study were obtained from successive proliferation subcultures on gelled medium. The bioreactor used in the temporary immersion culture system consisted of two compartments. Explants were placed in the upper compartment and the lower compartment was filled with culture medium. The upper compartment was connected with an air filter; the lower compartment was connected to an air pump, filter, and 3-way solenoid valve. During operation, the lower compartment was pressurized with air, which pushed the culture medium to the upper compartment through a connecting tube. The explants were immersed in the medium for a while (20 min); air bubbles agitated the cultures during immersion, and refreshed the area in the bioreactor head space by scavenging the exhausted air. The pressure in the lower compartment was released with the help of the solenoid valve to bring the medium back to the lower compartment when the immersion process was over. This process was repeated every 2 hours. The culture medium might be refreshed, or changed manually for stimulating different phases of tissue growth.

Escalona et al. (1999) performed a comparative study of pineapple micropropagation using solid medium, conventional liquid medium technology, and temporary immersion bioreactor. The pneumatically driven temporary immersion system, shown in Figure 2.5(b), consisted of two containers, one as a medium reservoir and the other one as a culture vessel, connected with glass and silicone tubes, filters, solenoid valves and air pumps. The liquid medium was pushed by filtered air to the container containing the explants (shoots of 2 to 3 cm in length) every 3 hours using an air pump. The medium kept the explants fully immersed for 2 min and was then pushed back by filtered air in the reverse direction. Filter paper was used to avoid continuous contact of liquid medium with the explants. It was possible to have a saturated filter paper with spent medium because of high frequency of operations (8 times in 24 h period); hence the spent medium might come in contact with new medium during the successive phases of cell culture. Also, because the high pressure air pushed the medium out of the culture vessel, this (pressure) would develop higher normal stresses on the propagules. The effect is not known yet. Similar design of temporary immersion system was used by Lorenzo et al. (1998) for sugarcane shoot formation and Jiménez et al. (1999) for production of potato microtubers.

2.1.3 Diffusion Bioreactor

Suspension cell culture of *Thalictrum rugosum* was carried out in a reactor equipped with hydrophobic polypropylene membrane, either arranged as a coil or a basket (Piehl et al., 1988). The purpose of the membrane was to supply oxygen to the medium through diffusion. The rotation of membrane coil or basket by means of

magnetic stirrer or eccentric shaft provided a gentle agitation to the medium as well as the cultures. This reduced the hydrodynamic shear stress, which would otherwise be caused by gas sparging or agitation mechanisms, and damage the tissues. No foam formation by damaged cells or cell debris was observed. Cell adhesion might cause clogging of the membrane. However this was not observed during the culture process. Instead of using a polypropylene membrane, Luttman et al. (1994) used silicone tubing to diffuse oxygen into the medium of a bioreactor, shown in Figure 2.6, for suspension culture of *Euphorbia pulcherrima,* and *Clematis tangutica*. The silicone tube, working as a permeable membrane for oxygen, nitrogen, and air, was given a helical shape with the help of a steel helical spring and inserted into the bioreactor. The dimension (diameter, length, and wall thickness) of the tube was decided based on the amount of embryogenic biomass to be produced. The chance of foam formation was much lower in this bioreactor because no bubble was produced during operation (unless the aeration pressure was raised above the bubble point).

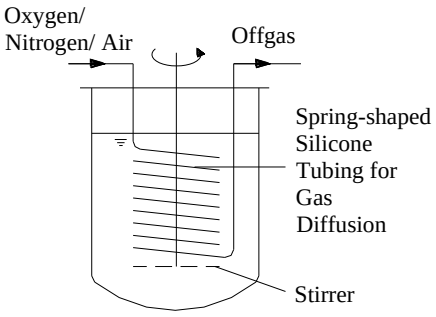

Figure 2.6 Diffusion Bioreactor having a helical shaped silicone tube permeable to O_2, N_2, and air that diffuse to the medium from the tube and the stirrer agitates the medium containing the culture (Luttman et al. 1994).

2.1.4 Perfusion Bioreactor

Perfusion bioreactors have been playing a vital role in the production of secondary metabolites. They are involved in continuous feeding of nutrients and harvesting of metabolites from spent medium during the culture period (Langer, 2011). They may be operated either mechanically (Su and Arias, 2003; De Dobbeleer et al., 2006) or pneumatically (Su et al., 1996). Several approaches (De Dobbeleer et al., 2006) have been applied in these bioreactor systems for an efficient removal of bio-products from the medium with a reduced degradation of metabolites. For example, continuous extraction of alkaloids secreted during hairy root culture was possible by circulating silicon oil in a two-liquid-phase bioreactor (Tikhomiroff et al., 2002); increased productivity of secondary metabolites was achieved by using resins *in situ* for cell suspension systems (Williams et al., 1992; Lee-Parsons and Shuler, 2002). Harvesting and purification of secondary metabolites were improved by using of resin (XAD-7) externally in the medium circulation loop (Klvana et al., 2005).

However, the major constraint of recovering metabolites from the culture medium was to retain majority of the cells by keeping the cells and the medium separate during perfusion culture. In achieving this, three techniques were widely used - centrifugation, filtration, and sedimentation (Su et al., 1996; Seki et al., 1997).

Filtration might have clogging problem (Tokashiki et al., 1990), and centrifugation might damage plant cells because of their shear sensitivity (De Dobbeleer et al., 2006). So gravitational sedimentation was considered as the most efficient way to

retain the cells and separate the medium containing secreted metabolites (Wang et al. 2010). However this method required an optimization of perfusion rate of the fresh medium, recirculation rate of the culture medium, and cell retention.

Attree et al. (1994) proposed a low-cost method based on perfusion technology to generate mature white spruce somatic embryos. A flat absorbent pad, used as a culture pad to support the embryos, was placed above the liquid culture medium in the cuboid shaped polypropylene culture chamber. This pad consisted of cotton wool, a 48 μm nylon mesh and a filter paper. The bioreactor was connected with the culture medium and spent medium reservoirs at two diagonally opposite corners of the base. The culture medium was pumped into the culture chamber at a rate of 60 ml/day for 7 weeks. The excess medium was collected in the spent medium reservoir by gravity. High quality mature embryos were recovered in this process. These embryos had higher desiccation tolerance and postgerminative growth compared to those cultured on agar medium.

Gravitational sedimentation technique was used by Su et al. (1996) for the suspension culture of A*nchusa officinalis* and continuous production of secreted protein throughout the culture period in a perfusion external loop airlift bioreactor, shown in Figure 2.7(a). A baffle was placed vertically to have a settling zone in the upper portion of the downcomer. Continuous removal of the medium with secreted metabolites was taken place from the settling zone and the perfusion medium was fed from the bottom of the riser to replenish nutrients for the cells. They achieved a maximum cell density of

2.16 times and an extracellular protein concentration of 2.36 times more in their system compared to batch culture.

A stirred tank perfusion bioreactor of 3.3 l working volume was used for the production of acid phosphatase (APase) while culturing A*nchusa officinalis* (Su and Arias, 2003). The bioreactor had an annular settling zone for continuous separation of cells and medium. The schematic of the bioreactor is shown in Figure 2.7(b). The bioreactor was made of glass with an annular stagnant zone because of the presence of a cylindrical baffle. An agitator with six blades on top (Rushton turbine) and three blades (to pump in upward direction) at the bottom was used for mixing. A sintered glass tube gas sparger of 140 µm pore size was placed below the impeller. Complete cell retention was possible at a perfusion rate of up to 0.4 vvd (vessel volume per day) achieving the APase production of about 300 units/l/d with a cell dry weight exceeding 20 g/l. The culture operation at a high packed cell volume (PCV over 70%) was avoided owing to declined oxygen uptake and reduced cell viability. Cells were removed from the bioreactor via bleed stream (at a rate of up to 0.11 vvd) that led to higher APase production and increased cell dry weight.

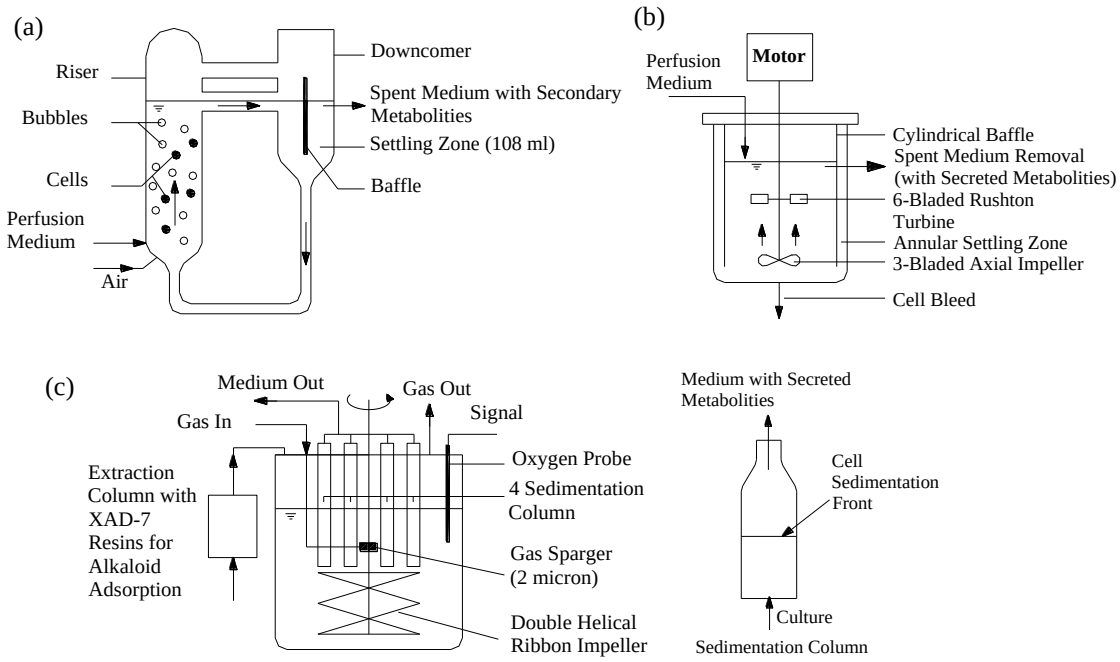

Figure 2.7 Perfusion Bioreactor; (a) Su et al. (1996), (b) Su and Arias (2003), (c) De Dobbeleer et al. (2006).

De Dobbeleer et al. (2006) developed a perfusion bioreactor, consisting of four sedimentation columns, a gas sparger, and a double-helical ribbon agitator (shown in Figure 2.7(c)) to extract secondary metabolites continuously from the cell suspension culture of *Eschscholzia californica*. The rotational speed of the agitator was optimized with the gap between the bottom of the sedimentation column and the top of the helical ribbon to have a stable cell sedimentation front and to minimize cell loss. The liquid medium with secreted secondary metabolites was circulated between sedimentation columns, fluidized resin (XAD-7 placed in an extraction column in the outer loop), and the bioreactor by a peristaltic pump.

Stirred tank perfusion bioreactor with a separate sedimentation unit was proposed by Wang et al. (2010). The bioreactor unit was equipped with a 4-blade agitator, gas sparger, and pH and dissolved oxygen probes. The spent medium was continuously removed from the bioreactor to the external sedimentation unit via overflow, and perfusion medium was fed into the bioreactor to replenish nutrients. As cell density increased in the bioreactor, more cells entered the settling column. So a harvest pipe was attached underneath the sedimentation unit to have cell bleed which led to high cell growth and reduced dead cell accumulation.

2.1.5 A few special types of bioreactors

2.1.5.1 Magnetically stabilized fluidized bed bioreactor

The concept of having fluidization of magnetized particles by a stream of fluid in presence of a uniform magnetic field (Rosensweig, 1979) was applied to design a magnetically stabilized fluidized bed bioreactor (Bramble et al., 1990). This bioreactor avoided the hydrodynamic instability and, therefore, achieved turbulent free, plug flow of solids. A schematic of this bioreactor is shown in Figure 2.8(a). The cells were attached to gel beads containing magnetizable solids. Then they were added to the bioreactor from the top and moved downward in a "lockstep fashion". After a certain period of culture, beads along with the spent cells were removed from the bottom using oxygen-enriched recycled and fresh liquid media that made the bed fluidized. Major advantages of this bioreactor includes high rate of oxygen transfer while causing a low-shear to the cells and elimination of support damage which would otherwise have resulted from particle collisions.

2.1.5.2 Immobilized plant cell bioreactor

In a plant cell bioreactor, the cells were immobilized by filtering them on a cotton matrix (commercially available terry cotton sheet) (Choi et al., 1995). About 85-90 g fresh weight of *Gossypium arboreum* cells were entrapped on a cotton sheet of 400 cm^2. To strengthen the immobilization of cells, the cotton cloth was spirally wound with a spacer (Goodloe 304 stainless steel woven packing). This way shear force on the cells by the immobilization matrix was eliminated. The immobilized cells were then placed in a plug flow type reactor (300 ml) as shown in Figure 2.8(b).

2.1.5.3 Reciprocating plate bioreactor

A reciprocating plate bioreactor, named after reciprocating motion of a plate stake in a bioreactor as shown in the schematic (Figure 2.8(c)), was used to investigate its potential for cell suspension culture. *Vitis vinifera* cells were used as a model culture in this bioreactor for their growth and viability (Gagnon et al., 1999). The bioreactor vessel was built with two concentric stainless steel tubes providing 17 l of working volume. The bioreactor consisted of six perforated stainless steel plates attached equispaced to a shaft operated by a variable speed motor. This resulted in a reciprocating motion to the plates and provided agitation and mixing in the culture medium. A gas sparger was placed at the bottom to provide aeration (or nitrogen) to the culture. The authors observed a significant decrease in O_2 transfer coefficient with increase in cell concentration in the bioreactor.

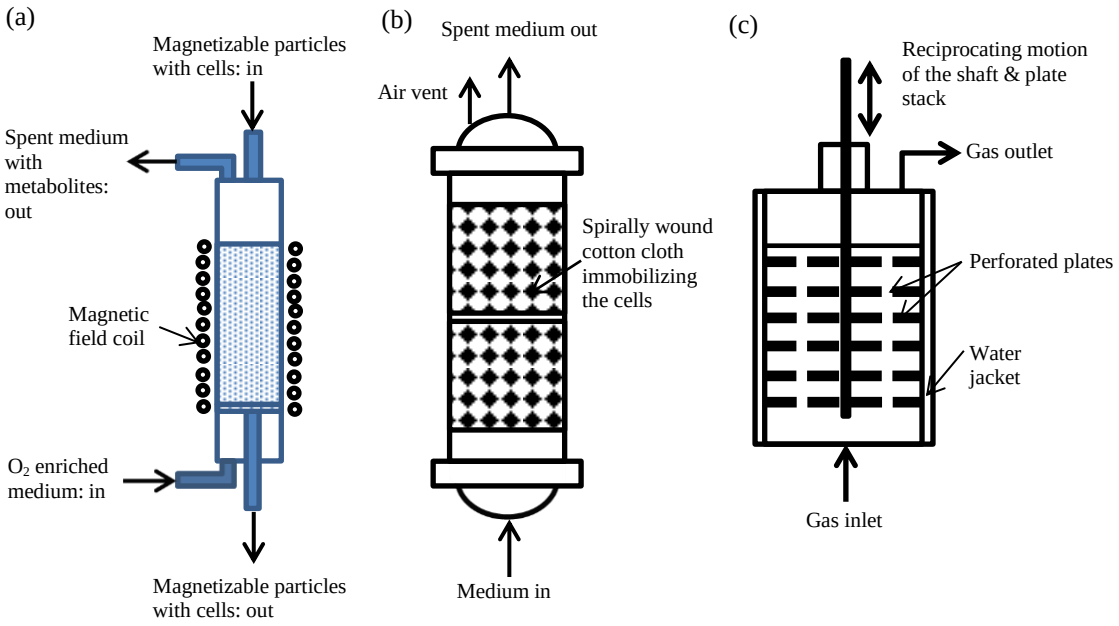
(a)
Magnetizable particles with cells: in
Spent medium with metabolites: out
Magnetic field coil
O_2 enriched medium: in
Magnetizable particles with cells: out
(b)
Spent medium out
Air vent
Spirally wound cotton cloth immobilizing the cells
Medium in
(c)
Reciprocating motion of the shaft & plate stack
Gas outlet
Perforated plates
Water jacket
Gas inlet

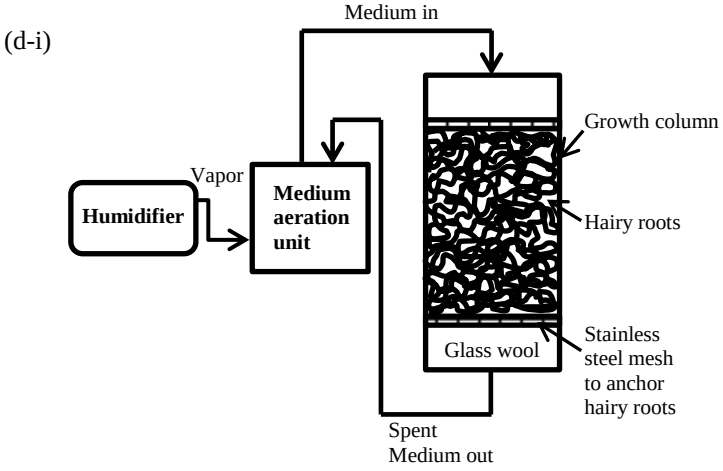
(d-i)
Medium in
Growth column
Vapor
Humidifier
Medium aeration unit
Hairy roots
Glass wool
Stainless steel mesh to anchor hairy roots
Spent Medium out

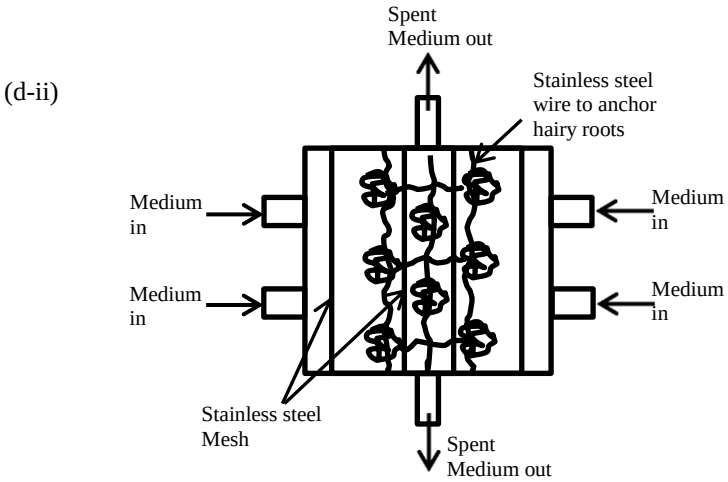
(d-ii)
Spent Medium out
Stainless steel wire to anchor hairy roots
Medium in
Medium in
Medium in
Medium in
Stainless steel Mesh
Spent Medium out

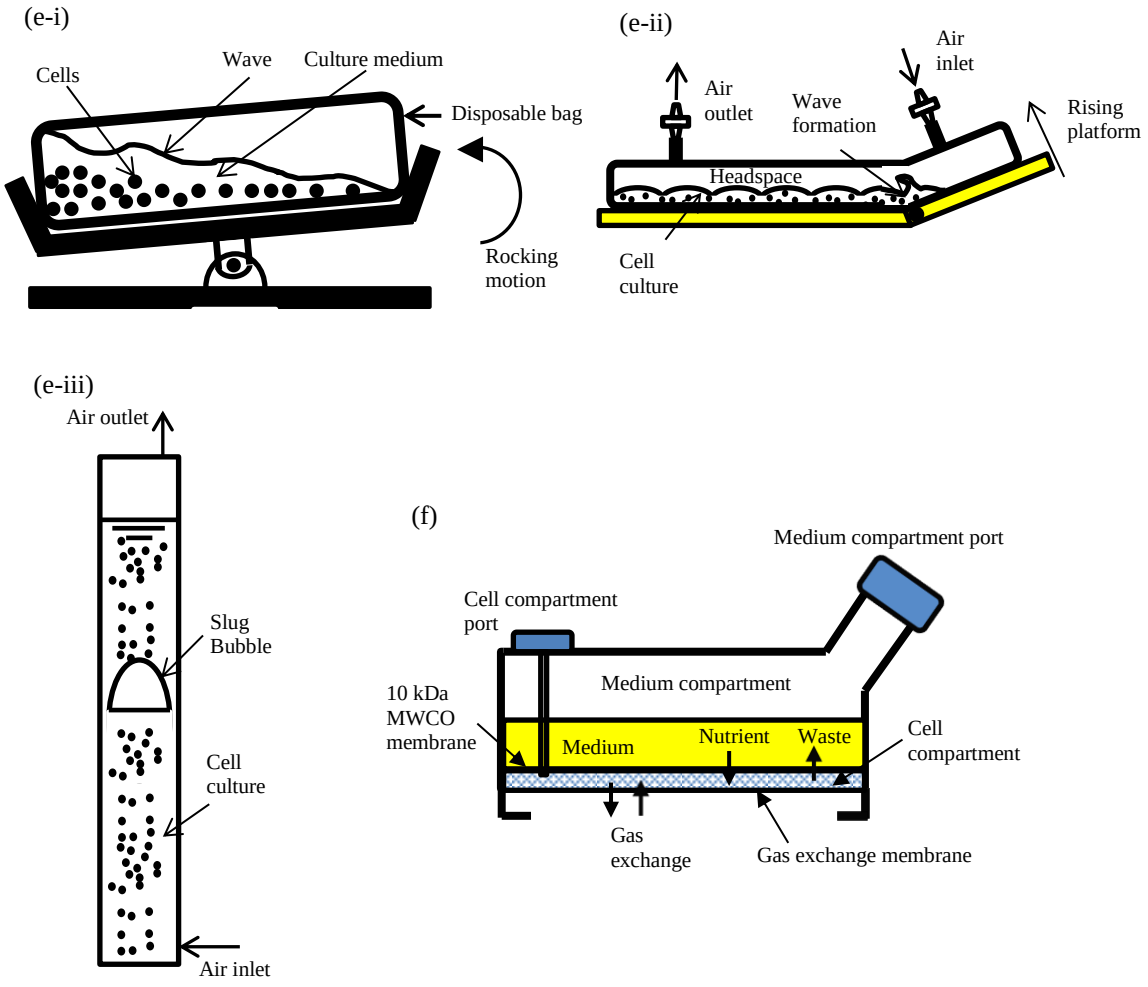

Figure 2.8 A few special types of bioreactors; (a) Magnetically stabilized fluidized bed bioreactor (Bramble et al., 1990), (b) Immobilized plant cell bioreactor (Choi et al., 1995), (c) Reciprocating plate bioreactor (Gagnon et al., 1999), (d) Flow bioreactors- (i) Single-column reactor, (ii) Radial flow reactor (Kino-oka et al., 1999), (e) Disposable bioreactors- (i) Wave bioreactor (Singh, 1999), (ii) Wave and Undertow bioreactor (Terrier et al., 2007), (iii) Slug bubble bioreactor (Terrier et al., 2007); (f) Membrane bioreactor (McDonald et al., 2005).

2.1.5.4 Flow bioreactor

Kino-oka et al. (1999) explained two types of flow bioreactors, namely single-column reactor (1 l) and radial flow reactor (1.5 l), used for high density hairy root culture of red beat. In single-column reactor, medium flowed from the top to the bottom of the reactor through hairy root cultures anchored to a stainless steel mesh (Figure 2.8(d-i)). In radial flow reactor (Figure 2.8(d-ii)) the hairy roots were anchored to stainless steel wires in between two concentric stainless steel meshes and fresh medium was introduced radially through four ports at the outer vessel. The spent medium was discharged from the two ports at the center of the reactor. Each reactor was connected to a medium aeration unit and a humidifier for operation.

2.1.5.5 Disposable bioreactor

Disposable bioreactor, with its name implying a one-time use culture vessel, was introduced to reduce production costs (Terrier et al., 2007), cross-contamination (Eibl et al., 2010), and cell damage due to gas bubbles and mechanical agitators (Singh, 1999). A disposable bioreactor causing wave agitation to the medium by rocking motion is shown in Figure 2.8(e-i) (Singh, 1999). The container of a disposable bioreactor is usually made of polyethylene, polystyrene, polytetrafluoroethylene, polypropylene, or ethylene vinyl acetate (Eibl et al., 2010). The rocking motion of the wave bioreactor was replaced by the wave and undertow (WU) mechanism and demonstrated by Terrier et al. (2007), shown in Figure 2.8(e-ii), for the production of isoflavones from tobacco and soya cell cultures. A 100 l working volume WU bioreactor container was placed on a horizontal table which was equipped with a platform at the side that rose periodically to induce wave and

undertow, and resulted in agitation and aeration in the culture medium. To investigate the performance of a pneumatically operated disposable bioreactor, the authors designed a 70 l working volume bubble column bioreactor with a vertical, flexible plastic cylinder, named slug bubble (SB) bioreactor that intermittently generated a large bubble occupying almost the entire cross-section of the tube(Figure 2.8(e-iii)). When the bubble moved up, a thin film of medium flowed downward along the wall as a falling film and an enhanced mixing and mass transfer occurred at the rear of the bubble.

2.1.5.6 Membrane bioreactor

Membrane bioreactor provides a convenient means of aeration to the cell culture in bioreactor without generating bubbles, and therefore, reduces the possibility of cell damage due to hydrodynamic shear. It may also be featured with a special membrane for specific molecular cut-off (MWCO) to supply nutrients to the cells and for separation of metabolites. This feature was introduced in a two-compartment (nutrient medium compartment and cell compartment) bioreactor (Figure 2.8(f)), named CELLine 350 from Integra Biosciences, Chur, Switzerland. It was used for the production of Human α-1 antitrypsin protein from transgenic rice cell culture (McDonald et al., 2005). About 7-10 ml of concentrated rice cells were packed in the cell compartment which was in between a 10kDa MWCO membrane and a gas exchange membrane. Initially the medium compartment was filled with 65 ml of medium in addition to 25 ml which was poured in to wet the MWCO membrane. For homogeneity of nutrients in the medium, the bioreactor was agitated at 70 rpm using an orbital shaker in the dark at 25^0C. Instead of a separate gas exchange membrane, the aerated medium was fed into a tubular membrane

bioreactor to enhance the extraction of secondary metabolites from *Beta vulgaris* and *Catharanthus roseus* cells using a low-level electric current (Yang et al., 2003). A ceramic membrane tube, made of high purity alumina with hydrophilic property of the surface, was used to separate the cells from the flow of medium in the bioreactor. The membrane bioreactor is suitable for reduced shear on cell walls, improved supply of nutrients and O_2 to the cells, and ease of separation of cell-secreted products since these are retained in the cell compartment. However due to expansion of cell compartment because of osmotic flux and increased biomass (McDonald et al., 2005), low durability of the MWCO membrane might restrict long-term and scaled up cell culture in membrane bioreactor.

2.2 Key Parameters for efficient Bioreactor Systems

A bioreactor system ensures the most optimal environment for growth and development of plant cells. However providing required nutrients and sufficient aeration to the culture without causing damage to the cells present a significant challenge for the design and operation of a well-functioning bioreactor. The key parameters associated with bioreactor design include (i) shear- different systems may generate different amount of shear, which affect applicability of a system for shear sensitive or shear insensitive culture, (ii) gas exchange- ease of transfer of fresh oxygen in sterile condition into the bioreactor and removal of bi-product gases out of the system, and maintaining desired gas composition in bioreactor, (iii) sterility- ease of maintaining the bioreactor sterility throughout the entire culture process makes it a well-functioning system, (iv) exchange of medium- addition of fresh medium conveniently without disturbing sterility to restore

nutrients level in the depleted medium or removal of spent medium improves performance of the bioreactor, (v) synchronization- a better performing bioreactor ensures the synchronized development of embryos. Details of these parameters and their influence on performance of bioreactors have been discussed below.

Shear- Shear stress is caused in both mechanically and pneumatically operated bioreactors due to mechanical agitation and aeration respectively. It plays a vital role in the suspension culture by affecting membrane integrity, cell growth, mitochondrial activity, size of clumps, morphology, release of proteins and phenolic compounds (intracellular metabolites), rate of formation of secondary metabolites, metabolic functions, enzyme levels in the cell, and even cell lysis (Wongsamuth and Doran, 1997; Namdev and Dunlop, 1995; Choi et al., 1995, Sun & Linden, 1999). At a favorable intensity, it affects cell growth and primary metabolism in plant cells by dispersing cell aggregates into suitable sizes, which favors nutrients and gas transfer and increases mitochondrial activity and intracellular protein content (protein expression) (Shi et al. 2003). However, plant cells are in general shear sensitive because they are relatively larger in size and have fragile, rigid wall and extensive vacuoles (Scragg, 1995; Hooker et al., 1990). Even a low shear stress (threshold varies from species to species) causes cell damage if it acts on the cells for a significant amount of time. Cell viability of *Perilla frutescens* reduced with shearing time in the rotating drum bioreactor in an experiment conducted by Zhong et al. (1994) in a low shear environment. They optimized an average shear rate of 20 to 30 s^{-1} caused by a marine impeller that resulted in maximum specific growth rate and yield.

Ballica & Ryu (1993) observed a significant drop in cell-yield at an aeration rate above 1.0 vvm in an internal loop airlift bioreactor of suspension culture of *Datura stramonium*. However the behavior of the culture in presence of stress varies with plant species. The cell growth of *Taxus cuspidata*, cultured in bubble column bioreactor, was seized in the first two to four days because of initial damage of cell membranes; however, by adapting the hydrodynamic shear environment through activating the defense genes (Shi et al., 2003) later on, cells had better growth and viability compared to the culture in shake flask (Zhong and Yuan, 2009). Production of some secondary metabolites, such as phytoalexin, lignin, etc., in a series of metabolic activities under stress environment soothe the injury of plant cells while experiencing hydrodynamic stresses (Shi et al. 2003). Deposition of polysaccharide in the damaged area of the cell wall also facilitates the recovery (reviewed by Sun & Linden, 1999).

The intensity of hydrodynamic shear stress can be measured in terms of shear force index and power input per unit mass; Kolmogoroff eddy length scale would be a measure of cell viability when the turbulent shear prevails in the bioreactor (Chen and Huang, 2000).

Gas exchange- Aeration plays a significant role for cell growth and production of secondary metabolites in bioreactors. For a well-functioning bioreactor, both the gas-liquid and liquid (medium)-solid (cells) mass transfers are important to conduct the respiration (metabolic process) of plant cells (Curtis, 2005). Carbon dioxide (CO_2), ethylene (C_2H_4), ethanol (C_2H_5OH), and acetaldehyde (CH_3CHO) are typically produced

by respiring cultures (Thomas & Murashige, 1979; Perata & Alpi, 1991; Bieniek et al., 1995). Accumulation of these gases in the culture vessel inhibits growth of cultures (Biddington & Robinson, 1991; Jackson et al., 1985). Mostafa & Gu (2003) reported detrimental effect on cell growth and production of glycoprotein in a 1000 l stirred tank bioreactor due to increased level of dissolved CO_2. Schlatmann et al. (1993) observed that the gas composition was one of the reasons that affected the production of ajmalicine in stirred tank bioreactor with forced aeration; excretion of ajmalicine to the medium was much less in a low ventilated system, such as a recirculation bioreactor. In a stirred tank bioreactor equipped with a dual impeller (flat-blade and pitched-blade), Huang et al. (2002) achieved a shake flask-comparable cell growth and L-DOPA production with controlled aeration (0.06 vvm) and agitation (at 300 rpm) of suspension culture of *Stizolobium hassjoo*. Their study showed high oxygen transfer rate played a vital role in higher cell growth and metabolite production. However they hypothesized that excessive aeration (0.1 vvm in their case) striped-off CO_2 and ethylene, considered as essential gaseous metabolites, and reduced the bioreactor performance. This can be manifested in the study on *Taxus chinensis* cell culture which revealed that both cell growth and production of taxuyunnanine C (TC) increased with increase in concentration of ethylene in bubble column bioreactor (Pan et al., 2000). However Burg (1973) observed that ethylene inhibited cell division, and this might suppress embryo elongation (Bieniek et al., 1995).

Somatic embryogenesis of carrot is aided if the medium is saturated with dissolved oxygen (DO) (Jay et al., 1992; Teng et al., 1994). However, Kessell & Carr

(1972) observed that the critical level of DO concentration for growth and embryo differentiation of carrot (*Daucus carota*) tissue in suspension culture was around 16% of saturation value above which carrot somatic embryogenesis was inhibited. The discrepancy may be due to the culture of different cultivars of carrot (Teng et al., 1994). Hvoslef-Eide et al. (2005) reviewed that Preil et al. (1988) and Preil (1991) showed the depletion of excess CO_2 from the recirculating aeration system (silicone tube) helped to have improved growth of poinsettia cell cultures in bioreactors. In Applikon bioreactors for suspension culture of *Cyclamen persicum* Mill., Hohe et al. (1999) observed almost similar amount of CO_2 accumulation in the headspace (i.e. gas phase) and equal cell growth in bubble aeration system with headspace atmosphere in contact with outside environment through filter, and bubble free aeration system with recirculation of gas. As a control, in the Erlenmeyer flask they observed better gas exchange through the aluminum cap with eight times lesser CO_2 accumulation in the headspace, while having about four times cell growth compared to bioreactors. The cell growth increased with sweeping out CO_2 from the gas phase of bioreactor; on the other hand, more embryos developed in the bioreactor which accumulated CO_2. This was because of almost entirely presence of proembryogenic masses (PEMs) compared to that without CO_2 accumulation. In the latter case, large vacuolated cells were present along with PEMs.

Sterility- Plant cell culture can easily be contaminated by microbes since sucrose is a major ingredient of the culture media. So it has always been a logical concern to maintain sterilized environment inside the bioreactors during culture process which usually takes a long period of time (sometimes a few months). Especially liquid culture is more

vulnerable to contamination than solid culture. Contamination of cell culture is not only associated with cost but also substantial losses of labor and time.

***Exchange of medium*-** Ease of refreshing or changing the culture medium in the bioreactor, while maintaining the system sterility, is another requirement of a well-functioning bioreactor. In somatic embryogenesis, the developmental pathway of Norway spruce follows the sequential steps of initiation, proliferation, embryo differentiation, embryo maturation, desiccation, germination, and plant development (von Arnold et al., 2005). Each of these culture steps requires proper chemical treatment with step-specific medium. So exchange of medium is absolutely necessary for the continuation of culture process. The less complicated the exchange process is, the higher the probability of maintaining the system sterility.

***Synchronization*-** Synchronization of somatic embryo development is considered as one of the most crucial issues for large-scale clonal propagation (Barry-Etienne et al., 2002) and still remains a bottleneck of implementing somatic embryogenesis in industrial scale (Molle and Freyssinet, 1992). Asynchronized development along with abnormal morphology of somatic embryos, followed by maturation and germination, results in lower conversion to plants (Barry-Etienne et al., 2002). By synchronization, we here refer to simultaneous growth and development of somatic embryos while cultured in liquid and/or solid medium. Fully developed, polarized somatic embryos in the embryo differentiation phase can respond to maturation treatment and form mature somatic embryos (Sun, 2010). It may be assumed that the cells in a cluster of PEMs receive

different levels of nutrients due to their location within the cluster and this affects the growth of somatic embryos resulting in non-synchronous development. Low yield of plants from somatic embryos due to asynchronous development has hampered the practical implementations of somatic embryogenesis for large-scale clonal propagation of plants and agricultural goods. Bioreactors with the facility of disintegrating clusters to ensure nutrients at every location may be a good choice of achieving synchronous growth of somatic embryos.

2.3 Design of a Well-functioning Temporary Immersion Bioreactor System

After identifying key parameters of a well-functioning bioreactor based on the study of available bioreactor technologies, a temporary immersion bioreactor (Figure 2.9), has been designed in house for regeneration of somatic embryos through proliferation of embryogenic masses, embryo differentiation, and maturation of somatic embryos (von Arnold et al., 2005). The internal volume of the bioreactor is about 1L. A 0.2 µm air filter (PTFE Acro 50, VWR International) is connected to the lid of the bioreactor to avoid any contamination of cells as the air gets into the bioreactor from outside when it starts emptying. A polyamide screen of pore size of 150 µm is stretched and squeezed by a screen holder and placed inside the bioreactor. The purpose of the screen is to hold cells and tissues, and facilitate soaking intermittently, and draining liquid medium out of the bioreactor. This size is sufficiently small to hold cells and tissues and large enough to allow liquid medium pass through it. The bottom part of the bioreactor is connected with a silicone tube (Tygon; 7.9 mm I.D. and 11.1 mm O.D.). The other end of the tube is inserted into a bottle containing liquid culture medium. A 3-way

solenoid valve (110VAC; Conair) and an air pump are used to operate the system, and are controlled by an electronic timer.

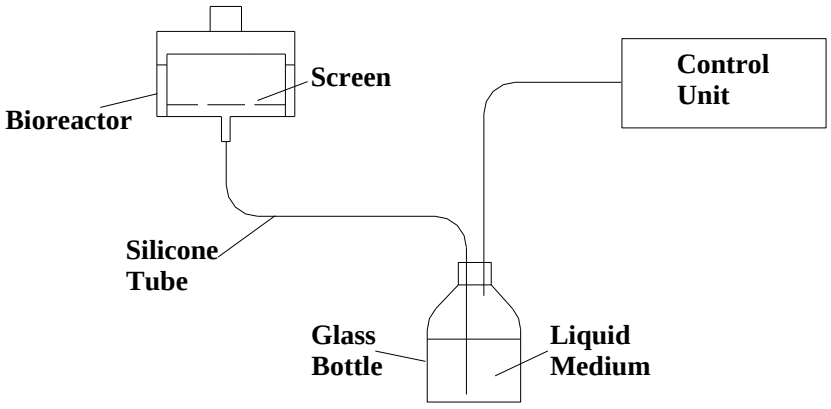

Figure 2.9 A temporary immersion bioreactor in an experimental setup. The air is pumped by an air pump to the glass bottle to push the culture medium to the bioreactor. When tissues on the screen are soaked with the medium, the air vents from the bottle to the atmosphere through a solenoid valve and let the medium gets back to the bottle due to gravity. The control unit consists of an air pump, a solenoid valve, and a timer.

2.4 Dispersion System

To provide more equal growth conditions to all somatic embryos and thus aid in growth and development of embryos, a dispersion system has been automated to apply a mechanical stress on proembryogenic masses by a glass disperser (Aidun and Egertsdotter, 2011/043731). The dispersion system is set up as shown in Figure 2.10 using the disperser with one end connected to a 1000 ml flask with an autoclavable silicone tube (L/S® 17). A peristaltic pump (Masterflex® L/S® Digital Drive, 115/230 VAC with Masterflex® L/S® Easy-Load® II pump head for high-performance precision tubing, fixed occlusion, SS rotor) is used to aspirate and dispense tissues through the disperser. The pump is connected to a flask through two solenoid valves and an air filter of 0.2 µm pore size (PTFE Acro 50, VWR International). During dispersion, the pump is run at a flow rate of 2500 ml/min.

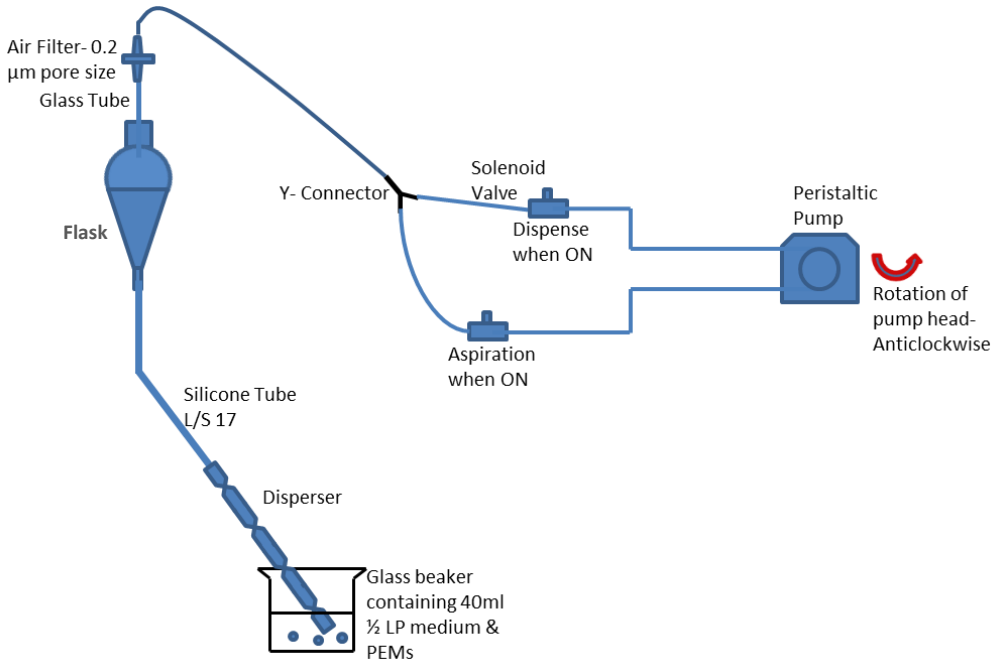

Figure 2.10 A Dispersion system is used to disperse clusters of PEMs before starting proliferation culture. Two solenoid valves, controlled by a timer, are used in the system, one for aspirating cells and tissues along with ½ LP liquid medium from a beaker through a disperser to a flask, and the other for dispensing tissues from the flask to the beaker. The solenoid valves are opened alternatively so that aspiration (8s) and dispense (6s) take place sequentially.

CHAPTER 3

EFFECT OF DISPERSION ON SOMATIC EMBRYOGNENESIS OF NORWAY SPRUCE (*Picea abies*)

To gain insight into the role of dispersion on proembryonic masses (PEMs) for synchronized development and yield of mature embryos, clusters of immature embryos have been dispersed by using a dispersion system and redistributed on the screen of a newly designed temporary immersion bioreactor to a more uniform spatial distribution. Non-dispersed PEMs are cultured in the bioreactors as controls. Effect of dispersion on embryo maturation is also studied on solid medium and discussed in this chapter.

3.1 Culture in Liquid Medium

3.1.1 Materials

3.1.1.1 Somatic embryogenic cell-lines

Two embryogenic cell lines, 11:12:02 and 11:12:04 of Norway spruce, originating from controlled crosses in the Swedish Norway spruce breeding program, were used in this study. The cell lines were maintained through proliferation/ multiplication of PEMs in the dark by subculturing every second week on solid half strength LP (½ LP) medium supplemented with 2,4-D (2,4-dichlorophenoxyacetic acid) and BAP (6-benzylaminopurine) in 9 cm petri plates. For maturation, PEMs were transferred to pre-maturation medium (DKM without growth regulators) for seven days before transferring to DKM maturation medium containing ABA (abscisic acid). During maturation for eight

weeks cells and tissues were subcultured biweekly with fresh DKM maturation medium. Details of nutrient media are provided in von Arnold and Clapham (2008).

3.1.2 Methods

3.1.2.1 Dispersion System

A dispersion system described in the previous chapter (Art. 2.4) was used to disperse the aggregates of PEMs. Before using for dispersion the parts starting from filter to disperser (Figure 2.10) were autoclaved for 40 minutes at a temperature of 121^0C and a pressure of 1.1 bar. The filter was autoclaved separately in a dry cycle and the other parts were autoclaved in a wet cycle. After autoclaving they were assembled together in a sterile hood. For each bioreactor, 2 g of PEMs aggregates was dispersed in 50 ml ½ LP liquid medium contained in a 200 ml glass beaker by passing them through the disperser (the strain rate was in the order of $10^3 s^{-1}$).

3.1.2.2 Culture of dispersed and non-dispersed PEMs in temporary immersion bioreactors

Twelve bioreactors of cell lines 11:12:02 and 11:12:04 were set up by spreading out the dispersed PEMs on bioreactor screens. As controls, same amount of non-dispersed aggregates of PEMs were transferred from solidified proliferation medium in petri plates to each of six replicate bioreactors of each cell line by forceps.

Temporary immersion bioreactor (Figure 2.9) was used for regeneration of somatic embryos through proliferation of embryogenic masses (both dispersed and non-dispersed), embryo differentiation, and maturation of somatic embryos. Each glass bottle

of a bioreactor system contained 500 ml of ½ LP liquid proliferation medium. The liquid medium immersed the tissues for a period of 1 minute in every 12 h. After 12 - 14 days, proliferation medium was replaced by pre-maturation medium, and the bioreactors were operated at the same immersion frequency for 7 days. Then the embryos were cultured in maturation medium for 8 weeks in the bioreactors to complete their development at the same immersion frequency. The used medium was replaced with the fresh medium in every 2 weeks.

3.1.2.3 Dispersion on somatic embryo development

To study the effect of dispersion on embryo maturation, the PEMs were multiplied in proliferation medium for one subculturing cycle, and then taken through pre-maturation and maturation as described above. After eight weeks of maturation, embryos were harvested from three different locations of the culture in each dispersed bioreactor; the total number of somatic embryos in a bioreactor and the number of mature embryos per unit fresh weight (FW) at the start of proliferation treatment were determined. Depending on the number of embryos matured in a control bioreactor, either all embryos or a portion of mature embryos at three different locations in each bioreactor was collected. The length of each harvested embryo was measured using image analysis.

One may describe the developmental stage of an embryo in terms of level of development parameter, q_i, where in this study we assume that q_i represents the length of an embryo. To evaluate the level of synchronization of embryo growth and development,

we assume that if the average length of somatic embryos with a length interval, δ, is defined as

$$\bar{q} \equiv \frac{\sum_{i=1}^{n} q_i}{n} \quad (3.1)$$

then

$$Q \equiv \int_0^{\infty} D(\bar{q}) d\bar{q} \quad (3.2)$$

where, $D(\bar{q})$ is the sum of lengths of all embryos in the length interval, δ.

The normalized distribution function is defined as $\varphi(\bar{q}) \equiv \frac{D(\bar{q})}{Q}$, when

$$\int_0^{\infty} \varphi(\bar{q}) d\bar{q} = 1 \quad (3.3)$$

As a measure of synchronization, full widths at 50% (also known as full width at half maximum (FWHM)), 66%, and 75% of maximum of the function $\varphi(\bar{q})$ are used.

3.1.2.4 Image analysis of mature embryos

Images of dispersed PEMs, cultures in the bioreactors at the end of maturation, and mature embryos after harvest were acquired by a DSLR camera (Nikon D5100). In each cell line, three samples of dispersed PEMs submerged in the liquid medium were collected, poured into petri plates, and photographed for estimating their size distributions. Each sample contained 651 ± 155 dispersed PEMs. The area occupied by each piece of dispersed PEMs was obtained from image analysis using ImageJ 1.48v (National Institute of Health, Bethesda, MD, USA) and considered as its dimension. The mean and standard deviation of the sizes of dispersed aggregates in a cell line were estimated from three replicates.

At the end of the maturation treatment dispersed bioreactors were opened under sterile conditions and the cultures were photographed before and after harvesting of mature embryos. Two images of each bioreactor culture were analyzed in ImageJ to estimate the area occupied by harvested mature embryos. In each bioreactor, an average of 18% area of dispersed PEMs was occupied by 173 and 145 harvested embryos of cell lines 11:12:02 and 11:12:04 respectively. Since the embryos developed homogeneously all over the dispersed PEMs, the number of embryos per g FW of PEMs in dispersed bioreactor was estimated from the number of harvested embryos and the area occupied by them.

The images of 1037 and 1176 mature embryos at harvest from dispersed and non-dispersed PEMs respectively of cell line 11:12:02 and 727 and 573 mature embryos from dispersed and non-dispersed PEMs respectively of cell line 11:12:04 were acquired by a DSLR camera (Nikon D5100). These embryos were collected from twenty two bioreactors. After acquisition of images, they were transferred to a computer. Except the regions of interest in each image, the rest was trimmed using GIMP 2.8.10. Then the final image was converted into a binary image using ImageJ 1.48v. For each embryo, the length of major axis of the ellipse drawn around the embryo was acquired in ImageJ. The axis length was considered as the length of an embryo. The number of embryos was then obtained in each of embryo length intervals of 0.0 – 1.0 mm, 1.0 – 2.0 mm, 2.0 – 3.0 mm, 3.0 – 4.0 mm, and 4.0 – 5.0 mm, giving δ as 1mm.

3.1.2.5 Statistical analysis

Data were available from the experiment of dispersion on maturation of somatic embryos in liquid medium for dispersed and non-dispersed PEMs. Variables derived from the experiments included (a) number of mature embryos per gram FW of PEMs, (b) number of mature embryos per bioreactor, (c) average length of embryos, (d) widths of the curve of $\varphi(\bar{q})$ at 50%, 66%, and 75% of maximum, (e) coefficient of variation (CV) of lengths of embryos, and (f) confidence interval of coefficient of variation. The number and length of embryos, and width of the curve, $\varphi(\bar{q})$, were normally distributed. Descriptive statistics including means and standard deviations are reported herein. Differences between dispersed and control cultures in terms of average lengths of somatic embryos, number of embryos per gram FW of PEMs, number of embryos in a bioreactor, and width of the curve, $\varphi(\bar{q})$, were assessed by independent two sample *t*-test. When sample sizes are either equal or different and variances of two populations are assumed unequal, then the *t* statistic for testing population means is calculated as,

$$t = \frac{\widehat{\mu_1} - \widehat{\mu_2}}{SE_{\widehat{\mu_1} - \widehat{\mu_2}}} \tag{3.4}$$

where

$$SE_{\widehat{\mu_1} - \widehat{\mu_2}} = \sqrt{\frac{s_1^2}{m_1} + \frac{s_2^2}{m_2}} \tag{3.5}$$

s_k^2, m_k, and $\widehat{\mu_k}$ are the variance, the sample size (with $k = 1, 2$), and estimated mean of *k*-th population respectively. The level of synchronization of embryos from dispersed and non-dispersed PEMs was examined by the coefficient of variation. The coefficient of variation (CV), defined as the ratio of standard deviation to the mean, is a useful measure of variation from the mean within a data set (Daniel and Cross, 2013). Coefficient of

variation of lengths of embryos from dispersed and non-dispersed cultures allowed the hypothesis testing of whether lengths of embryos from non-dispersed PEMs were more widely distributed compared to that obtained from dispersed PEMs. Therefore it was an effective measure of synchronization of embryo development as it determined whether the data (here the length of embryos) was more spread out from the mean. The 90% confidence interval of CVs was computed by the McKay method (Vangel, 1996) as below.

$$\kappa = \left\{ \begin{array}{l} CV\left[\left(\frac{\chi^2_{df,1-\alpha_s/2}}{df+1}-1\right)CV^2+\frac{\chi^2_{df,1-\alpha_s/2}}{df}\right]^{-1/2}, \\ \quad CV\left[\left(\frac{\chi^2_{df,\alpha_s/2}}{df+1}-1\right)CV^2+\frac{\chi^2_{df,\alpha_s/2}}{df}\right]^{-1/2} \end{array} \right\} \qquad (3.6)$$

where, κ, CV, α_s, df, and χ^2 represent a $[100 * (1-\alpha_s)\%]$ confidence interval of CV, the coefficient of variation, level of significance, degree of freedom, and chi-square value (obtained from a statistics software, R, version 3.1.2 (The R Foundation for Statistical Computing)) respectively.

3.1.2.6 Germination of mature somatic embryos

Mature somatic embryos were harvested from bioreactors and desiccated for 3 weeks. Embryos were then placed on solid AD-1 germination medium for 1 week in darkness, 2 weeks under red light, and 3 weeks under white light. AD-1 germination medium had the following composition per liter. Macroelements: KNO_3 764 mg, NH_4NO_3 173 mg, KH_2PO_4 381 mg, $MgSO_4.7H_2O$ 533 mg, $CaCl_2.2H_2O$ 83 mg. Iron and

microelements were as for DKM medium. Organic compounds: sucrose 30 g, casein hydrolysate 0.5 g, thiamine 1 mg, inositol 50 mg.

3.1.3 Results and discussion

3.1.3.1 Size distributions of dispersed aggregates of PEMs and effect of dispersion on proliferation

The size distributions of dispersed PEMs of *Picea abies* in Figure 3.1 showed that an average of 80% of dispersed PEMs was equal to or less than 0.2 mm^2. This ensured to more PEMs, when they were dispersed, having access to surrounding gases inside the bioreactor and nutrients from the culture medium compared to the tissues inside the non-dispersed PEMs.

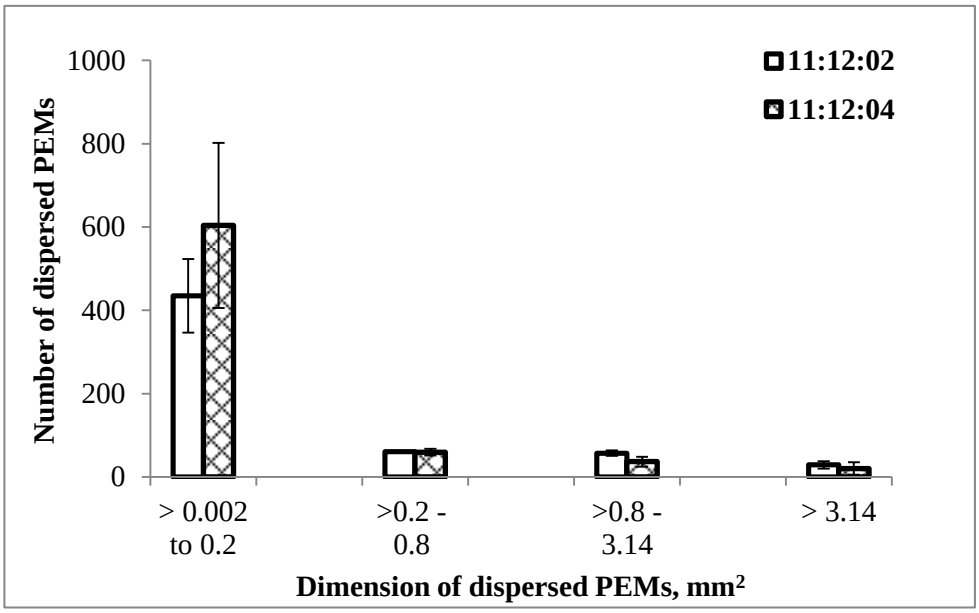

Figure 3.1 Size distribution of dispersed aggregates of PEMs of cell lines 11:12:02 and 11:12:04 of *Picea abies*. The clusters of PEMs in ½ LP liquid medium passed through the dispersion system several times (until all the dispersed pieces could pass the disperser without blocking) and then pictured. The pictures were analyzed using ImageJ to estimate the size distributions of dispersed PEMs. The error bars show standard deviations of three replicates of each cell line.

Dispersion and redistribution of immature embryos at early stages of development had a positive influence on proliferation of cells. Osuga and Komamine (1994), and Suehara et al. (1998) showed that large clusters of carrot cells were not suitable for *in vitro* propagation. After dispersion of aggregates, proliferation increased in all embryogenic cell lines of Norway spruce tested to date (data not shown). However the growth rate of PEMs in general varies between cell lines. From Figure 3.2, it is obvious that the proliferation rate was much higher in bioreactors that contained dispersed PEMs

compared to non-dispersed PEMs in control bioreactors. The initial weights of dispersed (Figure 3.2 (a)) and non-dispersed (Figure 3.2(b)) PEMs were 2.15 g and 2.19 g respectively. The final weights after 2 weeks of proliferation were not obtained to avoid cell damage while transferring PEMs in and out of a bioreactor for weighing and the possibility of contamination. However weights at the end of maturation treatment of two cell lines were obtained in a separate experiment; the average growth of dispersed PEMs were observed as 5.54x (11:12:02) and 9.25x (11:12:04) and that of non-dispersed PEMs were 2.05x (11:12:02) and 2.14x (11:12:04) of initial weights. Out of twenty four bioreactors used in this test, twelve were used for dispersed (three were contaminated) and twelve were used for non-dispersed PEMs culture (one was contaminated).

(a)  (b) 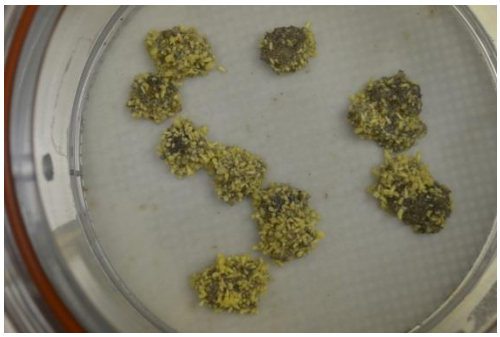

Figure 3.2 (a) Dispersed PEMs of cell line 11:12:04 of *Picea abies* with initial fresh weight (before proliferation) of 2.15 g. (b) Clusters of PEMs of cell line 11:12:04 of *Picea abies* with initial fresh weight of 2.19 g. The pictures show that the proliferation rate in (a) was much higher than that in (b).

3.1.3.2 Effect of dispersion on development of mature embryos

Enhanced development of somatic embryos was observed from PEMs of both cell lines dispersed at the beginning of proliferation (Figure 3.3 (a, b)). The number of mature embryos per gram FW of PEMs of cell line 11:12:02 increased from 128 in non-dispersed PEMs to 545 in dispersed PEMs (Table 3.1). The number of mature somatic embryos was 4.25 times more in dispersed PEMs compared to that in non-dispersed and this difference was statistically significant in independent two-sample *t*-test with *p*-value < 0.01. In cell line 11:12:04, the number of mature embryos per gram FW of PEMs was 123 and 388 in non-dispersed and dispersed PEMs respectively; the difference was also statistically significant with *p*-value < 0.01. Because of a large number of embryos matured in dispersed compared to non-dispersed bioreactors, only a portion of embryos, i.e., 15% (11:12:02) and 18% (11:12:04), was harvested from each bioreactor; these values were much smaller compared to non-dispersed bioreactors from which 75% and 59% of total embryos were harvested from each bioreactor of cell line 11:12:02 and 11:12:04 respectively. It may be inferred from these observations that dispersion resulted in more PEMs coming into direct contact with nutrients and gases than was the case for the PEMs of non-dispersed aggregates.

Dispersion introduces a substantial strain to the aggregates of PEMs. However it did not show an unfavorable impact on proliferation of PEMs and maturation of somatic embryos. In cell line 11:12:04, the average embryo lengths were 2.77 and 2.73 mm in dispersed and non-dispersed PEMs respectively (Table 3.2). By following independent two-sample *t*-test, it was shown that the difference was statistically insignificant with *p*

value = 0.49. After following similar statistical analysis for cell line 11:12:02, it was found that the difference between the average lengths of mature embryos in dispersed (3.05 mm) and non-dispersed (2.92 mm) PEMs was statistically significant with *p*-value < 0.01; the length of somatic embryos from dispersed PEMs was larger than that from non-dispersed PEMs. Therefore dispersion did not hamper the development and maturation of embryos of this cell line.

(a)

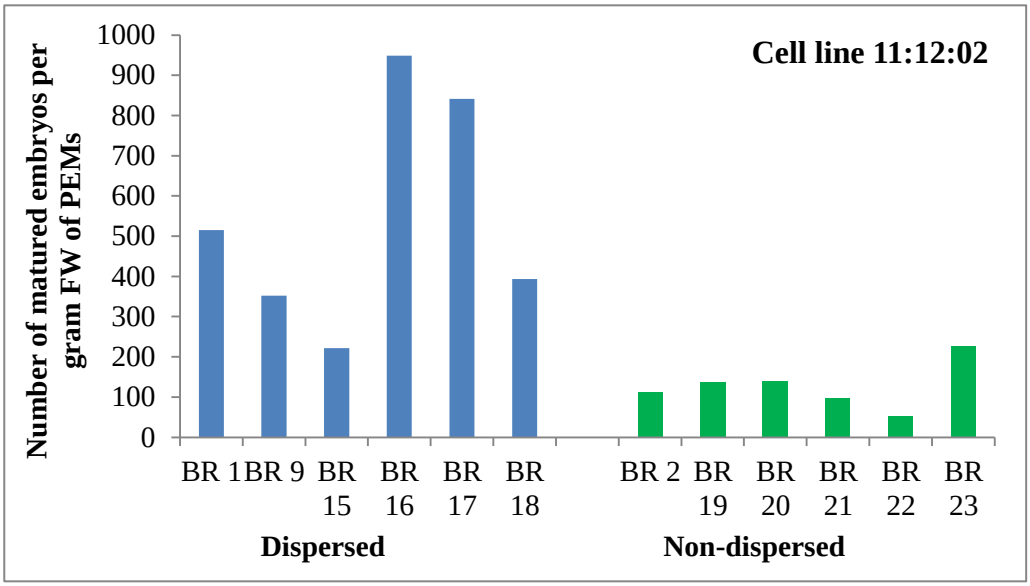

(b)

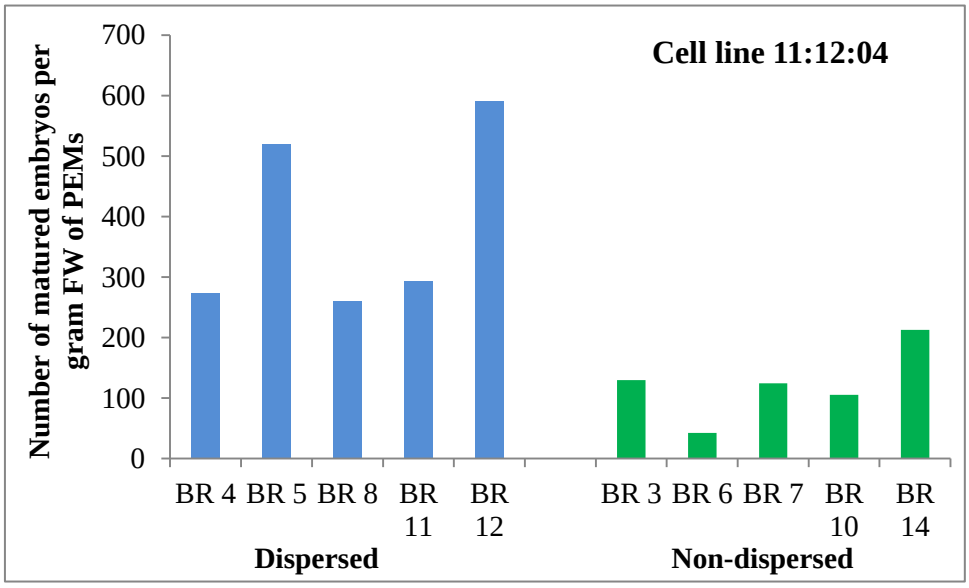

Figure 3.3 Bar graphs showing the number of mature embryos developed per gram of FW in different bioreactors containing dispersed PEMs and PEMs clusters of two cell lines of *Picea abies*; (a) 11:12:02, (b) 11:12:04.

Table 3.1 Yield of mature somatic embryos from dispersed and non-dispersed PEMs of two cell lines of Norway spruce cultured in temporary immersion bioreactors. Both cell lines had six replicates for each culture condition. Tissues in one of the bioreactors cultured cell line 11:12:04 were brownish and embryos did not mature, and another bioreactor of the same cell line was contaminated. Differences between the number of mature embryos from dispersed and non-dispersed PEMs were in each case statistically significant by the independent two-sample *t*-test at 90% confidence level (*p*-values were less than 0.01)

Cell line	Culture condition	Number of mature embryos (Mean ± SD) per g FW of PEMs	Number of mature embryos (Mean ± SD) per bioreactor
11:12:02	Dispersed PEMs	545.37 ± 288.75	1129 ± 594
	Non-dispersed PEMs	128.01 ± 58.0	261 ± 122
11:12:04	Dispersed PEMs	387.8 ± 155.85	828 ± 332
	Non-dispersed PEMs	122.82 ± 61.08	196 ± 89

Table 3.2 Lengths of mature somatic embryos of *Picea abies* developed from dispersed and non-dispersed PEMs in the bioreactors. Lengths were measured by an image analysis software, ImageJ

Cell line	Culture condition	Length of embryos (mm), (Mean ± SD)	Coefficient of variation (CV)
11:12:02	Dispersed	3.05 ± 0.74	0.24
	Non-dispersed	2.92 ± 0.77	0.27
11:12:04	Dispersed	2.77 ± 0.87	0.31
	Non-dispersed	2.73 ± 0.84	0.31

Dispersion of tissues followed by several subcultures in the bioreactors for proliferation, embryo differentiation, and embryo maturation yielded synchronized embryos of cell line 11:12:02 (Figure 3.4). By performing independent two-sample *t*-test, the difference between full width at half maximum (FWHM) of six bioreactors contained dispersed PEMs (1.47 mm) and six bioreactors cultured non-dispersed PEMs (1.65 mm) (Figure 3.5) was statistically significant (*p*-value = 0.05). Similarly differences in widths of $\varphi(\bar{q})$ at 66% (p = 0.05) and 75% (p = 0.07) of maximum were also statistically significant. At 66% of maximum of the normalized distribution function, widths were 1.08 and 1.25 mm for dispersed and non-dispersed PEMs respectively and at 75% of maximum of $\varphi(\bar{q})$, the corresponding widths were 0.88 and 1.03 mm. Therefore the shorter widths of the function $\varphi(\bar{q})$ at three different locations in dispersed PEMs of cell line 11:12:02 represented synchronized development of somatic embryos due to dispersion. However, the full width at 50% (p = 0.16), 66% (p = 0.27), and 75% (p = 0.34) of maximum of the function $\varphi(\bar{q})$ for dispersed PEMs are larger than the corresponding widths of non-dispersed PEMs of cell line 11:12:04 (Figure 3.5). Hence dispersion did not improve the level of synchronization of somatic embryo development from dispersed PEMs of cell line 11:12:04 of *Picea abies*.

For cell line 11:12:02, the coefficient of variation in case of dispersed PEMs was smaller with 90% confidence interval of (0.23, 0.25), using the McKay method, compared to that in clusters (90% confidence interval was (0.26, 0.28)) (Table 3.2). Hence dispersion helped to develop synchronized embryos for this cell line. However for

cell line 11:12:04, the coefficients were equal; therefore, dispersion did not improve synchronized growth of embryos.

3.1.3.3 Germination of embryos

Of the harvested mature somatic embryos from dispersed PEMs, 74% (11:12:02) and 50% (11:12:04) were germinated with having roots of 1 cm or longer, and 67% (11:12:02) and 61% (11:12:04) of the somatic embryos from non-dispersed PEMs were converted to germinants with roots of 1 cm or longer (Table 3.3). Therefore, more somatic embryos from dispersed PEMs of cell line 11:12:02 were germinated, but this was not the case for cell line 11:12:04.

Table 3.3 Number of mature embryos from dispersed and non-dispersed PEMs of two cell lines cultured in the germination medium, number of germinants, and germinants having roots of 1 cm or longer

Cell line	11:12:02		11:12:04	
	Dispersed PEMs	Non-dispersed PEMs	Dispersed PEMs	Non-dispersed PEMs
Number of somatic embryos cultured in germination medium	1006	994	605	608
Number of germinants	865	922	340	465
Number of germinants having roots of 1 cm or longer	748	670	303	373
Projected number of germinants (based on embryos harvested and germinated)	5766	1229	1888	788

(a)

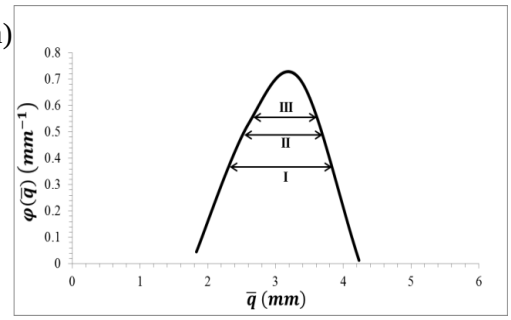
III
II
I
$\varphi(\bar{q})\ (mm^{-1})$
$\bar{q}\ (mm)$

(b)

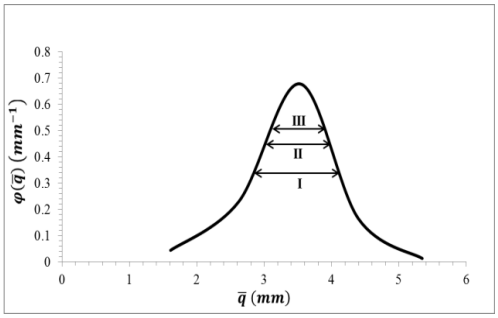
III
II
I
$\varphi(\bar{q})\ (mm^{-1})$
$\bar{q}\ (mm)$

(c)

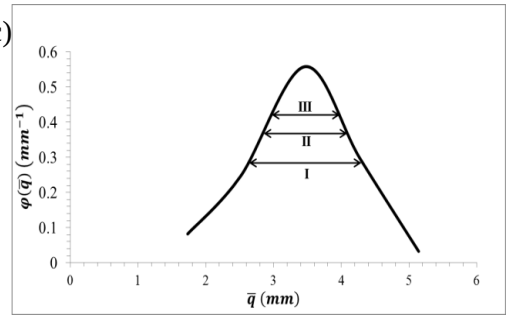
III
II
I
$\varphi(\bar{q})\ (mm^{-1})$
$\bar{q}\ (mm)$

(d)

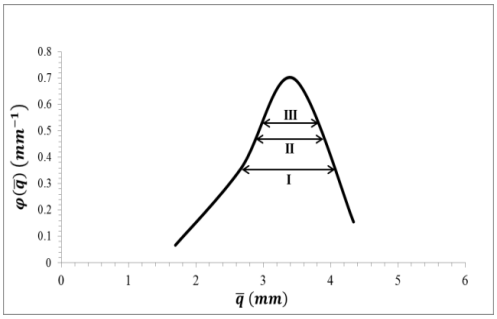
III
II
I
$\varphi(\bar{q})\ (mm^{-1})$
$\bar{q}\ (mm)$

(e)

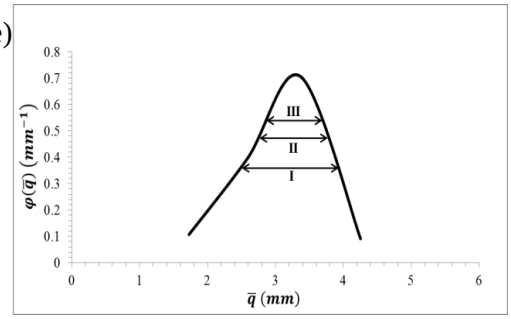
III
II
I
$\varphi(\bar{q})\ (mm^{-1})$
$\bar{q}\ (mm)$

(f)

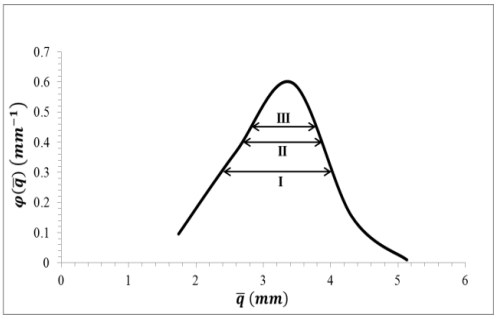
III
II
I
$\varphi(\bar{q})\ (mm^{-1})$
$\bar{q}\ (mm)$

(g)

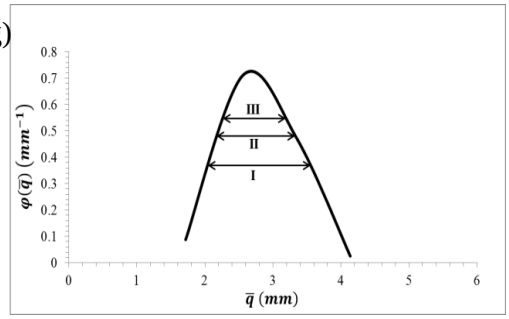
III
II
I
$\varphi(\bar{q})\ (mm^{-1})$
$\bar{q}\ (mm)$

(h)

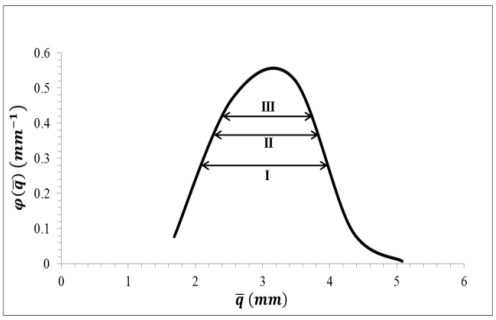
III
II
I
$\varphi(\bar{q})\ (mm^{-1})$
$\bar{q}\ (mm)$

(i)

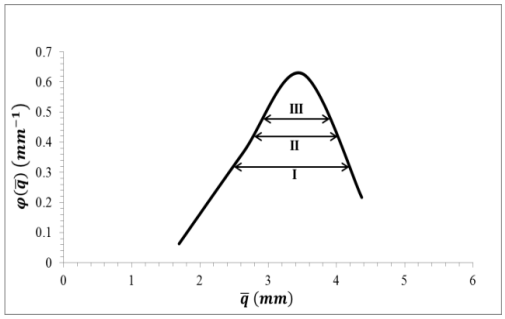
III
II
I
$\varphi(\bar{q})\ (mm^{-1})$
$\bar{q}\ (mm)$

(j)

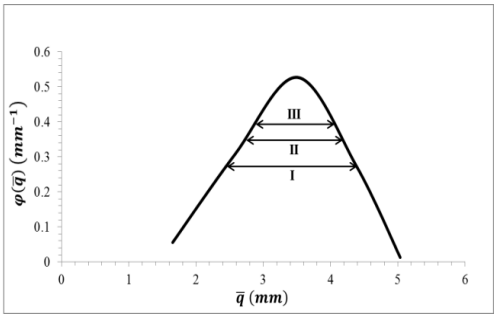
III
II
I
$\varphi(\bar{q})\ (mm^{-1})$
$\bar{q}\ (mm)$

(k)

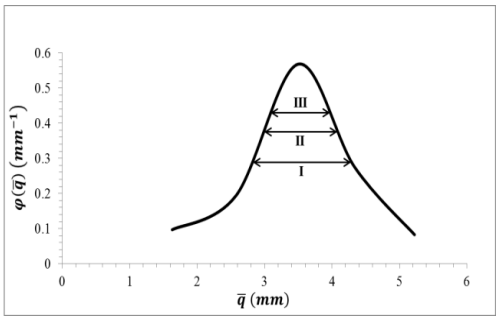
III
II
I
$\varphi(\bar{q})\ (mm^{-1})$
$\bar{q}\ (mm)$

(l)

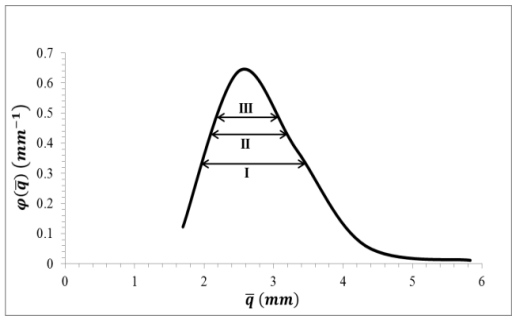
III
II
I
$\varphi(\bar{q})\ (mm^{-1})$
$\bar{q}\ (mm)$

(m)

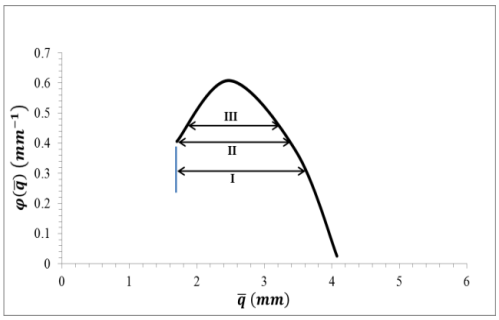
III
II
I
$\varphi(\bar{q})\ (mm^{-1})$
$\bar{q}\ (mm)$

(n)

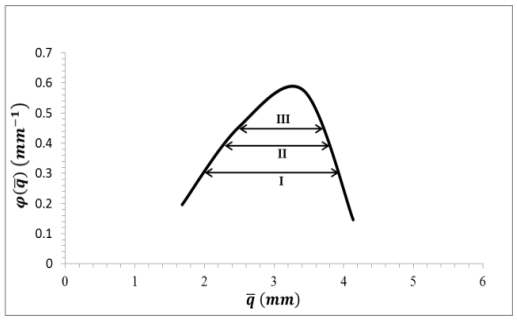
III
II
I
$\varphi(\bar{q})\ (mm^{-1})$
$\bar{q}\ (mm)$

(o)

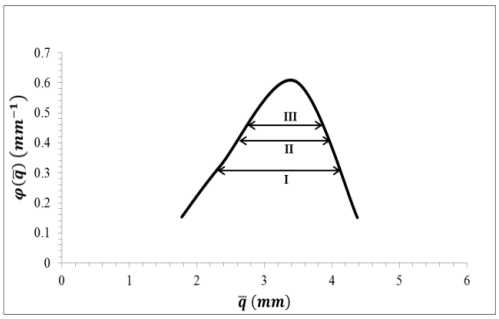
III
II
I
$\varphi(\bar{q})\ (mm^{-1})$
$\bar{q}\ (mm)$

(p)

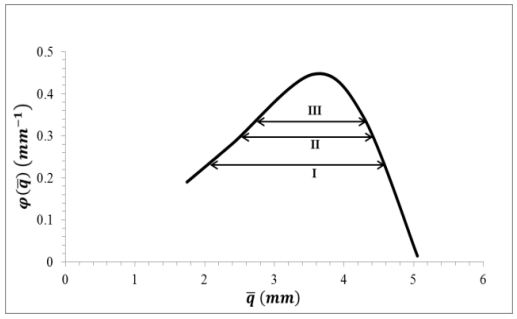
III
II
I
$\varphi(\bar{q})\ (mm^{-1})$
$\bar{q}\ (mm)$

(q)

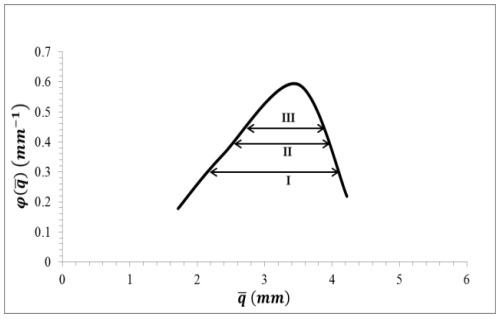
III
II
I
$\varphi(\bar{q})\ (mm^{-1})$
$\bar{q}\ (mm)$

(r)

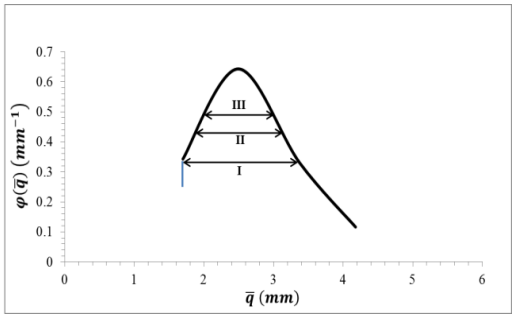
III
II
I
$\varphi(\bar{q})\ (mm^{-1})$
$\bar{q}\ (mm)$

(s)

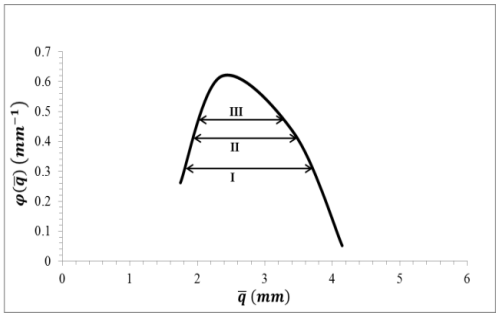
III
II
I
$\varphi(\bar{q})\ (mm^{-1})$
$\bar{q}\ (mm)$

(t)

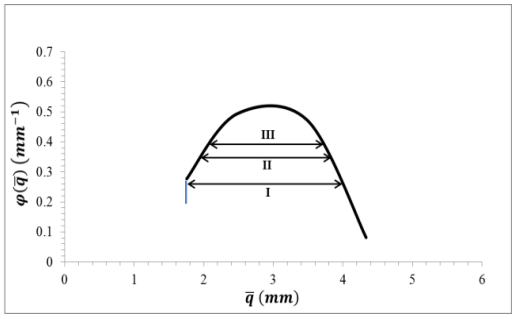
III
II
I
$\varphi(\bar{q})\ (mm^{-1})$
$\bar{q}\ (mm)$

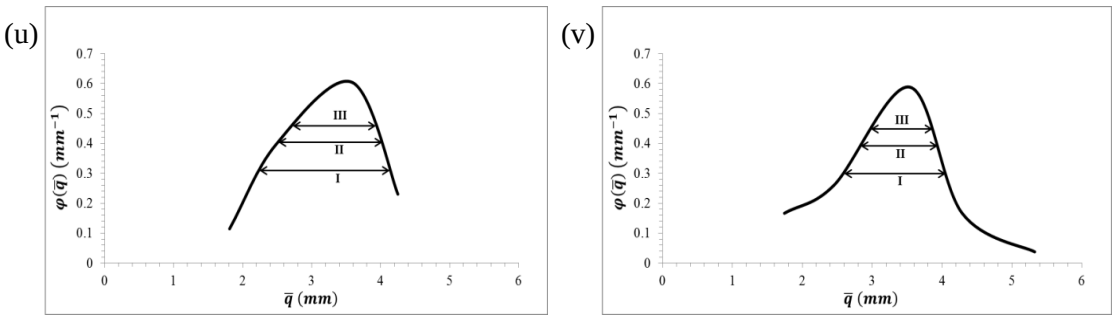

Figure 3.4 Level of synchronized development of somatic embryos of Norway spruce of cell lines 11:12:02 (a – l) and 11:12:04 (m – v). These plots are for different dispersed and control bioreactors. Plots (a – f and m – q) represent the distribution function, $\varphi(\overline{q})$, with respect to the average length in 1 mm interval of mature somatic embryos formed from dispersed PEMs. Similarly plots (g – l and r – v) represent that of in controls. I, II, and III represent full width at half (50%), 66%, and 75% of maximum of the function $\varphi(\overline{q})$ respectively. Their pertaining values are (a) 1.5, 1.15, & 0.92 mm; (b) 1.25, 0.95, & 0.78 mm; (c) 1.65, 1.23, & 1.0 mm; and (d) 1.4, 1.0, & 0.83 mm; (e) 1.42, 1.0, 0.82 mm; (f) 1.6, 1.17, & 0.95 mm; (g) 1.5, 1.15, & 0.92 mm; (h) 1.85, 1.55, & 1.33 mm; (i) 1.68, 1.24, & 0.97 mm; (j) 1.93, 1.43, & 1.17 mm; (k) 1.45, 1.08, & 0.88 mm; (l) 1.5, 1.1, & 0.88 mm; (m) 1.88, 1.65, & 1.35 mm; (n) 1.9, 1.5, & 1.2 mm; (o) 1.8, 1.3, & 1.05 mm; (p) 2.5, 1.85, & 1.55 mm; (q) 1.9, 1.4, & 1.15 mm; (r) 1.65, 1.25, & 1.0 mm; (s) 1.87, 1.5, & 1.25 mm; (t) 2.2, 1.85, & 1.64 mm; (u) 1.88, 1.5, &1.2 mm; (v) 1.45, 1.07, & 0.86 mm.

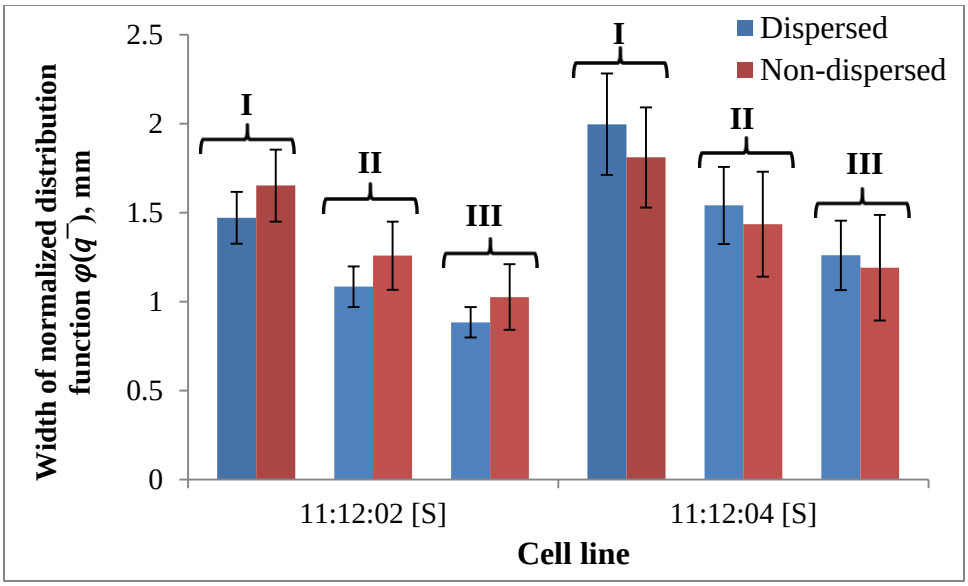

Figure 3.5 The average values and standard deviations of widths at 50% (FWHM) (I), 66% (II), and 75% (III) of maximum of the normalized distribution function, $\varphi(\bar{q})$, for mature embryos from dispersed and non-dispersed PEMs of different cell lines. The widths are shorter in dispersed PEMs than in non-dispersed PEMs of cell line 11:12:02, meaning a more synchronized development of mature embryos after dispersion of this cell line. However for cell line 11:12:04, widths of the function $\varphi(\bar{q})$ are shorter in non-dispersed PEMs. Differences between widths of $\varphi(\bar{q})$ for dispersed and non-dispersed PEMs are statistically significant by independent two sample *t*-test for cell lines followed by [S] in abscissa.

3.2 Culture on Solid Medium

3.2.1 Materials

3.2.1.1 Plant materials

Four embryogenic cell lines, 11:12:02, 11:12:04, 09:73:06, and 09:77:03 of Norway spruce, maintained through proliferation of PEMs in the dark by subculturing every second week on solid half strength LP (½ LP) medium supplemented with 2,4-D and BAP, were used in this study. For maturation, PEMs were transferred to solidified pre-maturation medium which was DKM (solidified using phytagel) without a growth

regulator. PEMs were cultured for seven days on this medium and then transferred to solidified DKM maturation medium containing ABA (abscisic acid). After every two weeks during eight weeks of culture, PEMs were moved to fresh solidified DKM maturation medium.

3.2.2 Methods

The dispersion system, dispersion on somatic embryo maturation, image analysis, statistical analysis, and germination of mature embryos followed the similar methods as explained above in "3.1 Culture in Liquid Medium" with a few exceptions. So to avoid repetitions only the exceptions in the methods are explained here.

3.2.2.1 Dispersion of PEMs aggregates, and culture of aggregates and dispersed PEMs

Half a gram of PEMs aggregates were dispersed in 40 ml ½ LP liquid medium using the dispersion system and procedure as described above. Three replicates each of cell lines 11:12:02, 11:12:04, 09:73:06, and 09:77:03 were set up by spreading 40 ml of the dispersed PEMs through pipetting onto a filter paper (Whatman, Grade 2, 7 cm) placed on solid proliferation medium in a 9 cm petri plate. Excess liquid medium was removed by pipetting. As a control, the same amount of non-dispersed aggregates of PEMs was transferred to solidified proliferation medium in petri plates by forceps. After 12 - 14 days of culture on proliferation medium, the tissues were transferred to pre-maturation medium (DKM). The dispersed PEMs were transferred to next culture stages along with the filter paper.

3.2.2.2 Image analysis

Samples of dispersed PEMs were photographed and analyzed as explained above. Each of three samples contained 557 ± 158 dispersed PEMs.

Images of somatic embryos from 24 plates containing an average of 129 and 78 mature embryos in each plate from dispersed and non-dispersed cultures respectively were analyzed using ImageJ and GIMP 2.8.10.

3.2.2.3 Statistical analysis

Similar statistical tests used in the experiment in liquid medium were performed in this study on solid medium for (a) number of mature embryos per gram FW of PEMs, (b) average length of embryos, (c) coefficient of variation (CV) of lengths of embryos, and (d) confidence interval of coefficient of variation. Differences between widths of the curves of normalized distribution function, $\varphi(\bar{q})$, for dispersed and non-dispersed cultures at 50%, 66%, and 75% of maximum were examined by Duncan Multiple Range Test, a non-parametric test (Tallarida and Murray, 1987). This test reduces the probability of falsely rejecting the null hypothesis, i.e., the equality of two sample means. In Duncan Multiple Range Test, the two sample means are significantly different if their absolute difference exceeds

$$W = Q(r, N - g) \times \sqrt{\frac{\hat{\sigma}^2}{m}}$$

where, g is the number of samples, m is the number of observations in each sample, N is total number of observations in g number of samples, r is the number of steps between two sample means, $\hat{\sigma}^2 = \sum_{k=1}^{g}(m_i - 1)s_k^2 / (N - g)$, is the residual mean square, s_k^2 is

the variance, and $Q(r, N-g)$ is the critical value obtained from the Q distribution table for corresponding α_s, r, and $(N-g)$.

3.2.3 Results and discussion

3.2.3.1 Size distributions of dispersed aggregates of PEMs and effect of dispersion on proliferation

Dispersion of aggregates of PEMs resulted in smaller aggregate units (Figure 3.6). The size range of dispersed aggregates varied between different cell lines ranging from a few microns to a few millimeters. More than 70% of dispersed aggregates were less than or equal to 0.2 mm^2 (Table 3.4).

Proliferation (or growth rate) of PEMs varies between cell lines. After dispersion of aggregates, proliferation increased in all embryogenic cell lines of Norway spruce tested. It was assumed that because of dispersion, more PEMs were able to come into direct contact with nutrients in the culture medium compared to PEMs in non-dispersed aggregates. Dispersion and redistribution of the immature embryos at early stages of development on solid medium thus had a positive influence on development.

(a) (b)

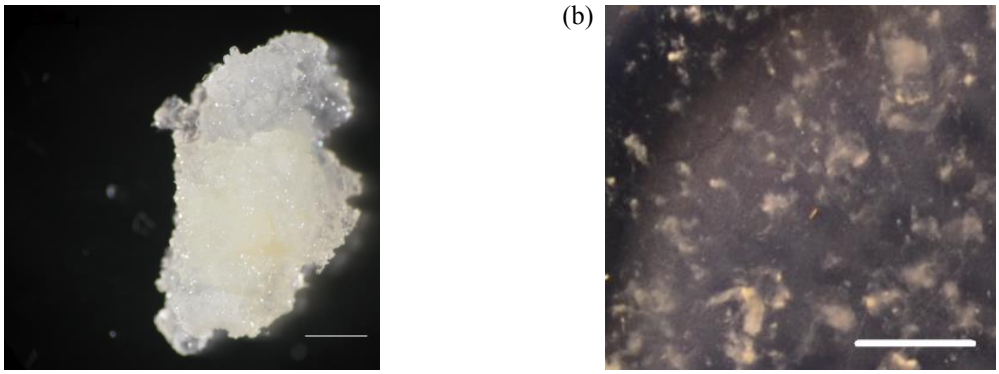

Figure 3.6 (a) Non-dispersed PEMs of *Picea abies*. Bar = 2mm; (b) Dispersed PEMs. Aggregates of PEMs in ½ LP liquid medium were passed through a dispersion system. Bar = 5mm.

Table 3.4 Size distributions of dispersed PEMs. After dispersion of aggregates of PEMs, more than 70% of dispersed PEMs were less than 0.2 mm^2 in size in all four cell lines and the mean values of sizes of dispersed aggregates varied with cell lines

	09:73:06	09:77:03	11:12:02	11:12:04
Percent of dispersed PEMs less than or equal to 0.2 mm^2	96.7%	95%	74.8%	80.8%
Size distribution of dispersed PEMs (mean ± sd) (mm^2)	0.15 ± 2.0	0.135 ± 1.36	0.32 ± 1.59	0.19 ± 1.14

3.2.3.2 Effect of dispersion on development of mature embryos

Dispersion resulted in a significant increase in yield of mature somatic embryos in cell lines 11:12:02, 09:77:03 and 09:73:06 (Figure 3.7). This could also be due to better access to nutrients for more PEMs after dispersion.

It is noted here that the average lengths of mature embryos from dispersed and non-dispersed PEMs of each cell line did not vary significantly within cell lines (Table 3.5). This means that dispersion, which caused strain on the PEMs, did not have unfavorable impact on maturation of embryos cultured on solid medium.

Dispersion was also found to increase the level of synchronization of the development of mature somatic embryos in cell lines 11:12:02 and 09:73:06 (Figures 3.8 and 3.9). The mean of full width at half maximum (FWHM) of $\varphi(\bar{q})$ of cell line 09:73:06 were 1.91 mm and 2.47 mm for dispersed and non-dispersed PEMs respectively with $\delta = 1\ mm$. For the cell line 11:12:02, the averages of FWHM of $\varphi(\bar{q})$ of three replicates contained dispersed PEMs and three replicates cultured non-dispersed PEMs were 0.97 mm and 1.45 mm respectively, with $\delta = 0.5\ mm$ for better resolution of the distribution function. Though widths of the function $\varphi(\bar{q})$ of dispersed PEMs of these two cell lines were shorter than that in non-dispersed PEMs, statistically the differences were not significant (p-value ≡ 0.25 in Duncan Multiple Range Test). Sizes of somatic embryos from dispersed PEMs were distributed as wide as non-dispersed PEMs. The full widths of $\varphi(\bar{q})$ at 66% and 75% of maximum were also verified for both dispersed and control

cultures (Figure 3.9), which also suggested similar level of synchronization of mature embryos after dispersion of cell lines 11:12:02 and 09:73:06.

The mean values of the full width at half maximum (FWHM), 66%, and 75% of maximum of the function $\varphi(\bar{q})$ for dispersed aggregates of PEMs were larger than those of non-dispersed aggregates of cell line 11:12:04 and 09:77:03 (Figure 3.9). Therefore, it would appear that dispersion did not improve the level of synchronization of mature somatic embryo development from dispersed PEMs of cell lines 11:12:04 and 09:77:03. For cell line 11:12:02, the coefficient of variation of lengths of mature embryos developed from dispersed PEMs (0.204 with 90% confidence interval of 0.189 - 0.221) was smaller than that from non-dispersed PEMs (0.271 with 90% confidence interval of 0.25 - 0.30). The confidence intervals were obtained by the McKay method. The CV values for dispersed and non-dispersed aggregates of PEMs were close for cell line 09:73:06 (Table 3.5). The CVs for cell lines 11:12:04 and 09:77:03 were greater for dispersed PEMs compared to non-dispersed PEMs (Table 3.5). Based on the CV values, it appears that dispersion stimulated synchronized development of mature embryos of cell line 11:12:02 and 09:73:06, but not of cell lines 11:12:04 and 09:77:03.

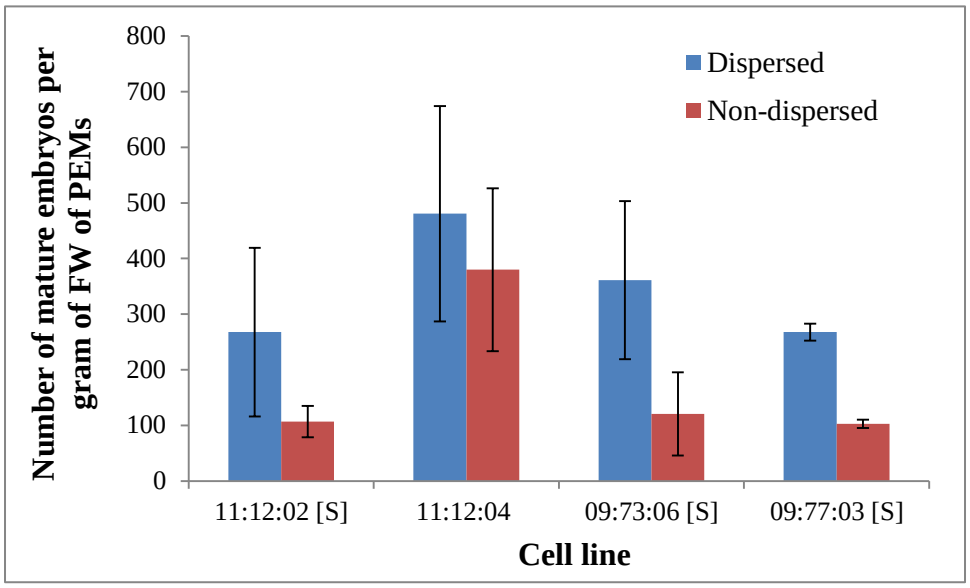

Figure 3.7 Number of mature embryos, developed from dispersed and non-dispersed PEMs, per gram of FW of different cell lines. In all four cell lines, dispersion resulted in increased yield of mature somatic embryos. The error bar shows the standard deviation in three replicates. Number of mature somatic embryos developed from a gram of fresh dispersed and non-dispersed PEMs are statistically different by independent two sample *t*-test at $p = 0.10$ for cell lines followed by [S] in abscissa.

Table 3.5 Lengths of mature somatic embryos of *Picea abies* developed from dispersed and non-dispersed PEMs on solid medium. Lengths were measured by an image analysis software, ImageJ

Cell line	Culture condition	Length of embryos (mm) (Mean ± SD)	Coefficient of variation (CV)
11:12:02	Dispersed	2.06 ± 0.42	0.204
	Non-dispersed	2.47 ± 0.67	0.272
11:12:04	Dispersed	2.55 ± 0.63	0.246
	Non-dispersed	2.32 ± 0.5	0.215
09:73:06	Dispersed	2.94 ± 1.04	0.354
	Non-dispersed	3.54 ± 1.29	0.364
09:77:03	Dispersed	2.42 ± 0.72	0.299
	Non-dispersed	2.12 ± 0.5	0.236

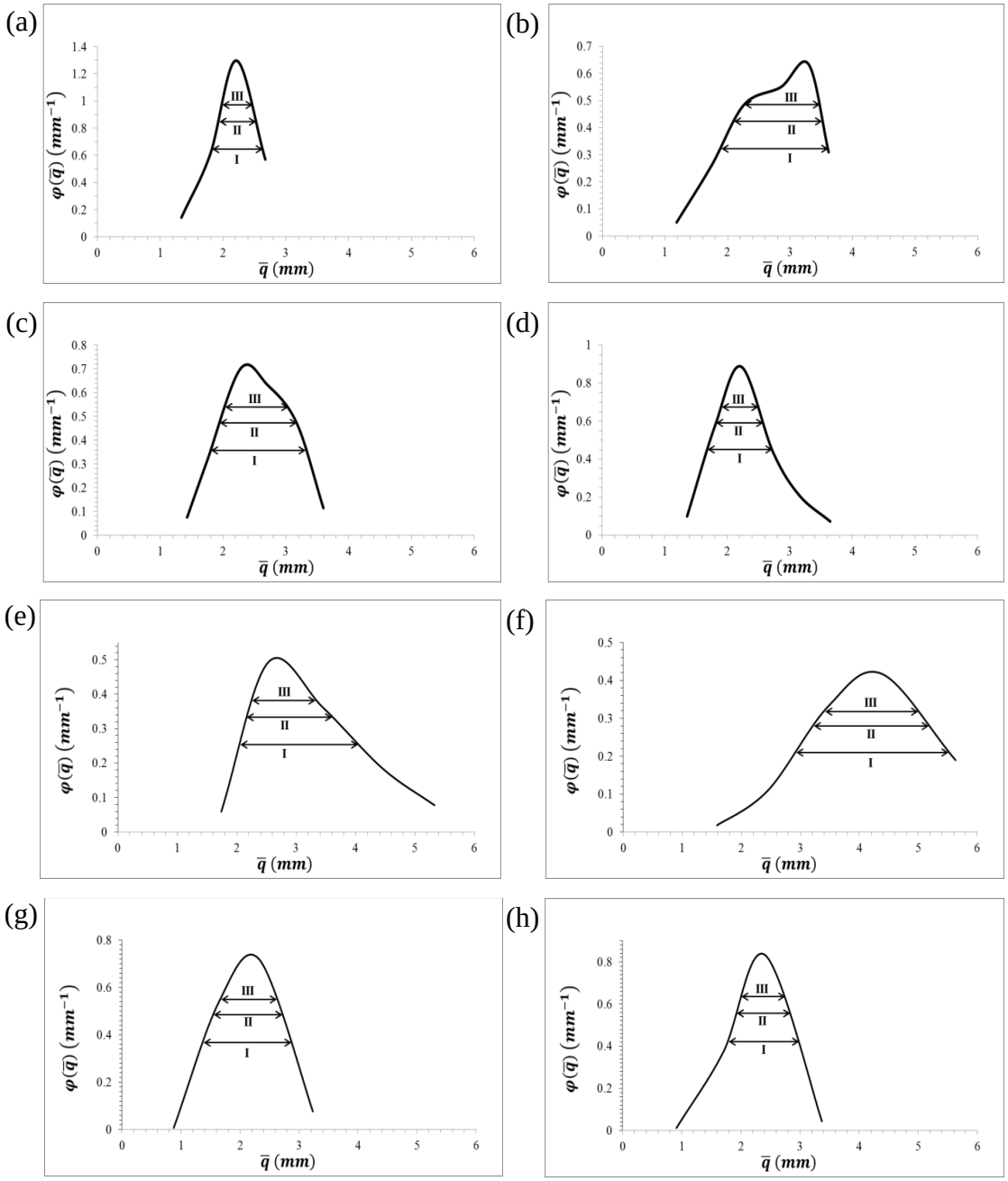

Figure 3.8 Level of synchronized development of mature somatic embryos of Norway spruce of cell lines 11:12:02 (a, b), 11:12:04 (c, d), 09:73:06 (e, f), and 09:77:03 (g, h). Plots (a, c, e, and g) represent the distribution function, $\varphi(\overline{q})$, with respect to the average length in an interval, δ, of mature somatic embryos formed from dispersed PEMs in a replicate of the corresponding cell line. Similarly plots (b, d, f, and h) represent that of in controls. I, II, and III represent full width at half (50%), 66%, and 75% of maximum of the function $\varphi(\overline{q})$ respectively. Their pertaining values are (a) 0.8, 0.58, & 0.48 mm; (b) 1.7, 1.4, & 1.2 mm; (c) 1.5, 1.22, & 1.0 mm; (d) 1.03, 0.75, & 0.58 mm; (e) 2.0, 1.42, & 1.05 mm; (f) 2.6, 1.95, & 1.58 mm; (g) 1.45, 1.15, & 0.93 mm; and (h) 1.18, 0.88, & 0.7 mm.

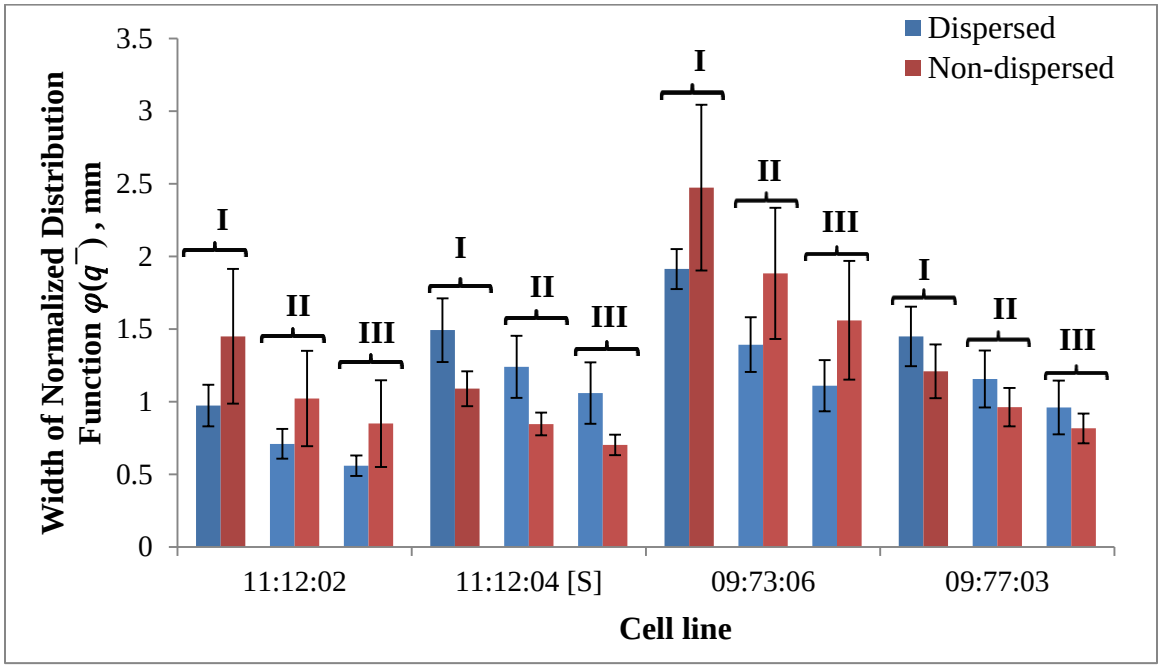

Figure 3.9 The average values of the full width at half maximum (FWHM) (I), 66% (II), and 75% (III) of maximum of the normalized distribution function, $\varphi(\bar{q})$ for mature embryos from dispersed and non-dispersed PEMs of different cell lines. The widths are shorter in dispersed PEMs than in non-dispersed PEMs of cell lines 11:12:02 and 09:73:06, meaning a more synchronized development of mature embryos after dispersion in these two cell lines. For cell line 11:12:04 and 09:77:03, the widths of function $\varphi(\bar{q})$ are shorter in non-dispersed PEMs. However, statistically the differences in widths of $\varphi(\bar{q})$ of dispersed and non-dispersed PEMs at 50%, 66%, and 75% of maximum are not significant by the Duncan Multiple Range Test at 90% confidence level, except cell line 11:12:04 as denoted by [S].

3.2.3.3 Germination of mature embryos

The germinants were photographed and counted. 60% (11:12:02) and 68% (11:12:04) of the harvested mature somatic embryos from dispersed PEMs were germinated with having roots of 1 cm or longer, and 55% (11:12:02) and 67% (11:12:04) of the harvested somatic embryos from non-dispersed aggregates of PEMs were converted to germinants with roots of 1 cm or longer (Table 3.6).

Table 3.6 Number of mature embryos from dispersed and non-dispersed PEMs of two cell lines cultured in the germination medium, number of germinants, and germinants having roots of 1 cm or longer

Cell line	11:12:02		11:12:04	
	Dispersed PEMs	Non-dispersed PEMs	Dispersed PEMs	Non-dispersed PEMs
Number of somatic embryos cultured in germination medium	182	136	222	267
Number of germinants	143	99	158	237
Number of germinants having roots of 1 cm or longer	109	75	150	178

CHAPTER 4

INTERMITTENT DISPERSION OF PROEMBRYOGENIC MASSES OF NORWAY SPRUCE IN A TEMPORARY IMMERSION BIOREACTOR

In traditional laboratory methods of cell suspension cultures, cells or aggregates of cells are suspended in culture medium in an Erlenmeyer flask and cultured under continuous agitation on a shaker table at a certain speed. This agitation causes a shear flow around cell clusters and helps to distribute nutrients in the medium amongst the embryos. Shaking or agitation is not effective enough to break the cell aggregates, and hyperhydricity has been an issue associated with this culture process. So it is necessary to introduce an efficient alternative to disintegrate clusters during proliferation of PEMs in liquid culture. Here an automated dispersion system integrated with the designed temporary immersion bioreactor has been proposed to break up the cell aggregates. A detailed experimental setup and procedure are described in the following sections.

4.1 Materials and Methods

4.1.1 Embryogenic cell lines

An embryogenic cell line, 09:86:02, of Norway spruce was used in this study. As described in Chapter 3, this cell line was also originated from controlled crosses in the Swedish Norway spruce breeding program and was maintained by subculturing in the dark in 9 cm petri plates containing PEMs on half strength LP (½ LP) solid medium supplemented with 2,4-D and BAP.

4.1.2 Setup of an auto-dispersion system

Dispersion of cell aggregates can be done in two different occasions, dispersion (i) at the beginning of culture process, and (ii) during proliferation of PEMs. Dispersion that occurs during proliferation of PEMs in a bioreactor is termed as auto-dispersion. An auto-dispersion system has been designed to integrate with a bioreactor to disperse PEMs at a pre-set time.

The purpose of an auto-dispersion system is to disperse PEMs intermittently during the proliferation phase of somatic embryogenesis. This reduces the human intervention. The auto-dispersion system consists of a glass aspirator/ disperser with four legs, a glass T-connector, a disperser made of glass (Aidun and Egertsdotter, 2011/043731), a flask (500 ml), air filter of 0.2 µm pore size (Acro 37 TF Vent Device with 0.2µm PTFE Membrane), and several 3-way normally closed solenoid valves (1/8 inch orifice, 3/32 inch exhaust, $C_v = 0.28$). The aspirator/ disperser is placed inside a bioreactor through a glass T-connector at the opening of the bioreactor lid such that the four open legs of the aspirator/ disperser touch the bioreactor screen (Figure 4.1). A glass disperser is connected to the aspirator/ disperser at one end and a flask at the other end through silicone tubes (Tygon, 7.9 mm I.D. and 11.1 mm O.D.). The opening of the flask is attached to a 0.2 µm air filter which is then connected to a manifold through silicone tube. Several solenoid valves and an air pump (BUSCH Miniseco SD 1004 B) are used to operate the auto-dispersion system. The pump and the solenoid valves are operated and controlled by a timer (PTC-15, Programmable Timing Controller).

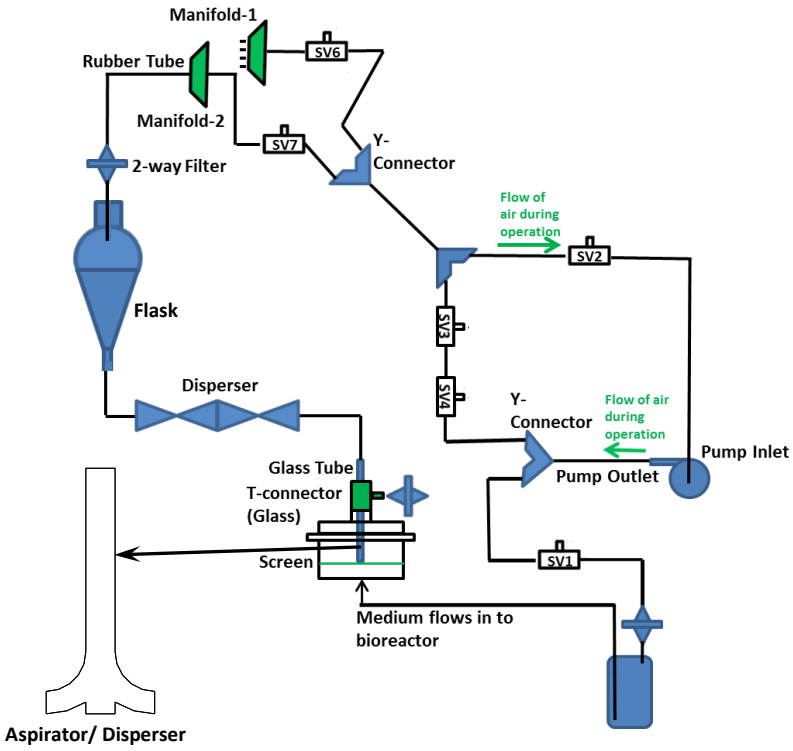

Figure 4.1 A Temporary immersion bioreactor with auto-dispersion system. Each bioreactor is equipped with an aspirator/ disperser, glass T-connector, disperser, flask, and air filters to disperse cell cultures intermittently during proliferation phase of somatic embryogenesis.

4.1.3 Operation of the auto-dispersion system

During operation, the air pump turns on and the solenoid valves, SV1, SV2, and SV7, are opened. The liquid medium flows through a silicone tube from a glass bottle to the bioreactor and soaks the dispersed PEMs. The auto-dispersion system starts operation as soon as the valves SV 2 and SV 7 are opened. However, the solenoid valves, SV 3 and SV4, are remained closed. This results in an aspiration of cells and tissues along with culture medium through the disperser to the flask. At the end of aspiration, the solenoid

valves SV3 and SV4 are opened and SV2 is closed. This causes the filtered air to push back the cell cultures to the bioreactor through disperser. During each run, the aspiration-dispense process is taken place three times to make sure that all the PEMs sitting on the screen pass through disperser during proliferation. The same air pump is used for aspiration and dispense of cells through disperser.

4.1.4 Culture of PEMs in control bioreactors and bioreactors with the auto-dispersion system

Eight bioreactors were set up with 1.5 g of PEMs to study the effect of auto-dispersion of PEMs during proliferation. To culture cell line 09:86:02, four bioreactors were used with auto-dispersion systems. In two of them PEMs were dispersed twice in a week (Group A) and two other were set to disperse the PEMs once in a week (Group B) during the proliferation phase of somatic embryogenesis of Norway spruce (Table 4.1). Four more bioreactors were setup to culture PEMs without auto-dispersion during proliferation; two of them cultured PEMs that were dispersed before start of proliferation in the experiment (Control A) and two of them had non-dispersed PEMs (Control B). Details of bioreactor setting and operation of auto-dispersion are given in Table 4.1.

Table 4.1 Detailed time line for auto-dispersion. Eight bioreactors were divided into four groups for each cell line; Group A and Group B consisted of four bioreactors connected to auto-dispersion systems, and Control A and Control B consisted of other four bioreactors. Auto-dispersion systems in two bioreactors of Group A were operated twice in a week and those in two other bioreactors of Group B were operated once in a week

Phase of somatic embryogenesis	Time	Group A	Group B	Control A	Control B
Proliferation	Day 1	Set up bioreactors with dispersed PEMs	Set up bioreactors with dispersed PEMs	Bioreactors with dispersed PEMs and no auto-dispersion	Bioreactors with non-dispersed PEMs
	Day 5	Auto-dispersed			
	Day 9	Auto-dispersed	Auto-dispersed		
	Day 13	Auto-dispersed			

4.2 Results and Discussion

4.2.1 Effect of auto-dispersion on development of mature embryos

A large number of embryos were formed in each case (Figure 4.2), i.e., in bioreactors contained dispersed (without auto-dispersion system) and non-dispersed PEMs, and bioreactors with auto-dispersion systems. Since there were too many mature embryos in the bioreactors, they were not counted. This cell line had a unique

characteristic of being dispersed when it came into contact with liquid medium. The PEMs continued to disperse when they were soaked two times a day with liquid culture medium in a bioreactor. So the dispersion before proliferation and during proliferation (auto-dispersion) did not have much impact on development of mature somatic embryos compared to that of non-dispersed PEMs.

4.2.2 Quality of mature embryos

The mature somatic embryos had hypocotyls and had clearly visible cotyledons, either small or large, and some of them did not (Figure 4.3). Since these embryos were not taken to the germination stage, it was not possible to determine whether those having no clearly visible cotyledons would germinate.

(a) 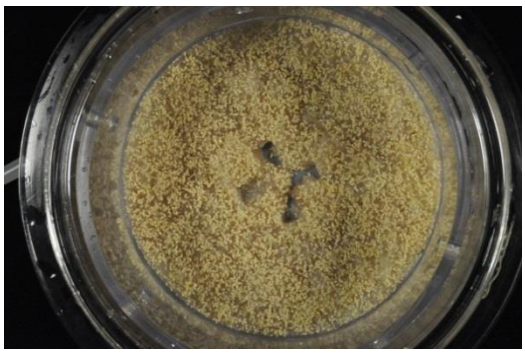 (b) 

(c) 

Figure 4.2 Embryos of Norway spruce of cell line 09:86:02 after 11weeks of culture; (a) embryos in auto-dispersed bioreactor (Group A, the impression at the center is due to the aspirator/ disperser), (b) embryos in a bioreactor from initially dispersed PEMs (Control A), (c) embryos from non-dispersed PEMs (Control B).

(a) 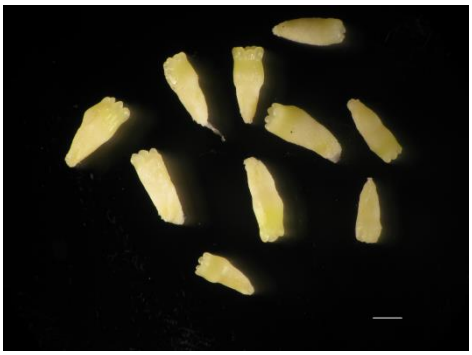 (b) 

Figure 4.3 Mature somatic embryos of Norway spruce of cell line 09:86:02; (a) embryos collected from a bioreactor in Control A, in which PEMs were dispersed before proliferation and not auto-dispersed, (b) embryos from a bioreactor in Group B, in which PEMs were auto-dispersed once in a week. Bar = 1mm.

CHAPTER 5

NUTRIENT DISTRIBUTIONS IN THE AGGREGATES OF PROEMBRYOGENIC MASSES OF NORWAY SPRUCE: A MATHEMATICAL MODEL AND EXPERIMENTAL STUDY

A mathematical model of nutrient uptake *in vitro* by tissue aggregates of *Picea abies* from ½ LP solidified medium supplemented with glucose has been developed to provide an insight into the distribution of sugar concentrations in aggregates of proembryogenic masses (PEMs) over the period of subculture. In a broader perspective, uptake of nutrient, especially glucose, sucrose, and fructose, from solidified culture medium by PEMs clusters of Norway spruce and estimation of nutrient concentrations in PEMs would help to gain insight into the role of dispersion of PEMs in proliferation and maturation of somatic embryos.

While subculturing aggregates of PEMs on solid medium, the regions that are close to or in contact with medium may get more nutrients compared to the regions that are away from medium. However it is noticed that somatic embryos develop and mature at all locations on the surfaces of a PEMs cluster exposed to air, though there is a possibility of variation of nutrient concentration in these locations. To investigate this, sugars have been considered as model nutrients in this work. They play a vital role as the main source of carbon in plant cell culture. Sucrose supplemented in the culture medium is generally hydrolyzed by sucrose synthase at the cell wall and transported into cells in the form of hexoses (review in Shin et al., 2003). Depletion of sucrose and fructose

usually results in hindrance of growth of plant cell suspension cultures (van Gulik et al., 1993).

Several mathematical models on nutrient uptake by plant cells and hairy root cultures have been proposed to date. Concentrations of intracellular phosphorus, sugars, nitrogen compounds and extracellular nitrate, ammonium, sugars, and phosphorus were investigated using these models for suspension culture of *Papaver somniferum, Eschscholtzia californica*, *Catharanthus roseus* cells and hairy roots of *Daucus carota*, and *Catharanthus roseus* (Cloutier et al., 2008 and the references therein). Here a mathematical model has been presented to evaluate the concentrations of nutrients in PEMs clusters, considered as a porous medium, cultured on solidified medium for a period of time. The model has been coupled to a model of nutrient concentrations in the medium. Model simulation of concentrations of sucrose, glucose, and fructose in a cluster of PEMs was compared to experimental observations. This model may eventually explore whether aggregates of PEMs get saturated with nutrients during the period of culture, and the time required for nutrient saturation of PEMs aggregates.

5.1 Materials and methods

5.1.1 Plant materials

An embryogenic cell line, 11:12:04, of Norway spruce was used in this experiment. The PEMs were maintained in the dark at 23^0- 25^0 C in 9 cm petri plates by subculturing every second week on solidified proliferation medium, half strength LP (½

LP) (Table 5.1 per von Arnold and Eriksson, 1981), supplemented with auxin and cytokinin.

Table 5.1 Nutrient concentration in the medium used in the experiment

	½ LP medium (g/L)	**½ LP medium (g/L) (glucose supplemented)**
Macro Elements (1.525 g/L)		
KNO_3	0.95	0.95
$MgSO_4 .7H_2O$	0.185	0.185
KH_2PO_4	0.17	0.17
$CaCl_2. 2 H_2O$	0.22	0.22
Micro Elements (0.00391 g/L)		
Zn-EDTA	2.36×10^{-3}	2.36×10^{-3}
KI	3.75×10^{-4}	3.75×10^{-4}
H_3BO_3	3.15×10^{-4}	3.15×10^{-4}
$MnSO_4 .H_2O$	8.45×10^{-4}	8.45×10^{-4}
$NaMoO_4 .2H_2O$	1.25×10^{-5}	1.25×10^{-5}
$CuSO_4. 5 H_2O$	1.25×10^{-6}	1.25×10^{-6}
$CoCl_2. 6 H_2O$	1.25×10^{-6}	1.25×10^{-6}
$FeSO_4 .7 H_2O$	6.95×10^{-3}	6.95×10^{-3}
Na-EDTA	9.3125×10^{-3}	9.3125×10^{-3}

Vitamins		
Pyridoxine (B6)	5×10^{-4}	5×10^{-4}
Nicotinic acid (B9)	1×10^{-3}	1×10^{-3}
Thiamin (B3)	2.5×10^{-3}	2.5×10^{-3}
NH_4NO_3	0.3	0.3
2,4-Dichlorophenoxyacetic acid	2.21×10^{-3}	2.21×10^{-3}
BA (6-Benzylaminopurine)	1×10^{-3}	1×10^{-3}
Sucrose	10	-
Glucose	-	5.243
Myoinositol	0.225	0.225

5.1.2 Methods

Each cluster of PEMs was divided into two pieces, top and bottom. The bottom portion represented the region of the cluster touching the solid medium directly. Each piece or sample weighed between 200 and 300 mg (fresh weight) and was placed in a 2.0 mL Eppendorf tube (VWR, Radnor, PA). Samples were collected at different time intervals as shown in Table 5.2 below. At each time, 5 aggregates of PEMs were dissected to have enough replicates for a robust estimate of sugar content at two locations in the cluster. Each sample was placed in an Eppendorf tube. A hole was made in the cap of each Eppendorf tube to allow vacuum while samples were in a freeze dryer; however caps were wrapped with parafilm and the Eppendorf tubes were placed in a paper bag.

Samples were then frozen rapidly in liquid nitrogen to stop metabolism and kept there for 30 min. After that samples were freeze dried at -49^{0}C in a freeze dryer (Labconco, Kansas City, MO) for a week. Each sample was transferred to a 2 mL Sarstedt screw cap micro tube, type I (VWR, Radnor, PA).

Samples were homogenized thoroughly in a bead mill (MM400, Retsch GmbH, Germany) using a 7 mm diameter stainless steel bead at a frequency of 30 Hz for 2 min to have a smooth consistency. Weights of homogenized samples were between 2 and 5 mg.

Table 5.2 Timeline of sample collection

Time Line	Number of PEMs Clusters	Media	Supplemented Sugar	Process	Fresh Weight of each sample
0 hr	5	½ LP	Sucrose	Cut each cluster of PEMs into two pieces (Top & Bottom)	200-300 mg
12 hr	5		Glucose		
24 hr	5		Glucose		
3 days	5		Glucose		
6 days	5		Glucose		
10 days	5		Glucose		

Glucose, sucrose, and fructose were extracted using 80% and 50% aq. ethanol (vol/vol). 250 µl of 80% ethanol was added to each homogenized sample in the micro tube and was heated in a heating block at 95^{o}C for 30 min. The samples were then centrifuged for 10 min at 13,000 g at room temperature to form pellets. The first supernatant (S1) was collected from each micro tube. To recover residual soluble sugars, ethanol extraction was repeated twice, heating each pellet with 150 µL of 80% aq. ethanol, centrifuge, collection of second supernatant (S2) and again heating each pellet with 250 µL of 50% aq. ethanol, centrifuge, collection of third supernatant (S3). In both cases, heating was carried out at 95^{o}C for 30 min. Pellets were discarded. 40 µL of each supernatant and four glucose standards (0, 0.25, 0.5 and 1 mM) were pipetted into each of 96 wells of a micro plate (Sarstedt, Nümbrecht, Germany). 160 µL of assay reagent, consisting of 3 mM $MgCl_{2,}$ 3 mM ATP, 1.3 mM NADP and 0.6 U Glucose-6-phosphate dehydrogenase (G6PDH), in 100 mM Hepes/KOH buffer (pH 7) (Roche Diagnostics GmbH, Mannheim, Germany) were then added to each of the wells.

Enzymatic assaying of soluble sugars was performed following the protocol of Stitt et al. (1989). In brief, in each well of the micro plate, 1 µl hexokinase (HK) (0.9 U/µl) (Roche), 1 µl phosphoglucose isomerase (PGI) (1.0 U/µl) (Roche) and excess amount of invertase (INV) (Sigma) were added sequentially in a 30 min interval. Glucose-6-phosphate (G6P) and fructose-6-phosphate (F6P) were produced from phosphorylation of glucose and fructose by ATP (adenosine triphosphate) during an enzymatic reaction catalyzed by hexokinase. Glucose-6-phosphate was oxidized to gluconate-6-phosphate with a reduction of NADP (nicotinamide adenine dinucleotide

phosphate) to reduced nicotinamide adenine dinucleotide phosphate (NADPH) in presence of glucose-6-phosphate dehydrogenase (G6PDH). Fructose-6-phosphate was converted to glucose-6-phosphate by the enzyme phosphoglucose isomerase. Conversion of sugars is shown below.

$$\text{ATP} + \text{Glucose} \xrightarrow{\text{HK}} \text{G6P} \xrightarrow{\text{G6PDH}} \text{NADPH}$$

$$\text{ATP} + \text{Fructose} \xrightarrow{\text{HK}} \text{F6P} \xrightarrow{\text{PGI}} \text{G6P} \xrightarrow{\text{G6PDH}} \text{NADPH}$$

$$\text{Sucrose} \xrightarrow{\text{INV}} \text{Glucose} + \text{Fructose} \underset{\text{HK}}{\overset{\text{PGI}}{\longrightarrow}} \text{G6P} \xrightarrow{\text{G6PDH}} \text{NADPH}$$

Absorbance, expressed by optical density (OD), of a monochromatic light of wave length 340 nm was determined using an Epoch micro plate spectrophotometer (Bio Tek Instrument Inc., Vermont, USA) and the value at which OD_{340} remained constant was converted to µg of sugar/ mg DW of plant tissues using the glucose standard curve.

5.2 Mathematical Model

Tissues are usually considered as porous medium having a cell phase and an extracellular phase (Nicholson, 2001). To develop a mathematical model of nutrient concentration distributions, an aggregate of PEMs may also be considered as a medium with a two phase system; its cell phase consists of cells and maturing embryos having suspensor cells connected to meristematic cells, and the extracellular phase is considered as interstices between cells as shown in Figure 5.1.

To develop the model, it is considered that a hemispherical PEMs aggregate of 7 mm in diameter is placed on solid nutrient medium contained in a petri plate as in Figure 5.2. Somatic embryos are matured at different locations in an aggregate of PEMs, either near the nutrient medium or away from the medium (Figure 5.2). The cluster of PEMs is considered as hemispherical in shape for simplicity. It is assumed that nutrients diffuse passively through the medium and the extracellular region in the PEMs cluster; whereas uptake of nutrients into the cells or maturing embryos requires facilitated diffusion, in which proteins at the cell membrane facilitate transportation of nutrients (ions/ molecules) from the extracellular region into the cytoplasm.

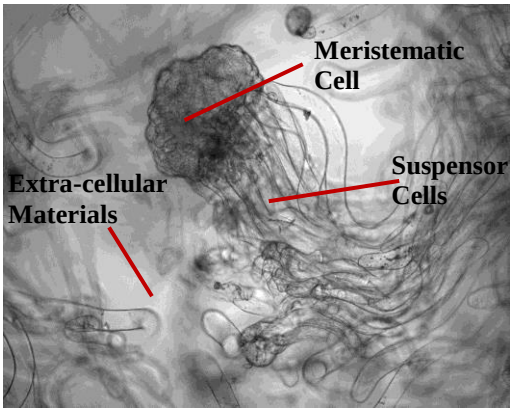

Figure 5.1 A maturing embryo entangled with the extra-cellular materials. A cluster of PEMs is dispersed in nutrient medium and embryos are suspended in the medium along with the extra-cellular materials.

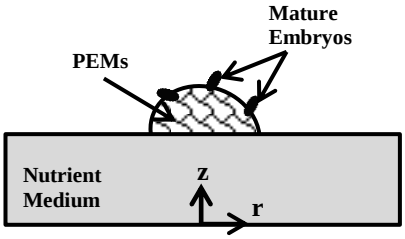

Figure 5.2 Somatic embryos are matured at different locations of the cluster. For the model the PEMs cluster is considered as hemispherical in shape.

Nutrients diffuse through medium to the region where the PEMs cluster is in contact with the medium. Transport of nutrients in the medium can be modeled by the diffusion equation

$$\frac{\partial C_{AM}}{\partial t} = \nabla \cdot (D_{AM} \nabla C_{AM}) \tag{5.1}$$

where, C_A is the concentration of a nutrient, A, in the medium containing different nutrients, D_A is the diffusion coefficient of the nutrient in the medium, and subscript M stands for nutrient medium.

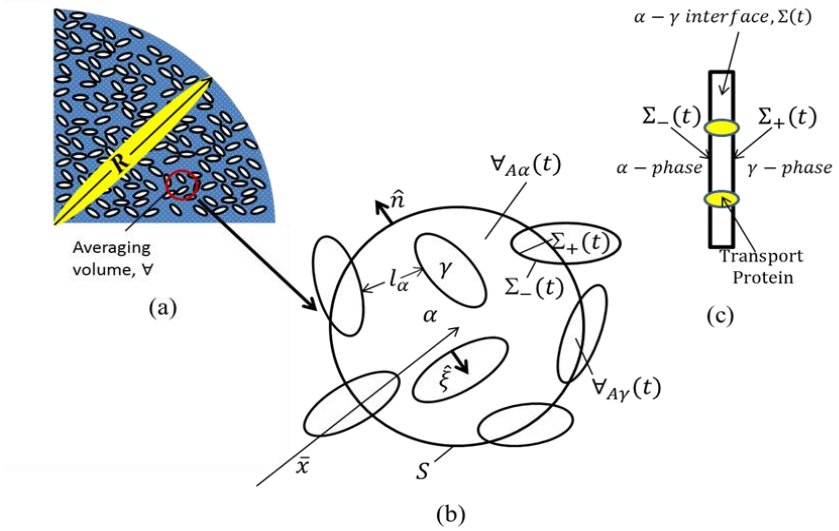

Figure 5.3 (a) Averaging volume, ∀, in a PEMs cluster of radium R; (b) Enlarged view of ∀, enclosed by a sureface S and contains the extracellular phase, α and the intracellular phase, γ. The two phases are separated by an interface, Σ. Volumes occupied by the $\alpha - phase$ and the $\gamma - phase$ are denoted by $\forall_{A\alpha}$ and $\forall_{A\gamma}$. The subscript, A , stands for a nutrient species. The location of ∀ is represented by its centroid, $\bar{x}$; (c) Enlarged view of $\alpha - \gamma$ interface showing the transport proteins; the side towards α is denoted by $\Sigma_-(t)$ and the side towards γ is denoted by $\Sigma_+(t)$. It is considered here as $\Sigma_-(t) = \Sigma_+(t)$.

Nutrients from the medium diffuse through the extracellular phase of the cluster of PEMs up to the outer region of cell membrane of each cell before the nutrients are taken up by the cells. It can be considered that diffusion through extracellular phase of a PEMs cluster is analogous to diffusion in a porous medium having two phases. So applying the diffusion equation over a PEMs cluster requires an averaging of variables on an appropriate length scale to smooth out discontinuities. Volume averaging technique

(Whitaker, 1999) will be used in this case to derive continuum equation for the defined two-phase system in the cluster. Figure 5.3 shows an averaging volume and the phases in it for mathematical modeling.

Transport of nutrient, A, in α and γ phases can be modeled by diffusion and diffusion-reaction equations respectively as follows.

$$\frac{\partial C_{A\alpha}}{\partial t} = \nabla \cdot (D_{A\alpha} \nabla C_{A\alpha}) \qquad \text{in the } \alpha - phase \qquad (5.2)$$

$$\frac{\partial C_{A\gamma}}{\partial t} = \nabla \cdot \left(D_{A\gamma} \nabla C_{A\gamma}\right) - \frac{\mu_A C_{A\gamma}}{C_{A\gamma} + K_A} \qquad \text{in the } \gamma - phase \qquad (5.3)$$

The 2nd term of RHS of the eq. (5.3) refers to absorption of nutrients by cells and maturing embryos according to the Michaelis-Menten enzyme kinetics.

To determine boundary conditions it is necessary to take into account the process of how nutrients enter cells. In this analysis, a cluster of PEMs is assumed to be axisymmetric for simplicity where the axis of rotation is z-axis. This reduces the 3D into a 2D model.

Most nutrients are taken in by proteins located in the outer membrane, known as transport proteins, from extracellular phase to the inside of a cell (Cambell & Reece, 2002). In this model, the uptake of nutrient into cells with the help of transport proteins is taken into consideration. The uptake process is considered based on the Michaelis-Menten enzyme kinetics (Barber, 1984). According to the enzyme kinetics mechanism, it

may be considered that when a nutrient, A, in the $\alpha - phase$ comes in contact with cell membrane forms a nutrient-protein complex. The decomposition of this complex results in release of the nutrient into cell cytosol by forward reaction as well as formation of original nutrient through reverse reaction. This can be presented symbolically as (Lakshminarayanaiah, 1984)

$$A_\alpha + P_T \underset{k_{-1}}{\overset{k_1}{\rightleftharpoons}} A_\alpha P_T \underset{k_{-2}}{\overset{k_2}{\rightleftharpoons}} P_T + A_\gamma \qquad \text{in } \Sigma(t) \qquad (5.4)$$

where A_α, P_T, $A_\alpha P_T$, and A_γ represent the nutrient, A, in α, transport protein, nutrient-protein complex, and the nutrient A in γ respectively.

Rate of formation of $A_\alpha P_T \equiv k_1 C_{A\alpha}[P_T] + k_{-2}[P_T]C_{A\gamma}$ (5.4a)

Rate of dissociation of $A_\alpha P_T \equiv (k_{-1} + k_2)[A_\alpha P_T]$ (5.4b)

So at the interfacial surface between α and γ, the flux from α to $\Sigma_-(t)$ and from $\Sigma_+(t)$ to γ are

$$\bar{J}_{\alpha\Sigma} \cdot \hat{\bar{\xi}} = k_1 C_{A\alpha}[P_T] - k_{-1}[A_\alpha P_T] \qquad (5.5)$$

and $$\bar{J}_{\Sigma\gamma} \cdot \hat{\bar{\xi}} = k_2[A_\alpha P_T] - k_{-2}[P_T]C_{A\gamma} \qquad (5.6)$$

Total concentration of transport protein in the cell membrane in averaging volume, ∀, may be defined as

$$P_0 = [P_T] + [A_\alpha P_T] \qquad (5.7)$$

To determine an expression of the concentration of nutrient-protein complex, it may be approximated that the change in concentration of nutrient-protein complex is negligibly small on the time scale of nutrient released to γ from nutrient-protein complex. Therefore,

$$\frac{d}{dt}[A_\alpha P_T] = 0 = k_1 C_{A\alpha}[P_T] - k_{-1}[A_\alpha P_T] - k_2[A_\alpha P_T] + k_{-2}[P_T]C_{A\gamma} \qquad (5.8)$$

Eq. (5.8) can then be solved for $[A_\alpha P_T]$ by applying eq. (5.7) for $[P_T]$ as

$$(k_{-1} + k_2)[A_\alpha P_T]$$
$$= k_1 C_{A\alpha}[P_T] + k_{-2}[P_T]C_{A\gamma} = k_1 C_{A\alpha}(P_0 - [A_\alpha P_T])$$
$$+ k_{-2} C_{A\gamma}(P_0 - [A_\alpha P_T])$$

and then by rearranging one can get,

$$\left(k_{-1} + k_2 + k_1 C_{A\alpha} + k_{-2} C_{A\gamma}\right)[A_\alpha P_T] = \left(k_1 C_{A\alpha} + k_{-2} C_{A\gamma}\right)P_0$$

Hence

$$[A_\alpha P_T] = \frac{(k_1 C_{A\alpha} + k_{-2} C_{A\gamma})P_0}{(k_{-1} + k_2 + k_1 C_{A\alpha} + k_{-2} C_{A\gamma})} \qquad (5.9)$$

Substituting eqs. (5.7 & 5.9) in eq. (5.5) gives (shown in Appendix B)

$$\bar{J}_{\alpha\Sigma} \cdot \hat{\bar{\xi}} = \left(\frac{k_2 k_1 C_{A\alpha} - k_{-1} k_{-2} C_{A\gamma}}{k_{-1} + k_2 + k_1 C_{A\alpha} + k_{-2} C_{A\gamma}}\right) P_0 \qquad (5.10)$$

Dividing the nominator and denominator in eq. (5.10) by $k_2 k_1$, it can be shown that

$$\bar{J}_{\alpha\Sigma} \cdot \hat{\bar{\xi}} = \left(\frac{C_{A\alpha} - \beta_1 C_{A\gamma}}{\beta_2 + \beta_3 + \beta_4 C_{A\alpha} + \beta_5 C_{A\gamma}}\right) P_0 \qquad (5.11)$$

where

$$\beta_1 = \frac{k_{-1}k_{-2}}{k_2 k_1};\ \beta_2 = \frac{k_{-1}}{k_2 k_1};\ \beta_3 = \frac{1}{k_1};\ \beta_4 = \frac{1}{k_2};\ \text{and } \beta_5 = \frac{k_{-2}}{k_2 k_1} \qquad (5.11a)$$

Similarly, substituting eq. (5.7 & 5.9) in eq. (5.6) gives

$$\bar{J}_{\Sigma\gamma} \cdot \hat{\bar{\xi}} = \left(\frac{C_{A\alpha} - \beta_1 C_{A\gamma}}{\beta_2 + \beta_3 + \beta_4 C_{A\alpha} + \beta_5 C_{A\gamma}}\right) P_0 \qquad (5.12)$$

So boundary conditions for the two phase system are

BC 1: $\bar{J}_{\alpha\Sigma} \cdot \hat{\bar{\xi}} = \left(\frac{C_{A\alpha} - \beta_1 C_{A\gamma}}{\beta_2 + \beta_3 + \beta_4 C_{A\alpha} + \beta_5 C_{A\gamma}}\right) P_0$ at $\Sigma_-(t)$, which is eq. (5.11).

BC 2: $\bar{J}_{\alpha\Sigma} = \bar{J}_{\Sigma\gamma}$ at the interface of α and γ (5.13)

Now in order to obtain a spatially smooth transport equation, a volume averaging technique (Appendix C) (Whitaker, 1967; Slattery, 1967) is applied to the set of equations above (eqs. 5.2, 5.3, 5.11, and 5.13). Concentration of nutrient, A, in α satisfies

$$\frac{\partial}{\partial t}\{\epsilon_\alpha \langle C_{A\alpha}\rangle^*\} = \nabla \cdot \epsilon_\alpha \{\overline{\overline{D}}_{A\alpha,eff} \cdot \nabla \langle C_{A\alpha}\rangle^*\} - \frac{a_v (P_0/\beta_4)\,\langle C_{A\alpha}\rangle^*}{(\beta_2/\beta_4)+(\beta_3/\beta_4)+\langle C_{A\alpha}\rangle^*} \tag{5.14}$$

while the concentration in γ can be set to zero with an assumption that the intracellular concentration of nutrient is negligibly small compare to extracellular concentration because of utilization of nutrient in the cell.

The numerator and dominator of the 2nd term in RHS of eq. (5.14) require further investigation. The term (P_0/β_4) in the numerator refers to the maximum rate of nutrient uptake $mol/cm^2 \cdot s$ to saturate transport proteins at the cell wall. So it can be written as

$(P_0/\beta_4) = \phi_{max}$ = Maximum uptake rate, $\left[\frac{mol}{cm^2 \cdot s}\right]$

The term $(\beta_2/\beta_4) + (\beta_3/\beta_4) = (k_{-1} + k_2)/k_1$ (from eq. (5.11a)) in the denominator indicates how quickly transport proteins will be saturated. Here $(k_{-1} + k_2)$ is the rate of dissociation of protein and nutrient, and k_1 is the rate of formation of nutrient-protein complex. Comparing to the Michaelis- Menten enzyme kinetics, it may be termed as

$(\beta_2/\beta_4) + (\beta_3/\beta_4) = K_m$ = Half-saturation constant, $\left[\frac{mol}{cm^3}\right]$

which is the concentration gradient at which the uptake rate is $^1/_2\,\phi_{max}$. Hence the governing equation, eq. (5.14), can be written as

$$\frac{\partial}{\partial t}\{\epsilon_\alpha\langle C_{A\alpha}\rangle^*\} = \nabla\cdot\epsilon_\alpha\{\overline{\overline{D}}_{A\alpha,eff}\cdot\nabla\langle C_{A\alpha}\rangle^*\} - \frac{\phi_{max}a_v\langle C_{A\alpha}\rangle^*}{K_m+\langle C_{A\alpha}\rangle^*} \quad (5.14a)$$

The set of governing equations, initial conditions, and boundary conditions to model the nutrient distribution in a PEMs cluster is then

$$\frac{\partial}{\partial t}\{\epsilon_\alpha\langle C_{A\alpha}\rangle^*\} = \nabla\cdot\epsilon_\alpha\{\overline{\overline{D}}_{A\alpha,eff}\cdot\nabla\langle C_{A\alpha}\rangle^*\} - a_v\frac{\phi_{max}\langle C_{A\alpha}\rangle^*}{K_m+\langle C_{A\alpha}\rangle^*} \quad (5.14a)$$

$$\frac{\partial C_{AM}}{\partial t} = \nabla\cdot(D_{AM}\nabla C_{AM}) \quad (5.14b)$$

Here a_v is estimated as (Appendix F)

$$a_v = \frac{\Sigma_-(t)}{\forall} = \frac{3(1-\epsilon_\alpha)}{r_0}$$

Boundary Conditions:

$$\langle C_{A\alpha}\rangle^* = C_{AM} \qquad @\ (r,\theta=0,t) \text{ and } (r,\theta=\pi,t) \quad (5.14c)$$

$$\bar{J}_M = -\bar{J}_{PEM} \qquad @\ (r,\theta=0,t) \text{ and } (r,\theta=\pi,t) \quad (5.14d)$$

$$\bar{J}_M = 0 \qquad @ \text{ the boundary of the medium} \quad (5.14e)$$

$$\bar{J}_{PEM} = 0 \qquad @ \text{ the boundary of the PEM} \quad (5.14f)$$

Initial conditions

$$\langle C_{A\alpha}\rangle^* = \mathcal{K} \qquad @\ t=0 \quad (5.14g)$$

$$C_{AM} = \mathcal{K}_M \qquad @\ t=0 \quad (5.14h)$$

5.3 Model Simulation

Simulation of nutrient uptake by a cluster of PEMs from solid medium, represented by eq. (5.14 (a-h)), has been performed in Comsol Multiphysics (Burlington, MA, USA). In this simulation, a hemispherical PEMs cluster of diameter 7 mm is placed on solidified medium of 4 cm square with 0.5 cm depth. We have assumed that the

volume fraction of α- phase (ϵ_α) in the cluster has not varied with growth of PEMs as well as the PEMs cluster. The initial concentrations of nutrients, eq. (5.14 (g & h)), in the medium have been obtained from the protocol followed to prepare the medium in Table 5.1 and that in the PEMs cluster have been estimated from the experiment described above in the Methods section. Initial estimates of various parameters for different nutrients have been taken from literatures (Jørgensen et al., 1979; Aksnes and Egge, 1991; Siegrist and Gujer, 1985; Stewart, 2003; Clarkson, 1981; Kreft *et al*., 2001; Barber, 1984; Fiksen et al., 2013; Osuga and Komamine, 1994) and the values used in the model is tabulated below (Table 5.3). The diffusivity of a nutrient in the PEMs cluster has been considered isotropic and the effective diffusivity tensor in eq. (5.14a) is used as a scalar quantity in the simulation. The growth rates of eight clusters have been experimentally obtained by culturing them in ½ LP solidified medium for 11 days. The average growth rate is introduced in terms of surface velocity of a cluster in the simulation. The surface velocity of 0.015 cm/day corresponds to a growth rate of 0.017 g/day using an average cluster density of 0.9 g/cm^3.

Table 5.3 Values of model parameters and initial conditions

Model parameter and Initial conditions	Glucose	Fructose	Sucrose
D_{AM}	3.47 x 10^{-5} cm^2/s	0.231 x 10^{-5} cm^2/s	1.157 x 10^{-5} cm^2/s
$D_{A\alpha,\ eff}$	0.579 x 10^{-5} cm^2/s	0.231 x 10^{-5} cm^2/s	0.174 x 10^{-5} cm^2/s
ϕ_{max}	1.39 x 10^{-6} µmol/cm^2-s	0.116 x 10^{-7} µmol/cm^2-s	0.116 x 10^{-7} µmol/cm^2-s
K_m	0.01 µmol/cm^3	0.01 µmol/cm^3	0.001 µmol/cm^3
r_0	25 x 10^{-4} cm	25 x 10^{-4} cm	25 x 10^{-4} cm
ϵ_α	0.9	0.9	0.9
$\mathcal{K}$	8.0 µmol/cm^3	23.0 µmol/cm^3	4.75 µmol/cm^3
$\mathcal{K}_M$	29.1 µmol/cm^3	0 µmol/cm^3	0 µmol/cm^3

5.4 Results and Discussion

5.4.1 Sensitivity of model parameters

Sensitivity of the model for each parameter has been determined by an average percent change over time in nutrient concentration in the PEMs cluster due to ±10% change of the nominal value of a parameter. Parameter interactions on model sensitivity

have been evaluated by changing the nominal values of a set of parameters by ±10% simultaneously. Since there are six parameters, the total number of parameter interactions is 57 ($(2^6 - 1)$ – number of parameters). Among the six parameters, the model has shown sensitivity to ϵ_α, ϕ_{max}, and r_0 for glucose uptake. With a change of nominal values of these parameters, predicted glucose concentrations have changed 10% or more. Among them the model is most sensitive to ϵ_α as shown in Figure 5.4, where increasing or decreasing its value increases or decreases the concentration of glucose in the cluster. The fraction of volume occupied by embryogenic cells and tissues in a cluster decreases if the volume fraction of $\alpha - phase$ increases and vice versa. More embryogenic cells in the cluster means more consumption of nutrients through metabolism. So residual concentration of nutrient decreases more rapidly with decrease in ϵ_α in the cluster which has been observed in the sensitivity plots for glucose, fructose, and sucrose. The model is also very sensitive to interactions between ϵ_α and other parameters. Though the model is sensitive to ϕ_{max}, and r_0, their simultaneous change does not impact on the predicted glucose concentrations in the cluster. Volume fraction of $\alpha - phase$ is also dominant on model sensitivity for fructose and sucrose. Changes in concentrations of these nutrients are much less than 10% for parameters other than ϵ_α.

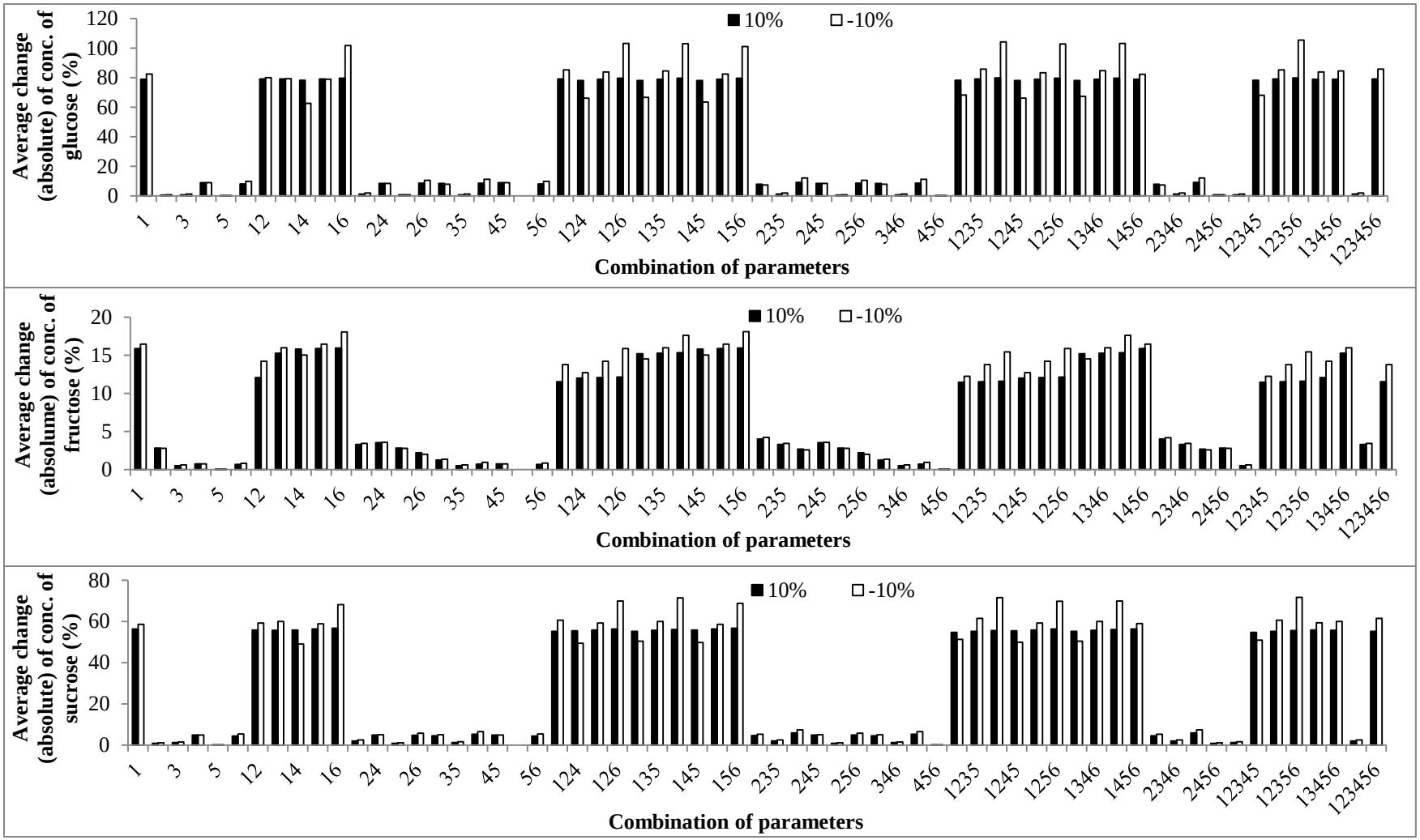

Figure 5.4 Determination of model sensitivity with ±10% change of each parameter and their combination to estimate the effect of parameter interactions on concentration distributions of nutrient in a PEMs cluster. Here 1- ϵ_α, 2 - .D_{AM}, 3 - $D_{A\alpha,eff}$, 4 - ϕ_{max}, 5 - K_m, 6 - r_0. Two and higher digit numbers represent combination of parameters.

5.4.2 Experiment and Simulation

5.4.2.1 Glucose concentrations in the medium and PEMs clusters

The nutritional model predicts the uptake and accumulation of glucose by the Norway spruce PEMs clusters from gel proliferation medium. In case of both top and bottom sections of the cluster, glucose concentration rapidly reached a maximum level in 12 hours, then uptake continued but at a lower rate compared to glucose consumption which was depicted by the start of a gradual decline of concentration close to the initial level almost at a constant rate (Figure 5.5(a)). A similar trend has been observed for sugar accumulation, though at a lesser rate, in hairy root culture of *Catharanthus roseus* by Cloutier et al. (2008), but their nutritional model simulated a sharp rise of intracellular sugar concentration to a maximum value in no time and remained constant during the culture period which was not in accordance with their experiment. A rapid increase in glucose accumulation in a PEMs cluster and a slow decrease to initial glucose concentration has been predicted by the model developed in this study. The predicted concentrations of glucose in the clusters are within ± σ (standard deviation, SD) of average observations at different time periods in the experiment, except concentrations on day 0.5 and 7. Concentrations on those days deviate from mean concentrations of glucose in top and bottom sections of PEMs clusters by 1.25 σ and1.56 σ respectively. Initially, before culture inoculation, average concentrations of glucose in top and bottom PEMs were 6.23 (SD = 3.92) and 7.11 (SD = 4.21) μmol/cm^3 respectively. After 10 days of culture on proliferation medium, when glucose uptake from the medium was followed by consumption in cells, concentrations in top and bottom PEMs reached 7.55 (SD = 4.37) and 5.14 (SD = 5.43) μmol/cm^3 respectively. The initial and final predicted

concentrations are 9.88 and 6.68 μmol/cm^3 respectively. So glucose may be considered as a limiting nutrient since in both experiment and simulation, final glucose concentrations approached initial concentrations. Therefore, this model can identify the limiting nutrient in somatic embryogenesis. The model also predicts glucose depletion in the medium due to nutrient uptake. The initial concentration in the medium was 29.1μmol/cm^3. However within 12 hours after inoculation, most of the samples gained higher glucose concentrations than initial medium concentration in the experiment. The rise of glucose concentrations in clusters was mainly due to higher concentration in the culture medium; additionally the hydrolysis of residual sucrose in PEMs clusters might lead to further increase in glucose concentrations. Autoclaving results in a more acidic tissue culture media which causes hydrolysis of sucrose in the medium with a pH between 3.5 and 5.8 (Wann et al., 1997). This implies that hydrolysis of sucrose is catalyzed in presence of hydrogen ions (H^+) according to the reaction below.

$$\underset{\text{(sucrose)}}{C_{12}H_{22}O_{11}} + H_2O + H^+ \rightarrow \underset{\text{(glucose)}}{C_6H_{12}O_6} + \underset{\text{(fructose)}}{C_6H_{12}O_6} + H^+$$

The initial pH of ½ LP medium supplemented with glucose was set to 5.8 before autoclaving. The pH of the medium containing glucose, maltose, or fructose instead of sucrose is reduced significantly after autoclaving (Owen et al., 1991), which makes the medium more acidic and therefore increases the availability of H^+. The diffusion or carrier transportation of hydrogen ions into the clusters would result in a higher rate of sucrose hydrolysis and a rapid increase in concentration of glucose following inoculation

on the fresh medium. A precise and accurate description of this phenomenon could improve the capacity of the nutrient model.

5.4.2.2 Sucrose concentrations in the medium and PEMs clusters

The predicted results of the model simulation of sucrose concentrations in a PEMs cluster follow the experimental sucrose concentrations in top and bottom sections of the clusters. In the experiment, when clusters were inoculated with the fresh medium, which was more acidic in nature owing to autoclaving the medium containing glucose, rapid hydrolysis of residual sucrose might have occurred between start of inoculation and 12 hours. This, along with diffusion of sucrose to the medium, resulted in a steeper fall of sucrose concentrations in the clusters (Figure 5.5(b)). A deceleration in sucrose breakdown started after 12 hours from inoculation and continued till day 2. Also diffusion of sucrose from the clusters to the medium resulted in a concentration jump in the medium as predicted by the model. By the time the catalytic property of the medium to hydrolyze sucrose was exhausted, the depletion rate of sucrose dropped markedly in the PEMs clusters, and concentrations remained almost similar from day 2 through the end of the culture period. The predicted sucrose concentrations in a cluster at different times are within $\pm \sigma$ of average concentrations of top and bottom sections of PEMs clusters together in the experiment except on day 7 when the predicted concentration is in the range of 1.21 σ.

5.4.2.3 Fructose concentrations in the medium and PEMs clusters

Sharp decline in concentrations of fructose was experimentally observed in both top and bottom PEMs in the first 12 hours after inoculation in glucose-containing ½ LP gel medium. Previously these PEMs clusters were subcultured in a proliferation medium containing 29.2 mM sucrose. So concentrations of free fructose still remained in a detectable range in the clusters after about 2 weeks of culture owing to synthesis of fructose from hydrolysis of sucrose. When the clusters were transferred to the glucose-containing medium, i.e., when there was no exogenous sucrose supplement, fructose synthesis was hindered. The residual fructose might have taken part in the glycolysis process where the sucrose was broken down in enzymatic pathways by invertases to form pyruvates leading to decrease in fructose concentrations in the clusters. Moreover, diffusion of fructose to the medium might also have played a major role in decreasing fructose concentrations in the PEMs clusters. This is represented by the predicted fructose concentrations in the medium in Figure 5.5(c). The model simulation of fructose concentrations in a PEMs cluster nicely fits with the experimental data showing a rapid decrease in concentration in the first 12 hours of inoculation, and after 2 days it becomes nearly stable. The concentrations predicted from the model at different times during the culture period are in the range of $\pm \sigma$ of mean concentrations of top and bottom sections of PEMs aggregates together in the experiment except on day 7 and day 10 when the model predictions are little underestimated, with concentrations within 1.77 σ and 1.13 σ respectively.

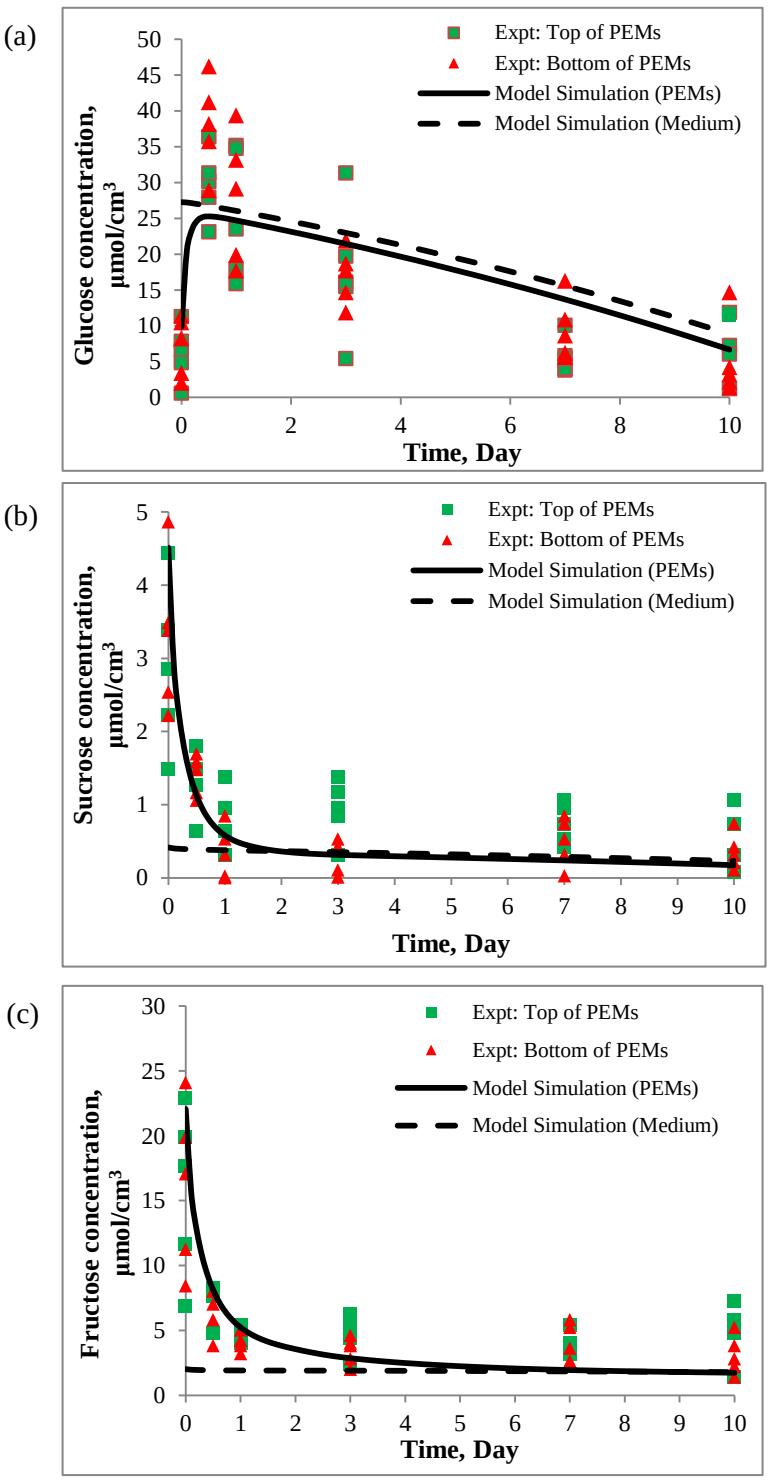

Figure 5.5 Nutrient concentrations from experiment and model simulation in PEMs clusters of Norway spruce cultured for 10 days on ½ LP solid medium supplemented with 29.1 mM glucose. Each cluster has been sliced into two parts, top and bottom. Nutrient concentrations in the medium are the predicted results from simulation; (a) glucose concentrations, (b) sucrose concentrations, (c) fructose concentrations.

CHAPTER 6

CONCLUSIONS AND CONTRIBUTIONS

6.1 Conclusions

This thesis has reported an investigation through a series of experiments and mathematical modeling on the effect of dispersion of proembryogenic masses of Norway spruce on somatic embryo development. The following conclusions can be made from this investigation.

Dispersion of PEMs at the beginning of proliferation resulted in an enhanced development of somatic embryos of Norway spruce in both liquid and solid culture. The embryo development increased two folds and three to five folds in dispersed PEMs compared to non-dispersed aggregates of PEMs in solid and liquid culture respectively. Bioreactor culture has shown higher yield of mature embryos compared to solid culture. This may be owing to better gas exchange and access of PEMs in the bioreactor to oxygen, which plays a vital role for metabolic processes of nutrients and provide energy for the growth of the cells (Forster and Estabrook, 1993). Though dispersion caused strain on aggregates of PEMs to be dispersed, it did not have an unfavorable impact on proliferation of PEMs and maturation of somatic embryos as indicated by the increased rate of proliferation and embryo maturation.

Dispersion improved synchronization of embryo development in one of two cell lines in liquid medium and two of four cell lines on solid medium. In cell line 11:12:02,

embryo development was more synchronized in dispersed compared to non-dispersed PEMs in both media. Though dispersion has ensured same nutritional environment to all PEMs, genetic differences among cell lines, and varying level of development of immature embryos in the culture might possibly be the reasons for still not having more synchronized growth of embryos in some cell lines.

Both the model simulation and the experiment have shown that clusters of PEMs were saturated with glucose, which serves as an energy source, in a few hours after inoculation on solid medium. So in PEMs clusters, there was no scarcity of nutrients that would inhibit the growth and development of somatic embryos. Though dispersion resulted in a large number of mature somatic embryos, it might not play the decisive role in synchronized development of embryos.

6.2 Contributions

This research has contributed to the knowledge of how disintegration of proembryogenic masses by dispersion before proliferation affects the enhancement and synchronization of somatic embryo development of Norway spruce and whether synchronized growth of somatic embryos is related to nutrient uptake and distribution in cell clusters.

A dispersion method developed recently (Aidun and Egertsdotter, Patent 2011/043731) has been automated for more rapid and controlled experiments. The disperser successfully dispersed the PEMs to a size equal to or less than 0.2 mm^2.

A temporary immersion bioreactor has been designed based on key parameters of a well-functioning bioreactor (identified by reviewing bioreactor technologies) such as shear, gas exchange, sterility, exchange of medium, and synchronization of embryo development, to investigate the effect of dispersion on embryo development.

A mathematical model using the Michaelis-Menten enzyme kinetics for the uptake of nutrients by cells and tissues has been developed to estimate nutrient distributions in a cluster of PEMs. The simulation of the model showed a rapid uptake of glucose from the medium within 12 hours (Figure 6.1) and then a steady drop in residual concentrations in the PEMs cluster over the period of culture. A similar trend of glucose uptake by PEMs clusters has been observed in enzymatic assaying of soluble sugars. The model simulation of fructose and sucrose concentrations in an aggregate of PEMs nicely fitted with the experimental data.

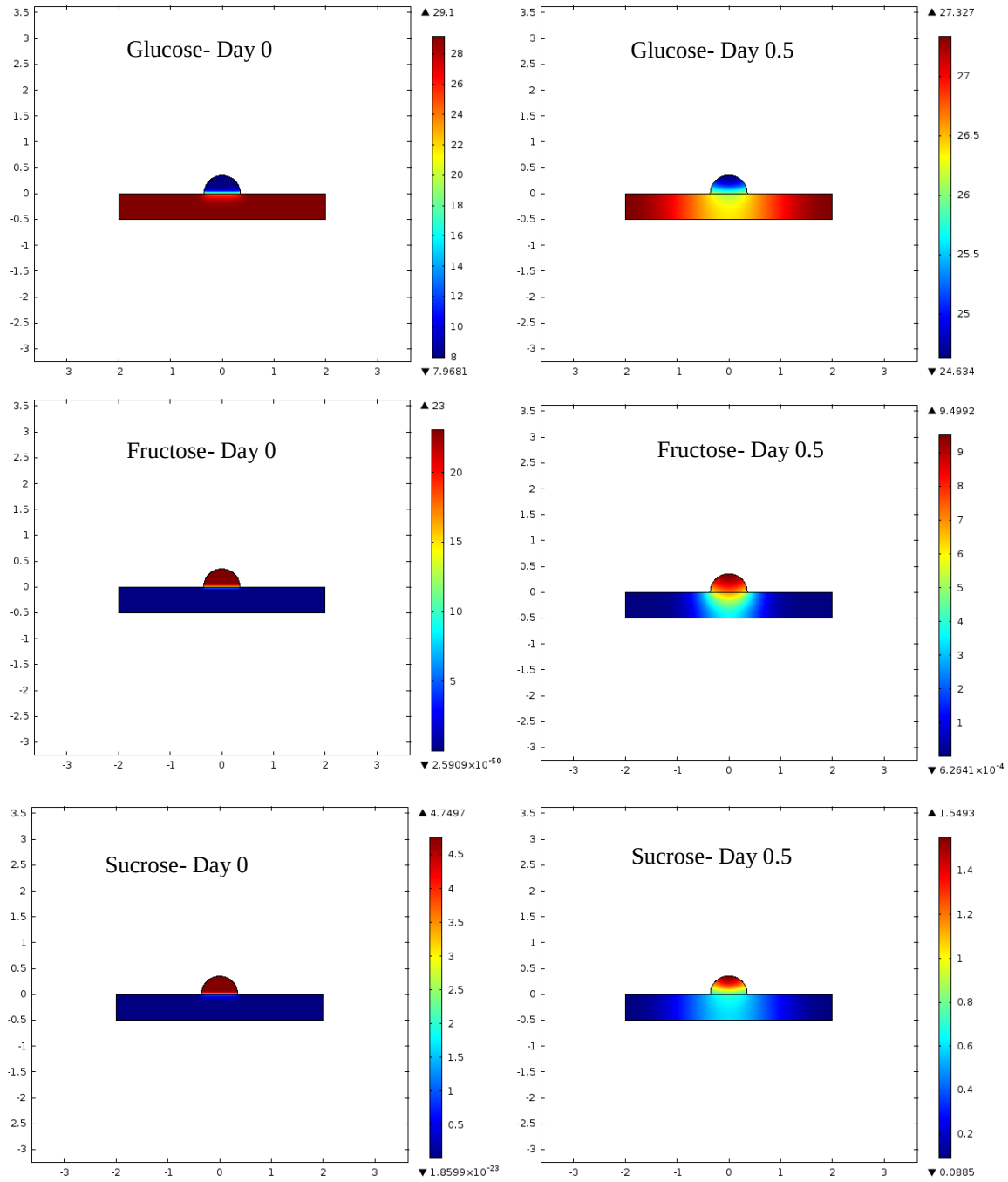

Figure 6.1 Model simulation showing nutrient (sugars) distributions in a PEMs cluster right before the start of culture (Day 0) and 12 hours after inoculation (Day 0.5). Initial concentrations of glucose, fructose, and sucrose in the PEMs cluster were 8, 4.75, 23 μmol/cm^3 respectively, and 29.1, 0, and 0 μmol/cm^3 respectively in the medium. Within 12 hours of subculture, the cluster of PEMs achieved nearly homogeneous distribution of glucose throughout.

CHAPTER 7

FUTURE WORK

In continuity of this work, a few suggestions are provided here for further investigation that would be of great interest.

Dispersion of clusters of PEMs has provided same nutritional environment to all PEMs and enhanced the development of somatic embryos of Norway spruce cultured in both liquid and solid medium. However synchronized growth of embryos in some cell lines has not been observed possibly owing to genetic differences among cell lines, and varying level of development of immature embryos in the culture. To become certain genetic markers of different cell lines can be identified. In this regard, variation in developmental stages of immature embryos in cultures of different cell lines may also be explored.

A nutrient may enhance (positive cooperativity) or interfere (negative cooperativity) the uptake of subsequent nutrient by the cells, or there may be no cooperativity. If there is a cooperativity with respect to nutrient binding to proteins at the cell membrane, a plot of uptake rate as a function of nutrient concentration is not hyperbolic as the Michaelis-Menten enzyme kinetics model, instead it may be a sigmoidal shape. In that case the Hill equation would be appropriate. In a case study, if the positive, negative, and no cooperativity are plotted against nutrient concentrations (Keener and Sneyd, 2009), the reaction velocities (uptake rate) do not vary in an order of

magnitude among these three cases. So no cooperativity during nutrient uptake has been assumed in the mathematical model developed in this research, since it might not impact on the prediction significantly. However, a study on nutrient cooperativity in plant cell culture would be beneficial to predict nutrient uptake more accurately. A mathematical expression of growth rate of cells may also be coupled to the model.

In this research, enzymatic analyses of sucrose, glucose, and fructose have been carried out to validate the mathematical model. Further investigation on other nutrients might extend the model capacity.

APPENDIX A: BIOREACTOR FOR PLANT CELL CULTURES

Stirred tank bioreactor		
Plant Species	**Author and Year**	**Observation**
Glycine max, *Pinus elliottii*	Treat et al. (1989)	Compared to flat blade impeller, smaller cell aggregates, higher cell viabilities (over 90%), equivalent biomass production (tangential design) using cell-lift impeller
Eschscholtzia californica	Taticek et al. (1990)	(Stirred tank & Bubble column); higher cell viability, and slower carbohydrate and oxygen (bubble column) uptake rates in the bioreactors compared to shake flasks
Catharanthus roseus, Nicotiana tabacum, Glycine max	Archambault et al. (1990)	(Stirred tank & Airlift); uniform and strong attachment of cells to the immobilizing structures introduced to these bioreactors and high cell retention (~96%) were achieved
Thalictrum rugosum	Facchini & DiCosmo (1990)	Growth and specific productivity of alkaloids were lower in immobilized cell culture in bioreactor compared to both immobilized and suspension culture in shake flasks
Tripterygium wilfordii	Pépin et al. (1991)	Cell immobilization resulted in comparable biomass production and carbohydrate uptake, and increased ammonium and nitrate uptake as that in suspension culture

Thalictrum rugosum	Kim et al. (1991b)	Berberine productivity in a bioreactor equipped with cell lift impeller and perfusion system was comparable to that in shake flask
Santalum album L.	Valluri et al. (1991)	Both cell lines had higher specific growth rate, lower fresh weight doubling time, and higher phenolics production in bioreactors compared to shake flask
Catharanthus roseus	Jolicoeur et al. (1992)	In bioreactors with double helical ribbon impellers (120 rpm), similar growth rate and biomass concentrations in high density cultures were achieved as in shake flasks
Catharanthus roseus	Schlatmann et al. (1994)	Higher concentration of dissolved O_2 resulted in increased ajmalicine production
Nicotiana tabacum	Ho et al. (1995)	Biomass productivity was hampered mainly due to shear stress caused by impeller agitation
Anchusa officinalis	Su et al. (1995)	Comparable cell density and rosmarinic acid production were achieved with controlled agitation, aeration, and dissolved O_2 concentration in a bioreactor and shake flask with intermittent medium exchange
Zea mays L.	Kovács *et al. (1995)*	Optimized pH (4.7) and dissolved O_2 concentration (40%) in the medium for higher haploid maize cells proliferation

Picea sitchensis	Moorhouse et al. (1996)	Demonstrated 2-way bubble free aeration and agitation system to develop mature somatic embryos
Trichosanthes kirilowii	Stoner et al. (1997)	Produced ribosome-inactivating protein in suspension culture
Lilium formolongi hort.	Godo et al. (1998)	Similar cell proliferation in shake flask and bioreactor; addition of BA to solid medium was favorable to shoot formation, but that was not the case in liquid medium; sucrose concentration also affected the shoot regeneration
Stizolobium hassjoo	Huang & Chen (1998)	Use of modified Murashige-Skoog (MS) medium in shake flasks and bioreactors enhanced the L-DOPA (3,4-dihydroxyphenylalanine) production
Xanthomonas campestris	Amanullah et al. (1998)	Among 4 different impellers maximum biomass production and xanthan productivity were resulted from highly viscous suspension cultures stirred by a pitched blade impeller (Prochem Maxflo T) and a 6-bladed Scaba SRGT impeller respectively
Cyclamen persicum Mill.	Hohe et al. (1999)	CO_2 accumulated in the bioreactors inhibited the cell growth

Digitalis lanata	Choi et al. (1999)	Cell growth was slightly lower than the control in aqueous two- phase polymer system, used in bioseparation or *in situ* extraction, of polyethylene glycol & dextran
Oryza sativa L.,	Moon et al. (1999)	(Stirred tank & Airlift); though agitation reduced the cell growth, use of cell immobilization supports effectively eliminated the hydrodynamic stresses on the cells
Catharanthus roseus	Keßler et al. (1999)	Production of ajmalicine & tryptamine varied with the size of cell aggregates (23-250µm)
Panax notoginseng	Zhong et al. (1999)	Cell density, biomass and saponin productivities were better in centrifugal impeller bioreactor than in turbine bioreactor & comparable to values in shake flask
Morinda elliptica	Abdullah et al. (2000)	Production medium enhanced cell growth and anthraquinone production than growth medium; continuous aeration increased growth rate in bioreactors with reduced number of impellers
Oryza sativa L.	Liu et al. (2000)	Reducing hydrodynamic shear on rice callus immobilized using polyurethane foam and stainless steel mesh increased the regeneration ability of cells

Stizolobium hassjoo	Chen & Huang (2000)	Better cell proliferation using flat blade than disk turbine impeller in the range of tested rpm; however variation of L-DOPA production was not that significant
Rice cell	Terashima et al. (2000)	Reduced glucose concentration in the fresh culture medium increased the production of recombinant human α_1-antitrypsin (rAAT)
Solanum chrysotrichum	Trejo-Tapia et al. (2001)	Analyzed the morphological of cell aggregates on broth rheology
Stizolobium hassjoo	Huang et al. (2002)	Investigated the importance of O_2 transfer rate and hydrodynamic shear on L-DOPA production
Taxus chinensis	Zhong et al. (2002)	Increased mixing rate and culture elicitation using methyl jasmonate favored cell growth and taxuyunnanine C production
Vaccinium pahalae	Meyer et al. (2002)	Optimized the irradiation, size of cell aggregates, and agitation rate for the production of anthocyanin
Nicotiana tabacum	Lee & Kim (2002)	Studied the effect of surface active agents to enhance cell growth and production of mGM-CSF
Taxus chinensis	Luo et al. (2002)	Feeding sucrose and causing dissolved O_2 tension (DOT) in the medium resulted in the

		maximum production of paclitaxel
Oryza sativa L.	Trexler et al. (2002)	Demonstrated the increase in production of recombinant Human α_1- antitrypsin (rAAT) using rice α-amylase (RAmy3D) promotor
Anchusa officinalis	Su & Arias (2003)	Use of bioreactor with continuous perfusion for production of acid phosphatase (APase)
Salvia officinalis L.	Bolta et al. (2003)	Investigated the effect of particle size (single cell and cell aggregates) on accumulation of ursolic acid
Panax ginseng	Jeong et al. (2003)	(Stirred tank & Bubble column); observed hairy root growth in bioreactors
Podophyllum hexandrum	Chattopadhyay et al. (2003)	Improved cell growth and podophyllotoxin production while having continuous cell retention
Panax notoginseng	Zhang & Zhong (2004)	Initial volumetric O_2 transfer coefficient greatly affected the cell growth and production of ginseng saponin & polysaccharide in high density culture
Elaeis guineensis Jacq.	Gorret et al. (2004)	Investigated the effect of nitrogen source, inoculum size, & conditioned medium on biomass production
Uncaria tomentosa	Trejo-Tapia et al. (2005)	Increased cell growth (also area of a single cell) and monoterpenoid oxindole alkaloid

		production compared to shake flask
Daucus carota, Picea abies, Betula pendula, Cyclamen persicum, Begonia cheimantha	Hvoslef-Eide et al. (2005)	Controlled environment and operating conditions improved cell growth in the bioreactors
Eschscholtzia californica, Catharanthus roseus	Hisiger & Jolicoeur (2005)	Investigated a multi-wavelength fluorescence probe for *in situ* estimation of biomass and secondary metabolites production
Lavandula vera MM	Pavlov et al. (2005)	Optimized the bioreactor operating conditions for biosynthesis of rosmarinic acid & resulted in the maximum yield 2x higher than shake flask culture
Nicotiana tabacum	Xu et al. (2005)	Produced a glycoprotein-based gum, gum arabic-8, using synthetic gene approach
Eschscholtzia californica	De Dobbeleer et al. (2006)	The bioreactor facilitated continuous extraction of secondary metabolites by keeping cells and cell aggregates separated from culture medium
Lilium formolongi Hort.	Ho et al. (2006)	(Stirred tank & Air lift); among four different types of bioreactors, only one (modified for low shear and more O_2 supply) was successful in cell growth and plant regeneration

Nicotiana tabacum	Lee & Kim (2006)	Perfusion culture enhanced cell growth and recombinant protein production
Azadirachta indica	Prakash & Srivastava (2006)	Increased cell growth and azadirachtin production were observed by eliminating nutrient limitations in the medium at different times from model simulation
Nicotiana tabacum L.	Cho et al. (2007)	Effectively used Pluronic F-68 (nonionic surfactant) to increase the level of extracellular hGM-CSF
Azadirachta indica	Prakash & Srivastava (2008)	Cell culture with addition of elicitor(s) in optimized concentrations increase azadirachtin production
Curcuma zedoaria Roscoe	Loc et al. (2008)	Secondary metabolites and antioxidant enzymes were extracted from cell cultures and the activities of antioxidant enzymes were accessed
Brugmansia candida	Cardillo et al. (2010)	Increased production of hairy root biomass and scopolamine and anisodamine in bioreactor compared to culture in Erlenmeyer flasks
Airlift bioreactor		
Thalictrum rugosum	Kim et al. (1991a)	Preventing clogging of draft tube by cell scraper at high cell density improved cell growth but lowered the extracellular berberine

		productivity; berberine production increased with addition of CO_2 and ethylene mixture
Datura stramonium	Ballica & Ryu (1993)	Aeration rate in the bioreactor had significant effect on cell growth and alkaloid production
Chenopodium rubrum L.	Fischer et al. (1994)	CO_2 enriched air injected through sparger of bioreactor equipped with florescent lamps favored the biomass growth enormously in a large-scale culture
Ipomoea batatas	Bieniek et al. (1995)	Mature embryos were formed, however shear damage in some embryos caused by sparged air was spotted; except having longer and reduced number of embryos in the bioreactor (purged), no significant morphological difference was observed with those developed in shake flask (closed)
Frangula alnus Mill.	Sajc et al. (1995)	Anthraquinones production increased through continuous extraction by non-aqueous solvent compared to immobilized culture in shake flask
Chenopodium rubrum	Fischer & Alfermann (1995)	Higher growth rate of cells was achieved with better illumination and supply of CO_2
Anchusa officinalis	Su et al. (1996)	Compared to batch culture higher cell density

		and protein concentration with continuous perfusion (a low level of osmotic concentration triggered perfusion)
Rhodiola sachalinensis	Jianfeng et al. (1998)	Similar yield of salidroside in shake flask and bioreactor cultures; no foam formation in the bioreactor
Picea sitchensis	Ingram & Mavituna (2000)	(Airlift, Stirred tank, & Bubble Column); both bubble column and stirred tank bioreactors produced maximum number of somatic embryos, matured on solid medium, of different cell lines
Panax notoginseng	Woragidbumrung et al. (2001)	Cell growth and ginseng polysaccharide production in regular and high density cultures were favored by using conditioned medium (spent medium)
Panax notoginseng	Hu & Zhong (2001)	Optimized the clearance between draft tube and bottom of the bioreactor for increased cell growth and production of ginseng saponin and polysaccharide
Beta vulgaris	Sánchez et al. (2002)	Rheological property of the medium changed with accumulation of extracellular proteins
Vitis vinifera, *Phytolacca*	Honda et al. (2002)	A viscous additive, carboxymethyl cellulose, supplemented medium increased the cell

Americana		growth and pigment production by reducing the turbulence in the culture
Taxus chinensis	Dong & Zhong (2002)	Enhanced taxuyunnanine C (TC) productivity was observed through combined use of methyl jasmonate, sucrose, and ethylene in inlet air
Taxus chinensis	Wang & Zhong (2002)	Elicitation of methyl jasmonate several times during the culture period enhanced taxuyunnanine C (TC) production
Panax notoginseng	Han & Zhong (2003)	Optimized the partial pressure of oxygen (pO_2) for cell growth, and production of ginseng saponin & polysaccharide
Sandalwood	Pal et al. (2003)	Analyzed the spent medium of somatic embryogenesis for various enzymes, arabinogalactan protein, and sandal oil
Taxus chinensis	Qian et al. (2005)	Enhanced production of taxuyunnanine C by adding sucrose and 2,3-dihydroxypropyl jasmonate to the culture
Panax notoginseng	Wang et al. (2005)	Established a protocol of methyl jasmonate elicitation to enhance the production of ginsenoside
Daucus carota L.	Mizukami et al. (2008)	Plantlets were regenerated successfully from hypocotyl segments
Bubble column bioreactor		

Perilla frutescens	Zhong et al. (1991)	Culture in the bioreactor with appropriate irradiation resulted in equivalent amount of anthocyanin pigment production as in shake flasks
Coffea arabica	Kurata & Furusaki (1993)	Even at low aeration rate cells were damaged and no alkaloid production in suspension, however immobilization of cells resulted in purine production; proper irradiation had also a favorable effect on alkaloid production
Lithospermum erythrorhizon	Sim & Chang (1993)	Increased shikonin production in the bioreactor than in shake flask; addition of n-hexadane in proper amount for *in situ* extraction enhanced shikonin production
Stevia rebaudiana	Akita et al. (1994)	200,000 plantlets were produced from shoots in a 500 L bioreactor (florescent lamps inside) in one batch; bubbles damaged the shoots right above the air sparger
Taxus baccata	Srinivasan et al. (1995)	Bubble column bioreactor resulted in more taxol production compared to Erlenmeyer flask and stirred tank; phosphate was considered as a growth limiting nutrient
Capsicum annuum	Mavituna & Buyukalaca	(Bubble column & Stirred tank); magnetically stirred bioreactor showed better performance in

	(1996)	mixing & embryo conversion from cells and cell clusters compared to bubble column bioreactor
Hyoscyamus muticus	Hsiao et al. (1999)	(Bubble column & Stirred tank); Effective specific growth rate of biomass was twice in plastic liners sterilized by autoclave compared to the one sterilized with ethylene oxide
Taxus chinensis	Pan et al. (2000)	(Bubble Column, Airlift, & Stirred tank); investigation of the effects of O_2, CO_2, ethylene & shear revealed that the addition of ethylene to inlet air at an optimal level increased both cell growth and taxane production in bubble column bioreactor
Panax ginseng C. A. Meyer	Choi et al. (2000)	Induced multiple adventitious roots in root segments of ginseng with profiles similar to field-grown ginseng roots
Panax notoginseng	Hu et al. (2001)	(Bubble column & Airlift); Increased productivity of biomass, ginseng saponin and polysaccharide in a high density culture by applying a fed-batch cultivation strategy
Daucus carota	Kim & Yoo (2002)	Optimized the sucrose concentrations for increased growth of hairy root culture and superoxide dismutase synthesis

Catharanthus roseus	Tikhomiroff et al. (2002)	Use of silicon oil in the bioreactor having hairy root cultures increased the specific yield of indole alkaloids
Eleutherococcus senticosus	Choi & Jeong (2002)	Early cotyledonary stage somatic embryos were developed in the bioreactors to investigate the dormancy characteristics with sucrose treatment
Hypericum perforatum L.	Zobayed et al. (2003)	Investigated the increase in synthesis of bioactive molecules, such as, hypericin, pseudohypericin, and hyperforin in bioreactor with regulated supply of carbon
Anoectochilus, apple, *Chrysanthemum*, garlic, ginseng, grape, *Lilium*, *Phalaenopsis* & potato	Paek et al. (2005)	(Bubble column & Temporary immersion); automated large-scale micropropagation in bioreactors
Eleutherococcus sessiliflorus	Shohael et al. (2005)	(Bubble column & Temporary immersion); large-scale production of mature somatic embryos
Eleutherococcus koreanum	Park et al. (2005)	Large-scale production of plantlets from adventitious roots explants via somatic

		embryogenesis
Panax ginseng	Thanh et al. (2006a & b)	Optimum concentrations of O_2 and CO_2 for cell growth and saponin production were established
Oldenlandia affinis	Seydel et al. (2009)	(Bubble Column & Airlift); Achieved expected productivity of cyclotide, kalata B1, from cell culture in the airlift bioreactor and maximum doubling time reduced to half compared to shake flask
Temporary immersion bioreactor		
Orchid, *Callistephus hortensis*, *Pheonix dactylifera* L., *Daucus carota* L., *Mitragyna inermis*	Tisserat and Vandercook (1985)	1.8 to 4 (varied with plant species) fold increase in fresh weight in the automated temporary immersion system compared to the manual system
Musa acuminata	Alvard et al. (1993)	Temporary immersion of the culture resulted in the highest multiplication rate among six different mode of treatments.
Hevea brasiliensis	Etienne et al. (1997)	Embryogenic induction in solid medium at lower concentration of growth regulators and then in temporary immersion without growth regulators & at lower concentration of $CaCl_2$

		and embryo development in temporary immersion resulted in maximum number of mature embryos among different treatments tested
Sugarcane	Lorenzo et al. (1998)	An optimized protocol resulted in increased shoot formation in the bioreactor compared to conventional protocol
Coffea arabica	Etienne-Barry et al. (1999)	Germinated embryos developed in the bioreactor from embryogenic masses; plantlets converted from germinated embryos depended on the density of somatic embryos in the bioreactor; high sucrose concentration in germination medium resulted in higher plant conversion and their subsequent growth
Solanum tuberosum L. (cvs. Desiree and Atlantic)	Jiménez et al. (1999)	Compared to cultures in solid medium, higher growth, more internodes per plant and absence of hyperhydricity were observed in temporary immersion culture
Ananas comosus L. Merr	Escalona et al. (1999)	Shoot multiplication rate was much higher in temporary immersion system compared to that in solid and liquid media
Camellia sinensis L.	Akula et al. (2000)	Temporary immersion was the most efficient among all other methods tested from

		multiplication of globular somatic embryos to germination
Coffea arabusta	Afreen et al. (2002)	A temporary root zone immersion system showed better success over modified RITA for plant development from somatic embryos and acclimatization
Coffea Arabica	Barry-Etienne et al. (2002)	Mature somatic embryos developed and germinated in the bioreactors; medium sized embryos (cotyledon area was 36%) resulted in highest conversion rate to plantlets
Hypericum perforatum L.	Zobayed and Saxena (2003)	(Temporary Immersion & Bubble column); comparative study of regeneration potential of different explants (root, shoot tip, leaf, hypocotyl, stem) and efficiency of bioreactors for shoot formation from root explants
Crescentia cujete	Murch et al. (2004)	Increased biomass production and longer and better quality plantlets were obtained in temporary immersion system
Saussurea medusa	Yuan et al. (2004)	Cell growth and flavonoids production were favored in the bioreactor
Pineapple culture	Pérez et al. (2004)	Observed the effect medium compositions (sucrose, inorganic salts, inositol, and thiamine) on shoot mass propagation and

		protease excretion
Fragaria ananassa	Hanhineva et al. (2005)	With less than half labor time, adventitious shoots were generated from leaf explants in bioreactors with comparable plantlet regeneration frequency on solid medium
Malus domestica	Zhu et al. (2005)	Optimized the shoot culture protocol to generate plantlets in the bioreactors
Eucalyptus clones	McAlister et al. (2005)	Increased productivity and plants with better acclimatization characteristics were observed in the bioreactor
Coffea arabica	Albarrán et al. (2005)	Optimized frequency and duration of immersion for increased growth, better quality somatic embryos, and higher conversion of embryos into plant
Banana hybrid "FHIA-18"	Kosky et al. (2006)	A qualitative study among plants regenerated from somatic embryos, shoot tips, and suckers was provided
Arnebia euchroma	Ge et al. (2006)	Increased shikonin production and cell growth compared to suspension culture
Beta vulgaris L.	Pavlov and Bley (2006)	Production of betalains from hairy root culture with optimized immersion frequency
Sugarcane	Snyman et al. (2007)	A huge number of somatic embryos were produced, germinated and regenerated into

		plantlets from immature leaf roll explants
Theobroma cacao L.	Niemenak et al. (2008)	Better development and increased number of somatic embryos were achieved in temporary immersion system (1 min immersion in every 6 hr) than in solid medium
Coffea arabica L. cvs. Caturra and Catuai	Gatica-Arias et al. (2008)	Higher proliferation of Catuaí callus was observed in Erlenmeyer flask, however 100% embryo germination was achieved in temporary immersion; 1 min of immersion in every 8 hr resulted in highest number of somatic embryos
Sugarcane (*Saccharum* spp.)	Mordocco et al. (2009)	Temporary immersion was successful in shoot generation from cultures established from leaf explants using a specific *in vitro* regeneration method
Cedrela odorata L.	Peña-Ramírez et al. (2010)	Shoot formation increased with using coconut water to the medium; shoot and root elongations increased in the bioreactor
Disposable bioreactor		
Potato, banana, fern, & gladiolus	Ziv et al. (1998)	Airlift type; shear damage of cells was greatly reduced in the disposable plastic film vessel; five to eightfold increase in biomass proliferation of meristematic clusters was

		observed
Populus tremula L.	Vinocur et al. (2000)	Thidiazuron (TDZ) enhanced bud-regeneration from roots compared to using benzyladenine (BA)
Taxus baccata	Bentebibel et al. (2005)	(Disposable (wave type), Airlift, & Stirred tank); successful use of bioreactors to increase paclitaxel production
Glycine max L., *Nicotiana tabacum*	Terrier et al. (2007)	(Disposable (wave-undertow, slug bubble) & Stirred tank); Disposable bioreactors resulted in comparable apparent growth rate of cells as stirred tank bioreactor and Erlenmeyer flasks; maintenance and operation of slug bubble bioreactor was simpler than wave & undertow bioreactor
Membrane bioreactor		
Beta vulgaris, *Catharanthus roseus*	Yang et al. (2003)	Investigated secondary metabolites production by applying steady and oscillatory electric fields while maintaining higher cell viabilities
Oryza sativa L.	McDonald et al. (2005)	Successfully produced α-1-antitrypsin, a human blood protein, from transgenic rice cell culture

Other types			
Bioreactor	**Plant Species**	**Author**	**Observation**

Type		**and Year**	
Magnetically stabilized fluidized bed (MSFB)	*Coffea arabica*	Bramble et al. (1990)	Reduced shear damage of cells in low shear environment in MSFB; cell growth was comparable but caffeine production was less in MSBF than in shake flask
Immobilized plant cell reactor	*Gossypium arboreum*	Choi et al. (1995)	Production of secondary metabolite increased through cell immobilization, permeabilization, and elicitation
Reciprocating plate bioreactor	*Vitis vinifera*	Gagnon et al. (1999)	Operation was not successful because of contamination and lack of optimized operating conditions (e.g. aeration, dissolved O_2 concentration, stripping off CO_2)
Rotating wall vessel bioreactor	*Taxus cuspidate*	Sun and Linden (1999)	Hydrodynamic shear stress improved the specific cell growth rate but reduced the Taxol production
Flow Bioreactor	Red beet hairy roots	Kino-Oka et al. (1999)	Hairy root elongation (DO conc.) & reduced viability at root-tip meristems (shear stress) in single column medium flow reactor, and uniform growth of hairy roots in radial flow reactor at optimal physical and operating conditions were observed

Ultrasonic nutrient mist bioreactor	*Artemisia annua* L.	Liu et al. (2003)	(Along with Airlift & Multi-plate radial flow bioreactor); nutrient mist bioreactor increased the growth of shoot culture and artemisinin synthesis the most among all tested bioreactors
Perfusion Bioreactor	*Eschscholtzia californica*	Gmati et al. (2004)	*In vivo* nuclear magnetic resonance was carried out for P^{31}

APPENDIX B: DERIVATION OF DIFFUSION FLUX, $\bar{J}_{\alpha\Sigma}$

Substituting eq. (5.7) for $[P_T]$ and eq. (5.9) for $[A_\alpha P_T]$ in eq. (5.5) results in

$$\bar{J}_{\alpha\Sigma} \cdot \hat{\bar{\xi}} = k_1 C_{A\alpha}(P_0 - [A_\alpha P_T]) - k_{-1} \frac{\left(k_1 C_{A\alpha} + k_{-2} C_{A\gamma}\right) P_0}{\left(k_{-1} + k_2 + k_1 C_{A\alpha} + k_{-2} C_{A\gamma}\right)} \tag{B1}$$

Again from eq. (5.9), the expression of $[A_\alpha P_T]$ results in eq. (B1) into

$$\bar{J}_{\alpha\Sigma} \cdot \hat{\bar{\xi}} =$$

$$k_1 C_{A\alpha} \left(P_0 - \frac{(k_1 C_{A\alpha} + k_{-2} C_{A\gamma}) P_0}{(k_{-1} + k_2 + k_1 C_{A\alpha} + k_{-2} C_{A\gamma})}\right) - k_{-1} \frac{(k_1 C_{A\alpha} + k_{-2} C_{A\gamma}) P_0}{(k_{-1} + k_2 + k_1 C_{A\alpha} + k_{-2} C_{A\gamma})} \tag{B2}$$

Factoring out P_0 from the 1st term of RHS of eq. (B2) gives

$$\bar{J}_{\alpha\Sigma} \cdot \hat{\bar{\xi}} = k_1 C_{A\alpha} \left(\frac{(k_{-1} + k_2) P_0}{k_{-1} + k_2 + k_1 C_{A\alpha} + k_{-2} C_{A\gamma}}\right)$$

$$- k_{-1} \frac{\left(k_1 C_{A\alpha} + k_{-2} C_{A\gamma}\right) P_0}{\left(k_{-1} + k_2 + k_1 C_{A\alpha} + k_{-2} C_{A\gamma}\right)} \tag{B3}$$

After subtracting the 2nd term from the 1st term in RHS of eq. (B3), one can get

$$\bar{J}_{\alpha\Sigma} \cdot \hat{\bar{\xi}} =$$

$$\left(\frac{k_{-1} k_1 C_{A\alpha} + k_2 k_1 C_{A\alpha} - k_{-1} k_1 C_{A\alpha} - k_{-1} k_{-2} C_{A\gamma}}{k_{-1} + k_2 + k_1 C_{A\alpha} + k_{-2} C_{A\gamma}}\right) P_0 \tag{B4}$$

Cancelling out $(k_{-1} k_1 C_{A\alpha})$ from the numerator in eq. (B4) results in

$$\bar{J}_{\alpha\Sigma} \cdot \hat{\bar{\xi}} = \left(\frac{k_2 k_1 C_{A\alpha} - k_{-1} k_{-2} C_{A\gamma}}{k_{-1} + k_2 + k_1 C_{A\alpha} + k_{-2} C_{A\gamma}}\right) P_0 \tag{B5}$$

which is eq. (5.10).

APPENDIX C: VOLUME AVERAGING

In an effort of developing spatially smooth transport equation, superficial average concentration and intrinsic average concentration will need to be used. The superficial average concentration for α and γ phases are defined as

$$\langle C_{A\alpha} \rangle = \frac{1}{\forall} \int_{\forall_\alpha(t)} C_{A\alpha} dV \tag{C1a}$$

and

$$\langle C_{A\gamma} \rangle = \frac{1}{\forall} \int_{\forall_\gamma(t)} C_{A\gamma} dV \tag{C1b}$$

respectively.

Intrinsic average concentrations for the two phases are defined as

$$\langle C_{A\alpha} \rangle^* = \frac{1}{\forall_\alpha(t)} \int_{\forall_\alpha(t)} C_{A\alpha} dV \tag{C2a}$$

and

$$\langle C_{A\gamma} \rangle^* = \frac{1}{\forall_\gamma(t)} \int_{\forall_\gamma(t)} C_{A\gamma} dV \tag{C2b}$$

Both $\forall_\alpha$ and $\forall_\gamma$ may vary with location ($\bar{x}$, the centroid of averging volume) of the averaging volume in the PEMs cluster and time (t) over which the PEMs grow (referring to the culture period). However for simplicity it is considered that the cells and maturing embryos are uniformly distributed, therefore, the phase volumes may only be the functions of time.

The averaging volume $\forall$ is

$$\forall = \forall_\alpha(t) + \forall_\gamma(t) \tag{C3}$$

which does not vary with time.

The superficial and intrinsic average contractions can be related with the help of volume fraction as

$$\epsilon_\alpha(t) = \epsilon_\alpha = \frac{\forall_\alpha(t)}{\forall} = \frac{\langle C_{A\alpha}\rangle}{\langle C_{A\alpha}\rangle^*}$$

i.e., $$\langle C_{A\alpha}\rangle = \epsilon_\alpha \langle C_{A\alpha}\rangle^* \qquad \text{(C4a)}$$

where, ϵ_α is the volume fraction of $\alpha - phase$. Similarly for the $\gamma - phase$

$$\langle C_{A\gamma}\rangle = \epsilon_\gamma \langle C_{A\gamma}\rangle^* \qquad \text{(C4b)}$$

To obtain the superficial average of the diffusion eq. (5.2) in α it can be written as

$$\frac{1}{\forall}\int\limits_{\forall_\alpha(t)} \frac{\partial C_{A\alpha}}{\partial t} dV = \frac{1}{\forall}\int\limits_{\forall_\alpha(t)} \nabla\cdot(D_{A\alpha}\nabla C_{A\alpha}) dV \qquad \text{(C5)}$$

The symbolic representation of this equation is

$$\left\langle \frac{\partial C_{A\alpha}}{\partial t}\right\rangle = \langle \nabla\cdot(D_{A\alpha}\nabla C_{A\alpha})\rangle \qquad \text{(C6)}$$

Applying the general transport theorem (Bird et. al. 2002, p. 824) to the LHS of eq. (C5) gives

$$\frac{1}{\forall}\left[\frac{\partial}{\partial t}\int\limits_{\forall_\alpha(t)} C_{A\alpha} dV - \int\limits_{\Sigma_-(t)} C_{A\alpha}\{\overline{w}_\Sigma\cdot\hat{\xi}\} dA\right] = \frac{1}{\forall}\int\limits_{\forall_\alpha(t)} \nabla\cdot(D_{A\alpha}\nabla C_{A\alpha}) dV$$

which can then be written as

$$\frac{1}{\forall}\frac{\partial}{\partial t}\int\limits_{\forall_\alpha(t)} C_{A\alpha} dV - \frac{1}{\forall}\int\limits_{\Sigma_-(t)} C_{A\alpha}\{\overline{w}_\Sigma\cdot\hat{\xi}\} dA = \frac{1}{\forall}\int\limits_{\forall_\alpha(t)} \nabla\cdot(D_{A\alpha}\nabla C_{A\alpha}) dV \qquad \text{(C7)}$$

It should be noted here that the $\alpha - phase$ may be bounded by both $\Sigma(t)$ and part of S surface, denoted as $S_\alpha(t)$. Since the averaging volume, $\forall$, always remain unchanged with location and time, any surface element on $S_\alpha(t)$ will not have a velocity with respect

to the centroid ($\bar{x}$) of $\forall$. However the interface $\Sigma(t)$ may be considered as a moving surface with respect to the centroid owing to the growth of the cells and maturing embryos.

Applying the symbolic representation, averaging eq. (C7) can be written as

$$\frac{\partial}{\partial t}\langle C_{A\alpha}\rangle - \frac{1}{\forall}\int_{\Sigma_-(t)} C_{A\alpha}\{\overline{w}_\Sigma \cdot \hat{\xi}\}dA = \langle \nabla \cdot (D_{A\alpha}\nabla C_{A\alpha})\rangle \qquad \text{(C8)}$$

In order to deal with the RHS of eq. (C8), it is necessary to apply the spatial averaging theorem (Whitaker 1973, 1985, 1999; Slattery 1990; Gray 1975) as a mathematical tool. Before that the divergence theorem will be applied to the RHS of eq. (C7) that results in

$$\frac{1}{\forall}\int_{\forall_\alpha(t)} \nabla \cdot (D_{A\alpha}\nabla C_{A\alpha})dV = \frac{1}{\forall}\int_{S_\alpha(t)} \hat{n} \cdot (D_{A\alpha}\nabla C_{A\alpha})dA + \frac{1}{\forall}\int_{\Sigma_-(t)} \hat{\xi} \cdot (D_{A\alpha}\nabla C_{A\alpha})dA \qquad \text{(C9)}$$

Also from Slattery (1967; eq. (8)) and Whitaker (1985; eq. (21)), it can be shown that (Appendix D)

$$\nabla \cdot \int_{\forall_\alpha(t)} \overline{\Psi}\, dV = \int_{S_\alpha(t)} \hat{n} \cdot \overline{\Psi}\, dA \qquad \text{(C10)}$$

Dividing eq. (C10) by $\forall$ gives

$$\nabla \cdot \frac{1}{\forall}\int_{\forall_\alpha(t)} \overline{\Psi}\, dV = \frac{1}{\forall}\int_{S_\alpha(t)} \hat{n} \cdot \overline{\Psi}\, dA \qquad \text{(C11)}$$

where $\overline{\Psi}$ is any parameter of either vector or tensor. Replacing $\overline{\Psi}$ with $D_{A\alpha}\nabla C_{A\alpha}$ in eq. (C11), one can obtain

$$\nabla \cdot \frac{1}{\forall}\int_{\forall_\alpha(t)} (D_{A\alpha}\nabla C_{A\alpha})\, dV = \frac{1}{\forall}\int_{S_\alpha(t)} \hat{n} \cdot (D_{A\alpha}\nabla C_{A\alpha})\, dA \qquad \text{(C12)}$$

Substituting eq. (C12) into eq. (C9) gives

$$\frac{1}{\forall}\int_{\forall_\alpha(t)} \nabla\cdot(D_{A\alpha}\nabla C_{A\alpha})dV$$

$$= \nabla\cdot\frac{1}{\forall}\int_{\forall_\alpha(t)} (D_{A\alpha}\nabla C_{A\alpha})\,dV + \frac{1}{\forall}\int_{\Sigma_-(t)} \hat{\xi}\cdot(D_{A\alpha}\nabla C_{A\alpha})dA \qquad \text{(C13)}$$

which can also be written as

$$\frac{1}{\forall}\int_{\forall_\alpha(t)} \nabla\cdot(D_{A\alpha}\nabla C_{A\alpha})dV = \nabla\cdot\frac{1}{\forall}\int_{\forall_\alpha(t)} (D_{A\alpha}\nabla C_{A\alpha})\,dV + \frac{1}{\forall}\int_{\Sigma_-(t)} \hat{\xi}\cdot(-\bar{J}_{\alpha\Sigma})dA$$

Then one may have

$$\frac{1}{\forall}\int_{\forall_\alpha(t)} \nabla\cdot(D_{A\alpha}\nabla C_{A\alpha})dV = \nabla\cdot\langle D_{A\alpha}\nabla C_{A\alpha}\rangle - \frac{1}{\forall}\int_{\Sigma_-(t)} \hat{\xi}\cdot(\bar{J}_{\alpha\Sigma})dA \qquad \text{(C14)}$$

Though $D_{A\alpha}$ is a function of pressure, temperature, and concentration (Reid et al., 1987; Whitaker, 1999), the pressure and temperature remain constant during the culture period of somatic embryogenesis.

Now eq. (C14) can be written as

$$\frac{1}{\forall}\int_{\forall_\alpha(t)} \nabla\cdot(D_{A\alpha}\nabla C_{A\alpha})dV = \nabla\cdot D_{A\alpha}\langle\nabla C_{A\alpha}\rangle - \frac{1}{\forall}\int_{\Sigma_-(t)} \hat{\xi}\cdot(\bar{J}_{\alpha\Sigma})dA \qquad \text{(C15)}$$

Applying the spatial averaging theorem (Whitaker, 1999) to $\langle\nabla C_{A\alpha}\rangle$ in eq. (C15) gives (Appendix D)

$$\langle\nabla C_{A\alpha}\rangle = \nabla\langle C_{A\alpha}\rangle + \frac{1}{\forall}\int_{\Sigma_-(t)} \hat{\xi}\,C_{A\alpha}\,dA \qquad \text{(C16)}$$

Combining eqs. (C15 & C16) results in

$$\frac{1}{\forall}\int_{\forall_\alpha(t)} \nabla\cdot(D_{A\alpha}\nabla C_{A\alpha})dV$$

$$= \nabla\cdot D_{A\alpha}\left\{\nabla\langle C_{A\alpha}\rangle + \frac{1}{\forall}\int_{\Sigma_-(t)} \hat{\xi}\, C_{A\alpha}\, dA\right\} - \frac{1}{\forall}\int_{\Sigma_-(t)} \hat{\xi}\cdot(\bar{J}_{\alpha\Sigma})dA \quad \text{(C17)}$$

With averaging symbol eq. (C17) becomes

$$\langle\nabla\cdot(D_{A\alpha}\nabla C_{A\alpha})\rangle = \nabla\cdot D_{A\alpha}\left\{\nabla\langle C_{A\alpha}\rangle + \frac{1}{\forall}\int_{\Sigma_-(t)} \hat{\xi}\, C_{A\alpha}\, dA\right\} - \frac{1}{\forall}\int_{\Sigma_-(t)} \hat{\xi}\cdot(\bar{J}_{\alpha\Sigma})dA \quad \text{(C18)}$$

Replacing $\langle\nabla\cdot(D_{A\alpha}\nabla C_{A\alpha})\rangle$ in eq. (B8) by the RHS of eq. (B18) gets the form of

$$\frac{\partial}{\partial t}\langle C_{A\alpha}\rangle - \frac{1}{\forall}\int_{\Sigma_-(t)} C_{A\alpha}\{\overline{w}_\Sigma\cdot\hat{\xi}\}dA$$

$$= \nabla\cdot D_{A\alpha}\left\{\nabla\langle C_{A\alpha}\rangle + \frac{1}{\forall}\int_{\Sigma_-(t)} \hat{\xi}\, C_{A\alpha}\, dA\right\} - \frac{1}{\forall}\int_{\Sigma_-(t)} \hat{\xi}\cdot(\bar{J}_{\alpha\Sigma})dA \quad \text{(C19)}$$

Applying the intrinsic average concentration shown in eq. (C4a), eq. (C19) becomes

$$\frac{\partial}{\partial t}\{\epsilon_\alpha\langle C_{A\alpha}\rangle^*\} - \frac{1}{\forall}\int_{\Sigma_-(t)} C_{A\alpha}\{\overline{w}_\Sigma\cdot\hat{\xi}\}dA$$

$$= \nabla\cdot D_{A\alpha}\left\{\nabla[\epsilon_\alpha\langle C_{A\alpha}\rangle^*] + \frac{1}{\forall}\int_{\Sigma_-(t)} \hat{\xi}\, C_{A\alpha}\, dA\right\}$$

$$- \frac{1}{\forall}\int_{\Sigma_-(t)} \hat{\xi}\cdot(\bar{J}_{\alpha\Sigma})dA \quad \text{(C20)}$$

The point concentration, $C_{A\alpha}$, in eq. (C20) may be eliminated by applying the spatial decomposition (Gray 1975) as

$$C_{A\alpha} = \langle C_{A\alpha}\rangle^* + \tilde{C}_{A\alpha} \quad \text{(C21)}$$

where $\tilde{C}_{A\alpha}$ represents the fluctuation of the intrinsic concentration in the averaging volume. So the 2nd term of RHS in eq. (C20) can be written as

$$\frac{1}{\forall}\int_{\Sigma_-(t)} \hat{\xi}\, C_{A\alpha}\, dA = \underbrace{\frac{1}{\forall}\int_{\Sigma_-(t)} \hat{\xi}\langle C_{A\alpha}\rangle^*\, dA}_{I_1} + \frac{1}{\forall}\int_{\Sigma_-(t)} \hat{\xi}\,\tilde{C}_{A\alpha}\, dA \tag{C22}$$

The intrinsic average concentration, $\langle C_{A\alpha}\rangle^*$, in I_1 is evaluated over the volume of $\alpha - phase$ (extracellular phase) in the averaging volume, $\forall$. So $\langle C_{A\alpha}\rangle^*$ should remain unchanged at any point in that phase of the concerned $\forall$ at any instance of time. Then I_1 can be written as

$$I_1 = \langle C_{A\alpha}\rangle^* \frac{1}{\forall}\int_{\Sigma_-(t)} \hat{\xi}\, dA = \langle C_{A\alpha}\rangle^* \frac{1}{\forall}\int_{\Sigma_-(t)} \hat{\xi}\,(1) dA \tag{C23}$$

Now invoking the spatial averaging equation for $\nabla\langle 1\rangle$, it can expressed as

$$\nabla\langle 1\rangle = \langle \nabla 1\rangle - \frac{1}{\forall}\int_{\Sigma_-(t)} \hat{\xi}\,(1) dA = -\frac{1}{\forall}\int_{\Sigma_-(t)} \hat{\xi}\,(1) dA \tag{C24}$$

So eq. (C23) becomes

$$I_1 = -\langle C_{A\alpha}\rangle^* \nabla\langle 1\rangle \tag{C25}$$

Applying the definition of averaging, as in eq. (C1a), in eq. (C25) gives

$$I_1 = -\langle C_{A\alpha}\rangle^* \nabla \frac{1}{\forall}\int_{\forall_\alpha(t)} (1) dV = -\langle C_{A\alpha}\rangle^* \nabla \frac{\forall_\alpha(t)}{\forall} = -\langle C_{A\alpha}\rangle^* \nabla \epsilon_\alpha \tag{C26}$$

Substituting I_1, eq. (C22) becomes

$$\frac{1}{\forall}\int_{\Sigma_-(t)} \hat{\xi}\, C_{A\alpha}\, dA = -\langle C_{A\alpha}\rangle^* \nabla\epsilon_\alpha + \frac{1}{\forall}\int_{\Sigma_-(t)} \hat{\xi}\,\tilde{C}_{A\alpha}\, dA \tag{C27}$$

Substituting eq. (C27) in eq. (C20) will result

$$\frac{\partial}{\partial t}\{\epsilon_\alpha\langle C_{A\alpha}\rangle^*\} - \frac{1}{\forall}\int_{\Sigma_-(t)} C_{A\alpha}\{\bar{w}_\Sigma \cdot \hat{\xi}\}dA$$

$$= \nabla \cdot D_{A\alpha}\left\{\langle C_{A\alpha}\rangle^*\nabla\epsilon_\alpha + \epsilon_\alpha\nabla\langle C_{A\alpha}\rangle^* - \langle C_{A\alpha}\rangle^*\nabla\epsilon_\alpha + \frac{1}{\forall}\int_{\Sigma_-(t)} \hat{\xi}\,\tilde{C}_{A\alpha}\,dA\right\}$$

$$-\frac{1}{\forall}\int_{\Sigma_-(t)} \hat{\xi}\cdot(\bar{J}_{\alpha\Sigma})dA$$

Cancelling out $\epsilon_\alpha\nabla\langle C_{A\alpha}\rangle^*$ gives

$$\frac{\partial}{\partial t}\{\epsilon_\alpha\langle C_{A\alpha}\rangle^*\} - \frac{1}{\forall}\int_{\Sigma_-(t)} C_{A\alpha}\{\bar{w}_\Sigma \cdot \hat{\xi}\}dA$$

$$= \nabla \cdot D_{A\alpha}\left\{\epsilon_\alpha\nabla\langle C_{A\alpha}\rangle^* + \frac{1}{\forall}\int_{\Sigma_-(t)} \hat{\xi}\,\tilde{C}_{A\alpha}\,dA\right\}$$

$$-\frac{1}{\forall}\int_{\Sigma_-(t)} \hat{\xi}\cdot(\bar{J}_{\alpha\Sigma})dA \qquad \text{(C28)}$$

If no growth condition is considered, or if it is assumed that the diffusion of a nutrient is much faster than the growth of cells and maturing embryos in a cluster, then the 2nd term in LHS of eq. (C28) can be neglected. This may eventually be the case of certain type of nutrients. van Gulik et al. (1993) reports that it takes only about 24 hr after inoculation for *Catharanthus roseus* cells in suspension culture to uptake phosphate; hence the growth of cells is then dependent on the intracellular phosphate pool instead of uptake rate. Eq. (C28) will then be reduced to

$$\frac{\partial}{\partial t}\{\epsilon_\alpha\langle C_{A\alpha}\rangle^*\} = \nabla\cdot D_{A\alpha}\left\{\epsilon_\alpha\nabla\langle C_{A\alpha}\rangle^* + \frac{1}{\forall}\int\limits_{\Sigma_-(t)}\hat{\xi}\,\tilde{C}_{A\alpha}\,dA\right\}$$

$$-\frac{1}{\forall}\int\limits_{\Sigma_-(t)}\hat{\xi}\cdot(\bar{J}_{\alpha\Sigma})dA \qquad \text{(C29)}$$

Gray (1975) has defined the tortuosity vector as

$$\epsilon_\alpha\bar{\tau}_\alpha = \frac{1}{\forall}\int\limits_{\Sigma_-(t)}\hat{\xi}\,\tilde{C}_{A\alpha}\,dA \qquad \text{(C30)}$$

which reduces the diffusion rate because of the system geometry and

$$\bar{\tau}_\alpha = \frac{1}{\forall_\alpha(t)}\int\limits_{\Sigma_-(t)}\hat{\xi}\,\tilde{C}_{A\alpha}\,dA \qquad \text{(C31)}$$

Introducing tortuosity vector in eq. (C29) gives

$$\frac{\partial}{\partial t}\{\epsilon_\alpha\langle C_{A\alpha}\rangle^*\} = \nabla\cdot[D_{A\alpha}\epsilon_\alpha\{\nabla\langle C_{A\alpha}\rangle^* + \bar{\tau}_\alpha\}] - \frac{1}{\forall}\int\limits_{\Sigma_-(t)}\hat{\xi}\cdot(\bar{J}_{\alpha\Sigma})dA \qquad \text{(C32)}$$

If the effective diffusivity tensor, $\bar{\bar{D}}_{A\alpha,eff}$, is defined as (as eq. 35 of Gray (1975))

$$\bar{\bar{D}}_{A\alpha,eff}\cdot\nabla\langle C_{A\alpha}\rangle^* = D_{A\alpha}\{\nabla\langle C_{A\alpha}\rangle^* + \bar{\tau}_\alpha\} \qquad \text{(C33)}$$

then eq. (C32) becomes,

$$\frac{\partial}{\partial t}\{\epsilon_\alpha\langle C_{A\alpha}\rangle^*\} = \nabla\cdot\epsilon_\alpha\{\bar{\bar{D}}_{A\alpha,eff}\cdot\nabla\langle C_{A\alpha}\rangle^*\} - \frac{1}{\forall}\int\limits_{\Sigma_-(t)}\hat{\xi}\cdot(\bar{J}_{\alpha\Sigma})dA \qquad \text{(C34)}$$

If the intracellular concentration of a nutrient is negligibly small compare to the extracellular concentration because of utilization of the nutrient in the cell, then it can be inferred that

$$\langle C_{A\gamma}\rangle^* \approx 0 \qquad \text{(C35)}$$

This leads to a possibility of forming a boundary layer of nutrient of thickness, δ_γ, at the cell cytoplasm side of the interface, $\Sigma_+(t)$.

Now the order of magnitude analysis of transport equation, eq. (5.3), in $\gamma - phase$ is given by

$$\underbrace{\frac{\partial C_{A\gamma}}{\partial t}}_{O\left(\frac{\Delta C_{A\gamma}}{t^*}\right)} = \underbrace{\nabla \cdot \left(D_{A\gamma} \nabla C_{A\gamma}\right)}_{O\left(\frac{D_{A\gamma} \Delta C_{A\gamma}}{{\delta_\gamma}^2}\right)} - \underbrace{\frac{\mu_A C_{A\gamma}}{C_{A\gamma}+K_A}}_{O\left(\frac{\mu_A C_{A\gamma}}{C_{A\gamma}+K_A}\right)} \tag{C36}$$

Because of boundary layer at $\Sigma_+(t)$, it may be approximated that the change in concentration over the thickness of the boundary layer is in the order of concentration of nutrient, and can be expressed as

$$\Delta C_{A\gamma} = O(C_{A\gamma}) \tag{C37}$$

t^* refers to the characteristic time.

Using eq. (C36 & C37), the boundary layer thickness can be estimated as

$$\delta_\gamma = O\left[\sqrt{\frac{D_{A\gamma}\left(C_{A\gamma}+K_A\right)}{\mu_A}}\right] \tag{C38}$$

From eqs. (5.11, 5.13, & C36), it can be written as

$$\bar{J}_{\alpha\Sigma} \cdot \hat{\bar{\xi}} = \bar{J}_{\Sigma\gamma} \cdot \hat{\bar{\xi}} = \frac{D_{A\gamma} C_{A\gamma}}{\delta_\gamma} = O\left(\frac{C_{A\alpha} - \beta_1 C_{A\gamma}}{\beta_2 + \beta_3 + \beta_4 C_{A\alpha} + \beta_5 C_{A\gamma}} P_0\right) \tag{C39}$$

Substituting the order of magnitude of the boundary layer thickness (δ_γ) (eq. (C38)) in eq. (C39) gives

$$C_{A\gamma}\sqrt{\frac{D_{A\gamma}\mu_A}{\left(C_{A\gamma}+K_A\right)}} = O\left(\frac{C_{A\alpha} - \beta_1 C_{A\gamma}}{\beta_2 + \beta_3 + \beta_4 C_{A\alpha} + \beta_5 C_{A\gamma}} P_0\right) \tag{C40}$$

After some mathematical manipulations, as shown in Appendix E, eq. (C40) can be written as

$$\beta_1 C_{A\gamma} = \frac{O(C_{A\alpha})}{1+O\left[\frac{\sqrt{D_{A\gamma}\mu_A/(C_{A\gamma}+K_A)}}{\beta_1 P_0}(\beta_2+\beta_3+\beta_4 C_{A\alpha}+\beta_5 C_{A\gamma})\right]} \tag{C41}$$

If the inequality

$$\frac{\sqrt{D_{A\gamma}\mu_A/(C_{A\gamma}+K_A)}}{\beta_1 P_0}(\beta_2+\beta_3) \gg 1 \tag{C42}$$

satisfies for cells and immature embryos, then the $\gamma - phase$ concentration

$$\beta_1 C_{A\gamma} \ll C_{A\alpha} \tag{C43}$$

Hence the flux in eq. (5.11) be

$$\bar{J}_{\alpha\Sigma}\cdot\hat{\bar{\xi}} = \bar{J}_{\Sigma\gamma}\cdot\hat{\bar{\xi}} = \frac{C_{A\alpha}}{\beta_2+\beta_3+\beta_4 C_{A\alpha}}P_0 \qquad \text{at } \Sigma(t) \tag{C44}$$

provided that

$$\beta_5 C_{A\gamma} \ll (\beta_2+\beta_3+\beta_4 C_{A\alpha}) \tag{C45}$$

is also satisfied.

Now going back to the transport equation in $\alpha - phase$, eq. (C34) can be written as

$$\frac{\partial}{\partial t}\{\epsilon_\alpha\langle C_{A\alpha}\rangle^*\} = \nabla\cdot\epsilon_\alpha\{\bar{\bar{D}}_{A\alpha,eff}\cdot\nabla\langle C_{A\alpha}\rangle^*\} - \frac{1}{\forall}\int_{\Sigma\_(t)}\frac{C_{A\alpha}}{\beta_2+\beta_3+\beta_4 C_{A\alpha}}P_0\,dA \tag{C46}$$

Applying the spatial decomposition, eq. (C21), in the last term in RHS of eq. (C46) gives

$$\frac{1}{\forall}\int_{\Sigma\_(t)}\frac{C_{A\alpha}}{\beta_2+\beta_3+\beta_4 C_{A\alpha}}P_0\,dA = \frac{1}{\forall}\int_{\Sigma\_(t)}\frac{(\langle C_{A\alpha}\rangle^*+\tilde{C}_{A\alpha})(P_0/\beta_4)}{(\beta_2/\beta_4)+(\beta_3/\beta_4)+(\langle C_{A\alpha}\rangle^*+\tilde{C}_{A\alpha})}\,dA \tag{C47}$$

Using order of magnitude analysis, Whitaker (1999, p. 15 & 29) has shown that the spatial deviation of concentration, $\tilde{C}_{A\alpha}$, is associated with the small length-scale, l_α,

however the intrinsic average concentration, $\langle C_{A\alpha}\rangle^*$, may have significant changes over a larger length scale, R. Because $l_\alpha \ll R$, it may be concluded that

$$\tilde{C}_{A\alpha} \ll \langle C_{A\alpha}\rangle^* \tag{C48}$$

This reduces eq. (C47) to

$$\frac{1}{\forall}\int_{\Sigma_-(t)} \frac{C_{A\alpha}}{\beta_2+\beta_3+\beta_4 C_{A\alpha}} P_0\, dA = \frac{1}{\forall}\int_{\Sigma_-(t)} \frac{(P_0/\beta_4)\,\langle C_{A\alpha}\rangle^*}{(\beta_2/\beta_4)+(\beta_3/\beta_4)+\langle C_{A\alpha}\rangle^*}\, dA \tag{C49}$$

The RHS of eq. (C49) is the local estimation of the flux from α to γ. By the term "local", it is referred to that the integrand in RHS remains unchanged within the averaging volume, but it may change over the length-scale, R. So from eq. (C49), one can write

$$\frac{1}{\forall}\int_{\Sigma_-(t)} \frac{C_{A\alpha}}{\beta_2+\beta_3+\beta_4 C_{A\alpha}} P_0\, dA = \frac{a_v(P_0/\beta_4)\,\langle C_{A\alpha}\rangle^*}{(\beta_2/\beta_4)+(\beta_3/\beta_4)+\langle C_{A\alpha}\rangle^*} \tag{C50}$$

where,

$$a_v = \frac{\Sigma_-(t)}{\forall} = \text{the interface area } (\alpha-\gamma) \text{ to volume ratio} \tag{C51}$$

Substituting eq. (C50) into eq. (C46) gives

$$\frac{\partial}{\partial t}\{\epsilon_\alpha\langle C_{A\alpha}\rangle^*\} = \nabla\cdot\epsilon_\alpha\{\overline{\overline{D}}_{A\alpha,eff}\cdot\nabla\langle C_{A\alpha}\rangle^*\} - \frac{a_v(P_0/\beta_4)\,\langle C_{A\alpha}\rangle^*}{(\beta_2/\beta_4)+(\beta_3/\beta_4)+\langle C_{A\alpha}\rangle^*} \tag{C52}$$

which is eq. (5.14).

APPENDIX D: EXPRESSION OF $\langle \nabla C_{A\alpha} \rangle$

Let us consider the Figure D1, where two averaging volumes (red and black colored perimeters) with centroids separated by a distance $\Delta\eta$ at a time t along the line η having a unit vector $\hat{a}_\eta$. If $\Delta\eta \longrightarrow 0$, the two volumes coincide. ψ_α is a parameter in the $\alpha - phase$.

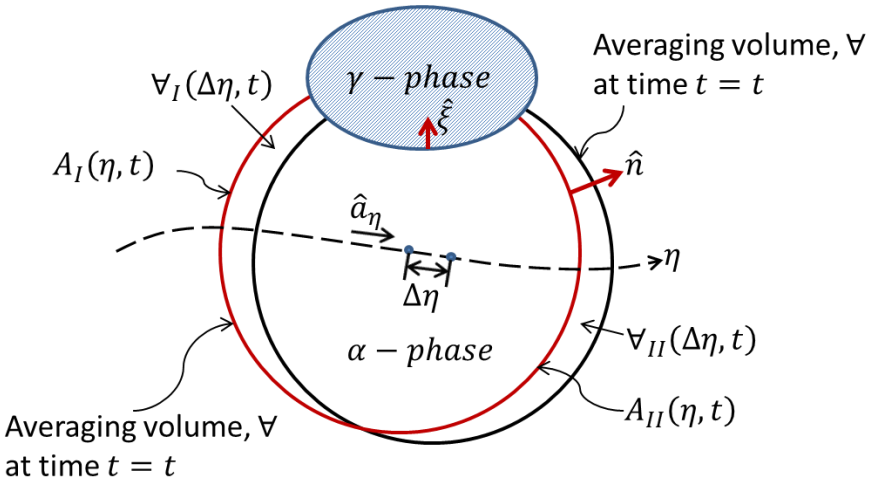

Figure D1 Two averaging volumes, shown in red and black perimeters, have centroids on η at a distance $\Delta\eta$ apart at time t. Each of the averaging volumes is a two phase system containing the $\alpha - phase$ and the $\gamma - phase$.

Hence,

$$\hat{a}_\eta \cdot \nabla \int\limits_{\forall_\alpha(\eta,t)} \psi_\alpha \, dV = \frac{d}{d\eta} \int\limits_{\forall_\alpha(\eta,t)} \psi_\alpha \, dV \tag{D1}$$

Introducing $\lim\limits_{\Delta\eta \to 0}$ in eq. (D2) gives

$$\hat{a}_\eta \cdot \nabla \int\limits_{\forall_\alpha(\eta,t)} \psi_\alpha \, dV = \lim_{\Delta\eta \to 0} \left[\frac{\int_{\forall_\alpha(\eta+\Delta\eta,t)} \psi_\alpha \, dV - \int_{\forall_\alpha(\eta,t)} \psi_\alpha \, dV}{\Delta\eta} \right] \tag{D2}$$

Since the common region in the numerator of RHS of eq. (D2) will be cancelled out, it can be written as

$$\frac{d}{d\eta} \int\limits_{\forall_\alpha(\eta,t)} \psi_\alpha \, dV = \lim_{\Delta\eta \to 0} \left[\frac{\int_{\forall_{II}(\Delta\eta,t)} \psi_\alpha \, d\forall_{II} - \int_{\forall_I(\Delta\eta,t)} \psi_\alpha \, d\forall_I}{\Delta\eta} \right] \tag{D3}$$

where,

$$d\forall_{II} = \left(\Delta\eta \, \hat{a}_\eta\right) \cdot \hat{n} \, dA_{II} \tag{D4a}$$

and

$$d\forall_I = \left(\Delta\eta \, \hat{a}_\eta\right) \cdot (-\hat{n}) \, dA_I \tag{D4b}$$

Substituting eqs. (D4a and D4b) in eq. (D3) gives

$$\frac{d}{d\eta} \int\limits_{\forall_\alpha(\eta,t)} \psi_\alpha \, dV = \int\limits_{A_{II}(\eta,t)} \psi_\alpha \left(\hat{a}_\eta \cdot \hat{n} \right) dA_{II} + \int\limits_{A_I(\eta,t)} \psi_\alpha \left(\hat{a}_\eta \cdot \hat{n} \right) dA_I \tag{D5}$$

$\Delta\eta$ and $\hat{a}_\eta$ are independent of averaging volumes. So eq. (D5) can be written as

$$\frac{d}{d\eta} \int\limits_{\forall_\alpha(\eta,t)} \psi_\alpha \, dV = \hat{a}_\eta \cdot \left[\int\limits_{A_{II}(\eta,t)} \psi_\alpha \, \hat{n} \, dA_{II} + \int\limits_{A_I(\eta,t)} \psi_\alpha \, \hat{n} \, dA_I \right] \tag{D6}$$

Considering that

$$S_\alpha(\eta,t) = A_I(\eta,t) + A_{II}(\eta,t) \tag{D7}$$

eq. (D6) will be reduced to

$$\frac{d}{d\eta}\int\limits_{\forall_\alpha(\eta,t)} \psi_\alpha \, dV = \hat{a}_\eta \cdot \int\limits_{S_\alpha(\eta,t)} \psi_\alpha \, \hat{n} \, dA \tag{D8}$$

Since

$$\frac{d}{d\eta} = \hat{a}_\eta \cdot \nabla \tag{D9}$$

from eq. (D1), eq. (D8) can be expressed as

$$\hat{a}_\eta \cdot \nabla \int\limits_{\forall_\alpha(\eta,t)} \psi_\alpha \, dV = \hat{a}_\eta \cdot \int\limits_{S_\alpha(\eta,t)} \psi_\alpha \, \hat{n} \, dA \tag{D10}$$

This results in

$$\nabla \int\limits_{\forall_\alpha(t)} \psi_\alpha \, dV = \int\limits_{S_\alpha(t)} \psi_\alpha \, \hat{n} \, dA \tag{D11}$$

In the vector form, eq. (D11) can be written as

$$\nabla \cdot \int\limits_{\forall_\alpha(t)} \bar{\psi}_\alpha \, dV = \int\limits_{S_\alpha(t)} \bar{\psi}_\alpha \cdot \hat{n} \, dA \tag{D12}$$

which is eq. (C10).

Now substituting $C_{A\alpha}$ for ψ_α in eq. (D11), one may find

$$\nabla \int\limits_{\forall_\alpha(t)} C_{A\alpha} \, dV = \int\limits_{S_\alpha(t)} C_{A\alpha} \, \hat{n} \, dA \tag{D13}$$

Dividing eq. (D13) by ∀ will result in

$$\nabla \frac{1}{\forall} \int\limits_{\forall_\alpha(t)} C_{A\alpha} \, dV = \frac{1}{\forall} \int\limits_{S_\alpha(t)} C_{A\alpha} \, \hat{n} \, dA \tag{D14}$$

Now using divergence theorem as

$$\int\limits_{\forall_\alpha(t)} \nabla C_{A\alpha} \, dV = \int\limits_{S_\alpha(t)} \hat{n} \, C_{A\alpha} dA + \int\limits_{\Sigma_-(t)} \hat{\xi} C_{A\alpha} dA \tag{D15}$$

Dividing eq. (D15) by ∀,

$$\frac{1}{\forall}\int_{\forall_\alpha(t)} \nabla C_{A\alpha}\, dV = \frac{1}{\forall}\int_{S_\alpha(t)} \hat{n}\, C_{A\alpha} dA + \frac{1}{\forall}\int_{\Sigma_-(t)} \hat{\xi} C_{A\alpha} dA \tag{D16}$$

Applying eq. (D11) for the 1st term of RHS in eq. (D16) and replacing ψ_α by $C_{A\alpha}$ results in

$$\frac{1}{\forall}\int_{\forall_\alpha(t)} \nabla C_{A\alpha}\, dV = \frac{1}{\forall}\nabla \int_{\forall_\alpha(t)} C_{A\alpha} dV + \frac{1}{\forall}\int_{\Sigma_-(t)} \hat{\xi} C_{A\alpha} dA \tag{D17}$$

In averaging notation, eq. (D17) can be written as

$$\langle \nabla C_{A\alpha} \rangle = \nabla \langle C_{A\alpha} \rangle + \frac{1}{\forall}\int_{\Sigma_-(t)} \hat{\xi} C_{A\alpha} dA \tag{D18}$$

which is eq. (C16).

APPENDIX E: EXPRESSION OF $C_{A\gamma}$

Multiplying eq. (C40) by $\left(\frac{\beta_2+\beta_3+\beta_4 C_{A\alpha}+\beta_5 C_{A\gamma}}{P_0}\right)$ gives

$$C_{A\gamma}\left\{O\left[\frac{\sqrt{D_{A\gamma}\mu_A/(C_{A\gamma}+K_A)}}{P_0}\left(\beta_2+\beta_3+\beta_4 C_{A\alpha}+\beta_5 C_{A\gamma}\right)\right]\right\}=O\left(C_{A\alpha}-\beta_1 C_{A\gamma}\right) \quad \text{(E1)}$$

Adding $\left(\beta_1 C_{A\gamma}\right)$ on both sides of eq. (E1) results in

$$C_{A\gamma}\left\{O\left[\frac{\sqrt{D_{A\gamma}\mu_A/(C_{A\gamma}+K_A)}}{P_0}\left(\beta_2+\beta_3+\beta_4 C_{A\alpha}+\beta_5 C_{A\gamma}\right)\right]\right\}+\beta_1 C_{A\gamma}=O(C_{A\alpha}) \quad \text{(E2)}$$

If $\beta_1 C_{A\gamma}$ is factored out in LHS, eq. (E2) becomes

$$\beta_1 C_{A\gamma}\left\{1+O\left[\frac{\sqrt{D_{A\gamma}\mu_A/(C_{A\gamma}+K_A)}}{\beta_1 P_0}\left(\beta_2+\beta_3+\beta_4 C_{A\alpha}+\beta_5 C_{A\gamma}\right)\right]\right\}=O(C_{A\alpha}) \quad \text{(E3)}$$

Finally eq. (E3) can be written as

$$\beta_1 C_{A\gamma}=\frac{O(C_{A\alpha})}{1+O\left[\frac{\sqrt{D_{A\gamma}\mu_A/\left(C_{A\gamma}+K_A\right)}}{\beta_1 P_0}\left(\beta_2+\beta_3+\beta_4 C_{A\alpha}+\beta_5 C_{A\gamma}\right)\right]} \quad \text{(E4)}$$

which is eq. (C41).

APPENDIX F: EXPRESSION OF INTERFACE AREA

It may be considered that the magnitude of the size of an averaging volume is $r_\forall = 3\ \mu m$, where $r_\forall$ is the radius of the averaging volume. It is approximately the size of an ion-selective micropipette tip used by Nicholson and Phillips (1981) to get a signal from the rat cerebellum. Since the cell radius is much higher than the radius of an averaging volume, the cell may occupy the whole averaging volume or a portion of it.

Volume occupied by the cell in the averaging volume = $(1-\epsilon_\alpha)\forall$ (F1)

Hence the surface area of the cell inside the averaging volume = $(4\pi r_0^2)\frac{(1-\epsilon_\alpha)\forall}{\frac{4}{3}\pi r_0^3} =$

$\frac{3(1-\epsilon_\alpha)\forall}{r_0}$ (F2)

Therefore,

$$a_v = \frac{\Sigma_-(t)}{\forall} = \frac{3(1-\epsilon_\alpha)\forall}{r_0}\frac{1}{\forall} = \frac{3(1-\epsilon_\alpha)}{r_0} \quad \text{(F3)}$$

REFERENCES

Abdullah M A, Ariff A B, Marziah M, Ali A M, Lajis N H (2000). Strategies to overcome foaming and wall-growth during the cultivation of Morinda elliptica cell suspension culture in a stirred-tank bioreactor. Plant Cell, Tissue Organ Cult. 60(3):205-212

Afreen F, Zobayed S M A, Kozai T (2002). Photoautotrophic culture of Coffea arabusta somatic embryos: development of a bioreactor for large-scale plantlet conversion for cotyledonary embryos. Ann Bot. 90:21-29

Aidun C K, Egertsdotter U. Method and device for dispersion of assemblies of biological material. Patent 2011/043731

Aitken-Christie J, Jones C (1987). Towards automation: Radiata pine shoot hedges in vitro. Plant Cell Tissue Organ Cult. 8: 185-196

Akita M, Shigeoka T, Koizumi Y, Kawamura M (1994). Mass propagation of shoots of Stevia rebaudiana using a large scale bioreactor. Plant Cell Rep. 13:180-183

Aksnes D L, Egge J K (1991). A theoretical model for nutrient uptake in phytoplankton. Mar Ecol Prog Ser. 70: 65-72

Akula A, Becker D, Bateson M (2000). High-yielding repetitive somatic embryogenesis and plant recovery in a selected tea clone, ‘‘TRI-2025’’, by temporary immersion. Plant Cell Rep. 19: 1140–1145

Albarrán J, Bertrand B, Lartaud M, Etienne H (2005). Cycle characteristics in a temporary immersion bioreactor affect regeneration, morphology, water and mineral status of coffee (*Coffea arabica*) somatic embryos. Plant Cell Tissue Organ Cult. 81:27–36

Alvard D, Cote F, Teisson C (1993). Comparison of methods of liquid medium culture for banana micropropagation: effects of temporary immersion of explants. Plant Cell, Tissue Organ Cult. 32:55-60

Amanullah A, Serrano-Carreon L, Castro B, Galindo E, Nienow A W (1998). The influence of impeller type in pilot scale Xanthan fermentations. Biotechnol Bioeng. 57(1): 95-108

Archambault J, Velosky B, Kurz, W G W (1990). Development of bioreactors for the culture of surface immobilized plant cells. Biotechnol Bioeng. 35:702-711

Arcuri E J, Nichols J R, Brix T S, Santamarina V G (1983). Thienamycin production by immobilized cells of Streptomyces cattleya in a bubble column. Biotechnol Bioeng. 15: 2399-2411

Attree S M, Pomeroy M K, Fowke L C (1994). Production of vigorous, desiccation tolerant white spruce (Picea glauca [Moench.] Voss.) synthetic seeds in a bioreactor. Plant Cell Rep. 13: 601-606

Atwell B J, Greenway H (1987). The relationship between growth and oxygen uptake in hypoxic rice seedlings. J Exp Bot. 38(3): 454-465

Ballica R, Ryu D Y (1993). Effects of rheological properties and mass transfer on plant cell bioreactor performance: production of tropane alkaloids. Biotechnol Bioeng. 42:1181-1189

Barber S A (1984). Soil Nutrient Bioavailability. John Wiley & Sons, Inc.

Barry-Etienne D, Bertrand B, Schlonvoigt A, Etienne H (2002). The morphological variability within a population of coffee somatic embryos produced in a bioreactor affects the regeneration and the development of plants in the nursery. Plant Cell, Tissue Organ Cult. 68(2):153-162

Barry-Etienne D, Bertrand B, Vasquez N, Etienne H (2002). Comparison of somatic embryogenesis-derived coffee (Coffea arabica L.) plantlets regenerated in vitro or ex vitro: Morphological, Mineral and Water Characteristics. Ann Bot 90:77-85

Bentebibel S, Moyano E, Palazón J, Cusidó R M, Bonfill M, Eibl R, Piñol T (2005). Effects of immobilization by entrapment in alginate and scale-up of paclitaxel and baccatin III production in cell suspension cultures of Taxus baccata. Biotechnol Bioeng. 89(6):647-655

Biddington N L, Robinson T H (1991). Ethylene production during anther culture of Brussel sprouts (Brassica oleracea var. gemmifera) and its relationship with factors that affect embryo production. Plant Cell, Tissue Organ Cult. 25:169-177

Bieniek M E, Harrell R C, Cantliffe D J (1995). Enhancement of somatic embryogenesis of Ipomoea batatas in solid cultures and production of mature somatic embryos in liquid cultures for application to a bioreactor production system. Plant Cell, Tissue Organ Cult. 41:1-8

Bolta Z, Baricevic D, Raspor P (2003). Biomass segregation in sage cell suspension culture. Biotechnol Lett. 25(1):61-65

Bramble J L, Graves D J, Brodelius P (1990). Calcium and phosphate effects on growth and alkaloid production in *Coffea arabica* experimental results and mathematical model. Biotechnol Bioeng. 37(9):859-868

Burg S P (1973). Ethylene in plant growth. Proc Na Acad Sci, USA. 70(2):591-597

Cardillo A B, Otálvaro A Á M, Busto V D, Talou J R, Velásquez L M E, Giulietti A M (2010). Scopolamine, anisodamine and hyoscyamine production by Brugmansia candida hairy root cultures in bioreactors. Process Biochem. 45(9):1577-1581

Chattopadhyay S, Bisaria V S, Srivastava A K (2003). Enhanced production of podophyllotoxin by Podophyllum hexandrum using in situ cell retention bioreactor. Biotechnol Prog. 19(3):1026-1028

Chattopadhyay S, Srivastava A K, Bisaria V S (2004). Production of Phytochemicals in Plant Cell Bioreactors. In: Srivastava P S, Narula A, Srivastava S (eds). Plant Biotechnology and Molecular Markers. Kluwer Academic Publishers, Dordrecht, The Netherlands. 120-121

Che P, Love T, Frame B, Wang K, Carriquiry A, Howell S. (2006). Gene Expression Patterns During Somatic Embryo Development and Germination in Maize Hi II Callus Cultures. Plant Mol Biol. 62:1-14

Chen H-B, Kao P-M, Huang H-C, and Shieh C-J (2010). Effects of using various bioreactors on chitinolytic enzymes productin by Paenibacillus taichungensis. Biochem Eng J. 49:337-342

Chen S Y, Huang S Y (2000). Shear stress effects on cell growth and L-DOPA production by suspension culture of *Stizolobium hassjoo* cells in an agitated bioreactor. Bioprocess Eng. 22: 5-12

Cho J M, Kwon J Y, Lim J A, Kim D I (2007). Increased hGM-CSF production and secretion with pluronic F-68 in transgenic Nicotiana tabacum suspension cell cultures. Biotechnol Bioprocess Eng. 12(6):594-600

Choi H J, Tao B Y, Okos M R (1995). Enhancement of secondary metabolite production by immobilized *Gossypium arboreum* cells. Biotechnol Prog. 11: 306-311

Choi S M, Son S H, Yun S R, Kwon O W, Seon J H, Paek K Y (2000**)**. Pilot-scale culture of adventitious roots of ginseng in a bioreactor system. Plant Cell, Tissue Organ Cult. 62(3):187-193

Choi Y E, Jeong J H (2002). Dormancy induction of somatic embryos of Siberian ginseng by high sucrose concentrations enhances the conservation of hydrated artificial seeds and dehydration resistance. Plant Cell Rep. 20(12):1112-1116

Choi Y S, Lee S Y, Kim D I (1999). Cultivation of Digitalis lanata cell suspension in an aqueous two-phase system. J Microbiol Biotechnol. 9(5):589-592

Clarkson D T (1981). Nutrient interception and transport by root systems. In Johnson C B (ed.), Physiological processes limiting plant productivity. London: Butterworths. 307-330

Cloutier M, Bouchard-Mrchand E, Perrier M, Jolicoeur M (2008). A Predictive Nutritional Model for Plant Cells and hairy Roots. Biotechnol Bioeng. 99(1):189-200

Curtis W R (2005). Application of bioreactor design principles to plant micropropagation. Plant Cell, Tissue Organ Cult. 81:255-264

Daie J, Chin C-K, Pitcher L (1987). Differential rates of sucrose and hexose transport by asparagus cell cultures. Plant Sci. 53:101-107.

Daniel W W, Cross C L (2013). Biostatistics: A Foundation for Analysis in the Health Sciences. Wiley & Sons, Inc. 10th Ed.

Debergh P, Aitken-Christie J, Cohen D, Grout B, Arnold S, Zimmerman R, Ziv M (1992). Reconsideration of the term 'vitrification' as used in micropropagation. Plant Cell, Tissue Organ Cult. 30(2):135-140

Debergh P, Harbaoui Y, Lemeur R (1981). Mass propagation of globe artichoke (Cynara scolymus): evaluation of different hypotheses to overcome vitrification with special reference to water potential. Physiol Plant. 53: 181-187

De Dobbeleer C, Cloutier M, Fouilland M, Legros R, Jolicoeur M (2006). A high-rate perfusion bioreactor for plant cells. Biotechnol Bioeng. 95(6):1126-1137

De Jong A J, Schmidt E D L, De Vries S C (1993). Early events in higher plant embryogenesis. Plant Mol Biol. 22(2): 367-377

Deo P C, Harding M R, Taylor M, Tyagi P A, Becker D K (2009). Somatic embryogenesis, organogenesis and plant regeneration in taro (*Colocasia esculenta* var. esculenta). Plant Cell Tissue Organ Cult. 99: 61-71

Domínguez A, Rivela I, Couto SR, Sanromán M A (2001). Design of a new rotating drum bioreactor for ligninolytic enzyme production by *Phanerochaete chrysosporium* grown on an inert support. Process Biochem. 37:549-554

Dong H D, Zhong J J (2002). Enhanced taxane productivity in bioreactor cultivation of Taxus chinensis cells by combining elicitation, sucrose feeding and ethylene incorporation. Enzyme Microb Technol. 31(1-2):116-121

Doran P M (1993). Design of reactors for plant cells and organs. In: Feichter A (ed.), Bioprocess Design Control. Springer-Verlag, Berlin. 48:116–169

Doran P M (1999). Design of mixing systems for plant cell suspensions in stirred reactors. Biotechnol Prog. 15:319-335

Egertsdotter U (1996). Regulation of somatic embryo development in Norway spruce (*Picea abies*). Agronomie. 16:603-608

Egertsdotter U, Mo L H, von Arnold S (1993). Extracellular proteins in embryogenic suspension cultures of Norway spruce (*Picea abies*). Physiol Plant. 88:315-321

Egertsdotter U, von Arnold S (1995). Importance of arabinogalactan proteins for the development of somatic embryos of Norway spruce (*Picea abies*). Physiol Plant. 93:334-345

Egertsdotter U, von Arnold S (1998). Development of somatic embryos in Norway spruce. J Exp Bot. 49:155-162

Eibl R, Kaiser S, Lombriser R, Eibl D (2010). Disposable bioreactors: the current state-of-the-art and recommended applications in biotechnology. Appl Microbiol Biotechnol. 86:41-49

El-Sayed A-H M M, Rehm H J (1987). Continuous penicillin production by Penicillium chrysogenum immobilized in calcium alginate beads. Appl Microbiol Biotechnol. 26:215-218

Escalona M, Lorenzo J C, Gonzales B L, Daquinta M, Borroto C G, Gonzales J I, Desjardine Y. (1999). Pineapple (Ananas cosmos L. Merr) micropropagation in temporary immersion systems. Plant Cell Rep. 18:743-748

Etienne-Barry D, Bertrand B, Vasquez N, Etienne H (1999). Direct soweing of Coffea Arabica somatic embryos mass-produced in a bioreactor and regeneration of plants. Plant Cell Rep. 19:111-117

Etienne H, Lartaud M, Michaux-Ferriere N, Carron M P, Berthouly M, Teisson C (1997). Improvement of somatic embryogenesis in *Hevea brasiliensis* (Müll. Arg.) using the temporary immersion technique. In vitro Cell Dev Biol- Plant. 33:81-87

Facchini P J, Dicosmo F (1991). Plant-cell bioreactor for the production of protobeberine alkaloids from immobilized Thalictrum rugosum cultures. Biotechnol Bioeng. 37(5):397-403

Fereol L, Chovelon V, Causse S, Triaire D, Arnault I, Auger J, Kahane R (2005). Establishment of embryogenic cell suspension cultures of garlic (*Allium sativum* L.), plant regeneration and biochemical analyses. Plant Cell Rep. 24: 319-325

Fiksen Ø, Follows M J, Aksnes D L (2013). Trait-based models of nutrient uptake in microbes extend the Michaelis-Menten framework. Limnol Oceanogr. 58(1):193-202

Filonova L H, Bozhkov P V, von Arnold S (2000). Developmental pathway of somatic embryogenesis in *Picea abies* as revealed by time-lapse tracking. J Exp Bot. 51(343): 249-264

Fischer U, Alfermann A W (1995). Cultivation of photoautotrophic plant-cell suspension in the bioreactor- influence of culture conditions. J Biotechnol. 41(1):19-28

Fischer U, Santore U J, Husemann W, Barz W, Alfermann A W (1994). Semicontinuous cultivation of photoautotrophic cell-suspension cultures in a 20-L airlift-reactor. Plant Cell, Tissue Organ Cult. 38(2-3):123-134

Forster R E, Estabrook R W (1993). Is oxygen an essential nutrient? Annu Rev Nutr. 13:383-403

Fu C-C, Wu W-T, Lu S-Y (2003). Performance of airlift bioreactors with net draft tube. Enzyme Microb Technol. 33:332-342

Fujimura M, Kato J, Tosa T, Chibata I (1984). Continuous production of L-arginine using immobilized growing Serratia marcescens cells: Effectiveness of supply of oxygen gas. Appl Microbiol Biotechnol. 19:79-84

Fung C J, Metchell D A (1995). Baffles increase performance of solid-state fermentation in rotating drum bioreactors. Biotechnol Tech. 9(4):295-298

Gagnon H, Thibault J, Cormier F, Do C B (1999). *Vitis vinifera* culture in a non-conventional bioreactor: the reciprocating plate bioreactor. Bioprocess Eng. 21(5):405-413

Gaspar T, Kevers C, Debergh P, Maene L, Paques M, Boxus P (1987). Vitrification: morphological, physiological, and ecological aspects. In: Bonga J M, Durzan D J (Eds). Cell and Tissue Culture in Forestry (vol. 1). Dordrecht, Holland: Martinus Nijhoff publishing, 152- 166

Gaspar T (1991). Vitrification in micropropagation. In: Bajaj Y P S (Ed). Biotechnology in Agriculture and Forestry (vol.17). Berlin: Springer-Verlag, 117-126.

Gaspar T, Kevers C, Franck T, Bisbis B, Billar J P, Huault C, Dily F L, Petit-Paly G, Rideau M, Penel C, Crevecoeur M, Greppin H (1995). Paradoxical results in the analysis of hyperhydric tissues considered as being under stress: questions for a debate. Bulg J Plant Physiol. 21(2-3):80-97

Gatica-Arias A M, Arrieta-Espinoza G, Esquivesl A M E (2008). Plant regeneration via indirect somatic embryogenesis and optimization of genetic transformation in Coffea Arabica L. cvs. Caturra and Catuaí. Electron J Biotechnol. 11(1):1-12

Ge F, Yuan X F, Wang X D, Zhao B, Wang Y C (2006). Cell growth and shikonin production of Arnebia euchroma in a periodically submerged airlift bioreactor. Biotechnol Lett. 28(8):525-529

Gmati D, Chen J K, Jolicoeur M (2004). Development of small-scale bioreactor: Application to in vivo NMR measurement. Biotechnol Bioeng. 89(2):138-147

Godo T, Kobayashi K, Tagami T, Matsui K, Kida T (1998). In vitro propagation utilizing suspension cultures of meristematic nodular cell clumps and chromosome stability of Lilium X formolongi hort. Sci Hort. 72(3-4):193-202

Gorret N, bin Rosli A K, Oppenheim S F, Willis L B, Lessard P A, Rha C K, Sinskey A J (2004). Bioreactor culture of oil palm (*Elaeis guineensis*) and effects of nitrogen source,

inoculum size, and conditioned medium on biomass production. J Biotechnol. 108(3):253-263

Grey D, Stepan-Sarkissian G, Fowler M (1987). Cell and tissue culture in forestry. In Bonga J, Durzan D J (eds.), Nutrient uptake. Nijhoff, Dordrecht. 1:31-60

Gupta P, Pullman G, Timmis R, Kreitinger M, Carlson W, Grob J, Welty E (1993). Forestry in the 21st century. The biotechnology of somatic embryogenesis. Bio/Technology. 11: 454–459

Guzzo F, Baldan B, Mariani P, LoSchiavo F, Terzi M (1994). Studies on the origin of totipotent cells in explants of *Daucus carota* L. J of Exp Bot. 45: 1427- 1432

Hakman I, von Arnold S (1985). Plantlet regeneration through somatic embryogenesis in Picea abies (Norway spruce). J Plant Physiol. 121:149-158

Han J, Zhong J J (2003). Effects of oxygen partial pressure on cell growth and ginsenoside and polysaccharide production in high density cell cultures of Panax notoginseng. Enzyme Microb Technol. 32(3-4):498-503

Hanhineva K, Kokko H, Karenlampi S (2005). Shoot regeneration from leaf explants of five strawberry (Fragaria x ananassa) cultivars in temporary immersion bioreactor system. In vitro Cell Dev Biol- Plant. 41(6):826-831

Hisiger S, Jolicoeur M (2005). Plant cell culture monitoring using an in situ multiwavelength fluorescence probe. Biotechnol Prog. 21(2):580-589

Ho C H, Henderson K A, Rorrer G L (1995). Cell-damage and oxygen mass-transfer during cultivation of Nicotiana tabacum in a stirred-tank bioreactor. Biotechnol Prog. 11(2):140-145

Ho C W, Jian W T, Lai H C (2006). Plant regeneration via somatic embryogenesis from suspension cell cultures of Lilium formolongi Hort. using a bioreactor system. In vitro Cell Dev Biol- Plant. 42(3):240-246

Honda H, Hiraoka K, Nagamori E, Omote M, Kato Y, Hiraoka S, Hobayashi T (2002). Enhanced anthocyanin production from grape callus in an air-lift type bioreactor using a viscous additive-supplemented medium. J Biosci Bioeng. 94(2):135-139

Honda H, Liu C, Kobayashi T (2001). Large-scale plant micropropagation. Adv Biochem Eng/Biotechnol. 72: 157-182

Honda H, Koyayashi T (2004). Large-scale micropropagation system of plant cells. Adv Biochem Eng/Biotechnol. 91: 105-134

Hohe A, Winkelmann T, Schwenkel H G (1999). CO_2 accumulation in bioreactor suspension cultures of *Cyclamen persicum* Mill. and its effect on cell growth and regeneration of somatic embryos. Plant Cell Rep. 18(10):863-867

Hooker B S, Lee J M, An G (1990). Cultivatiion of plant cells in a stirred vessel: effect of impeller design. Biotechnol Bioeng. 35:296-304

Hsiao T Y, Bacani F T, Carvalho E B, Curtis W R (1999). Development of a low capital investment reactor system: Application for plant cell suspension culture. Biotechnol Prog. 15(1):114-122

Hu W W, Zhong J J (2001). Effect of bottom clearance on performance of airlift bioreactor in high-density culture of Panax notoginseng cells. J Biosci Bioeng. 92(4):389-392

Hu W W, Yao H, Zhong J J (2001). Improvement of Panax notoginseng cell culture for production of ginseng saponin and polysaccharide by high density cultivation in pneumatically agitated bioreactors. Biotechnol Prog. 17:838-846

Huang S Y, Shen Y W, Chan H S (2002). Development of a bioreactor operation strategy for L-DOPA production using Stizolobium hassjoo suspension culture. Enzyme Microb Technol. 30: 779-791

Hvoslef-Eide A K, Olsen O A S, Lyngved R, Munster C, Heyerdahl P H (2005). Bioreactor design for propagation of somatic embryos. Plant Cell, Tissue Organ Cult. 81(3):265-276

Huang T-K, McDonald K A (2009). Bioreactor engineering for recombinant protein production in plant cell suspension cultures. Biochem Eng J. 45:168-184

Huang S Y, Chen S Y (1998**)**. Efficient L-DOPA production by Stizolobium hassjoo cell culture in a two stage configuration. J Biotechnol. 62(2):95-103

Huang S Y, Shen Y W, Chan H S (2002). Development of a bioreactor operation strategy for L-DOPA production using Stizolobium hassjoo suspension culture. Enzyme Microb Technol. 30: 779-791

Illing S, Harrison S T L (1999). The kinetics and mechanism of *Corynebacterium glutamicum* aggregate breakup in bioreactors. Chem Eng Sci. 54:441-454

Ingram B, Mavituna F (2000). Effect of bioreactor configuration on the growth and maturation of Picea sitchensis somatic embryo cultures. Plant Cell, Tissue Organ Cult. 61(2):87-96

Jackson M B, Fenning T M, Drew M C, Saker L R (1985). Stimulation of ethylene production and gas-space (aerenchyma) formation in adventitious roots of *Zea mays* L. by small partial pressures of oxygen. Planta. 165(4):486-492

Jay V, Genestier S, Courduroux J-C (1992). Bioreactor studies on the effect of dissolved oxygen concentrations on growth and differentiation of carrot (*Daucus carota* L.) cell cultures. Plant Cell Rep. 11:605-608

Jay V, Genestier S, Courduroux J-C (1994). Bioreactor studies on the effect of medium pH on carrot (*Daucus carota* L.) somatic embryogenesis. Plant Cell, Tissue Organ Cult. 36: 205-209

Jeong G T, Park D H, Hwang B, Woo J C (2003). Comparison of growth characteristics of Panax ginseng hairy roots in various bioreactors. Appl Biochem Biotechnol. 105:493-503

Jianfeng X, Jian X, Aiming H, Pusun F, Zhiguo S (1998). Kinetic and technical studies on large-scale culture of *Rhodiola sachalinensis* compact callus aggregates with air-lift reactors. J Chem Technol Biotechnol. 72(3):227-234

Jiménez E, Pérez N, de Feria M, Barbón R, Capote A, Chavez M, Quiala E, Pérez J C (1999). Improved production of potato microtubers using a temporary immersion system. Plant Cell, Tissue Organ Cult. 59(1):19-23

Jørgensen B B, Revsbech N P, Blackburn T H, Cohen Y (1979). Diurnal cycle of oxygen and sulfide microgradients and microbial photosynthesis in a cyanobacterial mat sediment. Applied and Environmental Microbiology. 38(1): 46-58

Jolicoeur M, Chavarie C, Carreau P J, Archambault J (1992). Development of a helical-ribbon impeller bioreactor for high-density plant cell suspension culture. Biotechnol Bioeng. 39:511-521

Kantarci N, Borak F, Ulgen K O (2005). Bubble column reactors. Process Biochem. 40:2263-2283

Keener J, James Sneyd J (2009). Mathematical Physiology I: Cellular Physiology. In: Antman S S, Marsden J E, Sirovich L. Interdisciplinary Applied Mathematics: Mathematical Biology. Springer, New York, NY. 2nd Ed.

Kessell R H J, Carr A H (1972). The effect of dissolved oxygen concentration on growth and differentiation of carrot (*Daucus carota*) tissue. J Exp Bot. 23:996-1007

Keβler M, ten Hoopen J G, Furusaki S (1999). The effect of the aggregate size on the production of ajmalicine and tryptamine in Catharanthus roseus suspension culture. Enzyme Microb Technol. 24:308-315

Kevers C, Coumans M, Coumans-Gilles M F, Gasper T (1984). Physiological and biochemical events leading to vitrification of plants cultured in vitro. Physiol Plant. 61:69-74

Kim D I, Cho G H, Pedersen H, Chin C K (1991a). A hybrid bioreactor for high-density cultivation of plant-cell suspensions. Appl Microbiol Biotechnol. 34(6):726-729

Kim D I, Pedersen H, Chin C K (1991b). Cultivation of *Thalictrum rugosum* cell suspension in an improved airlift bioreactor- stimulatory effect of carbon-dioxide and ethylene on alkaloid production. Biotechnol Bioeng. 38(4):331-339

Kim J H, Yoo Y J (2002). Optimization of SOD biosynthesis by controlling sucrose concentration in the culture of carrot hairy root. J Microbiol Biotechnol. 12(4):617-621

Kino-Oka R, Hitaka Y, Taya M, Tone S (1999). High-density culture of red beet hairy roots by considering medium flow condition in a bioreactor. Chem Eng Sci. 54(15-16):3179-3186

Klvana M, Legros R, Jolicoeur M (2005). In situ extraction strategy affects benzophenanthridine alkaloid production fluxes in suspension cultures of *Eschscholtzia californica*. Biotechnol Bioeng. 89:280-289

Komamine A, Matsumoto M, Tsukahara M, Fujiwara A, Kawahara R, Ito M, Nomura K, Fujimora T (1990). Mechanisms of somatic embryogenesis in cell cultures- physiology, biochemistry, and molecular biology. In: Nijkamp H J J, Van der Plas L H W, Van Aartrijk A (eds), In Progress in Plant Cellular and Molecular Biology. Kluwer Academic Publishers, Dordrecht, The Netherlands. 307-313

Komamine A, Murata N, Nomura K (2005). Mechanisms of somatic embryogenesis in carrot suspension cultures- morphology, physiology, biochemistry, and molecular biology. In Vitro Cellular and Developmental Biology- Plant. 41: 6-10

Kosky R G, Barranco L A, Pérez B C, Daniels D, Vega M R, Silva M F (2006). Trueness-to-type and yield components of the banana hybrid cultivar FHIA-18 plants regenerated via somatic embryogenesis in a bioreactor. Euphytica. 150: 63–68

Kovács G, Laszlo M, Rajkai G, Barnabas B (1995**)**. Monitoring of haploid maize cell suspension culture conditions in bioreactors. Plant Cell, Tissue Organ Cult. 43(2):123-126

Kreft J U, Picioreanu C, Wimpenny J W, van Loosdrecht M C (2001). Individual-based modeling of biofilms. Microbiology.147:2897-2912

Krishna H, Singh S K. (2007). Biotechnological advances in mango (*Mangifera indica* L.) and their future implication in crop improvement -- A review. Biotechnol Adv. 25:223-243

Kurata H, Furusaki S (1993). Immobilized Coffea Arabica cell culture using a bubble-column reactor with controlled light intensity. Biotechnol Bioeng. 42(4):494-502

Lakshmanan P, Geijskes R, Wang L, Elliott A, Grof C. (2006). Developmental and hormonal regulation of direct shoot organogenesis and somatic embryogenesis in sugarcane (Saccharum spp. interspecific hybrids) leaf culture. Plant Cell Rep. 25:1007-1015

Langer E S (2011). Trends in perfusion bioreactors- the next revolution in bioprocessing. BioProcess Int. 9(10):18-22

Lee-Parsons C W, Shuler M L (2002). The effect of ajmalicine spiking and resin addition timing on the production of indole alkaloids from *Catharanthus roseus* cell cultures. Biotechnol Bioeng. 79: 408-415

Lee S Y, Kim D I (2002). Stimulation of murine granulocyte macrophage-colony stimulating factor production by Pluronic F-68 and polyethylene glycol in transgenic Nicotiana tabacum cell culture. Biotechnol Lett. 24(21):1779-1783

Lee S Y, Kim D I (2006). Perfusion cultivation of transgenic *Nicotiana tabacum* suspensions in bioreactor for recombinant protein production. J Microbiol Biotechnol. 16(5):673-677

Liu C Z, Guo C, Wang Y-C, Ouyang F (2003). Comparison of various bioreactor on growth and artemisinin biosynthesis of Artemisia annua L. shoot cultures. Process Biochem. 39:45-49

Liu C Z, Moon K, Honda H, Kobayashi T (2000). Immobilization of rice (Oryza sativa L.) callus in polyurethane foam using a turbine blade reactor. Biochem Eng J. 4(3):169-175

Loc N H, Tuan C V, Binh D H N, Phuong T T B, Kim T G, Yang M S (2009). Accumulation of sesquiterpenes and polysaccharides in cells of zedoary (Curcuma zedoaria Roscoe) cultured in a 10 L bioreactor. Biotechnol Bioprocess Eng. 14(5):619-624

Lorenzo J C, Gonzalez B L, Escalona M, Teisson C, Espinosa P, Borroto C (1998). Suggarcane shoot formation in an improved temporary immersion system. Plant Cell, Tissue Organ Cult. 54:197-200

Luo J, Mei X G, Liu L, Hu D W (2002). Improved paclitaxel production by fed-batch suspension cultures of Taxus chinensis in bioreactors. Biotechnol Lett. 24(7):561-565

Luttman R, Florek P, Preil W (1994). Silicone-tubing aerated bioreactors for somatic embryo production. Plant Cell, Tissue Organ Cult. 39:157-170

Mandels M. 1972. The culture of plant cells. Adv Biochem Eng. 2:201-215

Mamun N H A, Egertsdotter U, Aidun C K (2015). Bioreactor technology for clonal propagation of plants and metabolite production. Front Biol. Advance online publication. doi: 10.1007/s11515-015-1355-1

Margaritis A, Wallace J B (1984). Novel bioreactor systems and their applications. Biotechnology. 2:447–453

Mavituna F, Buyukalaca S (1996). Somatic embryogenesis of pepper in bioreactors: a study of bioreactor type and oxygen-uptake rates. Appl Microbiol Biotechnol. 46:327-333

McAlister B, Finnie J, Watt M P, Blakeway F (2005). Use of the temporary immersion bioreactor system (RITA (R)) for production of commercial Eucalyptus clones in Mondi Forests (SA). Plant Cell, Tissue Organ Cult. 81(3):347-358

McDonald K A, Hong L M, Trombly D M, Xie Q, Jackman A P (2005). Production of human alpha-1-antitrypsin from transgenic rice cell culture in a membrane bioreactor. Biotechnol Prog. 21(3):728-734

Merkle S A, Dean J F D (2000). Forest tree biotechnology. Curr Opin in Biotechnol. 11:298-302

Meyer J E, Pepin M F, Smith M A L (2002). Anthocyanin production from Vaccinium pahalae: limitations of the physical micro environment. J Biotechnol. 93(1):45-57

Mizukami M, Takeda T, Satonaka H, Matsuoka H (2008). Improvement of propagation frequency with two-step direct somatic embryogenesis from carrot hypocotyls. Biochem Eng J. 38(1):55-60

Molle F, Fressinet G (1992). Les semences artificielles. Phytoma. 441:39–44.

Moon K H, Honda H, Kobayashi T (1999). Development of a bioreactor suitable for embryogenic rice callus culture. J Biosci Bioeng. 87(5):661-665

Moorhouse S D, Wilson G, Hennery M J, Selby C, tSaoir S M A (1996). Plant cell bioreactor with medium-perfusion for control of somatic embryogenesis in liquid cell suspensions. Plant Growth Regul. 20(1): 53-56

Morcillo F, Gagneur C, Adam H, Richaud F, Singh R. (2006). Somaclonal variation in micropropagated oil palm. Characterization of two novel genes with enhanced expression in epigenetically abnormal cell lines and in response to auxin. Tree Physiol. 26:585-594

Mordocco A M, Brumbley J A, Lakshmanan P (2009). Development of a temporary immersion system (RITAA (R)) for mass production of sugarcane (Saccharum spp. interspecific hybrids). In vitro Cell Dev Biol- Plant. 45(4):450-457

Mostafa S S, Gu X S (2003). Strategies for improved dCO_2 removal in large-scale fed-batch cultures. Biotechnol Prog. 19:45-51

Murch S J, Liu C Z, Romero R M, Saxena P K (2004). In vitro culture and temporary immersion bioreactor production of Crescentia cujete. Plant Cell, Tissue Organ Cult. 78(1):63-68

Namdev P K, Dunlop E H (1995). Shear sensitivity of plant cells in suspnesions- present and future. Appl Biochem Biotechnol. 54:109-131

Niemenak N, Saare-Surminski K, Rohsius C, Ndoumou D O (2008). Regeneration of somatic embryos in Theobroma cacao L. in temporary immersion bioreactor and analyses of free amino acids in different tissues. Plant Cell Rep. 27:667-676

Novak F J (1992). Musa (bananas and plantains). In: Hammerschlag, F. A.; Litz, R. E., eds. Biotechnology of perennial fruit crops. Wallingford, UK: CAB International. 449-488.

Ogbonna J C, Mashima H, Tanaka H (2001). Scale up of fuel ethanol production form sugar beet juice using loofa sponge immobilized bioreactor. Bioresour Technol. 76:1-8

Osuga K, Komamine A (1994). Synchronization of somatic embryogenesis from carrot cells at high frequency as a basis for the mass production of embryos. Plant Cell, Tissue Organ Cult. 39: 125-135

Owen H R, Wengerd D, Miller A R (1991). Culture medium pH influenced by basal medium, carbohydrate source, gelling agent, activated charcoal, and medium storage method. Plant Cell Rep. 10:583-586

Paek K Y, Chakrabarty D, Hahn E J (2005). Application of bioreactor systems for large scales production of horticultural and medicinal plants. In: Hvoslef-Eide A K, Preil W (eds). Liquid Culture systems for in vitro Plant Propagation. The Netherlands: Springer 95-116

Pal S, Das S, Dey S (2003). Peroxidase and arabinogalactan protein as by-products during somatic embryo cultivation in air-lift bioreactor. Process Biochem. 38(10):1471-1477

Pan Z-W, Wang H-Q, Zhong J-J (2000). Scale-up study on suspension cultures of *Taxus chinensis* cells for production of taxane diterpene. Enzyme Microb Technol. 27: 714-723

Pandey A (1992). Recent process developments in solid-state fermentation. Process Biochem. 27(2):109–117

Paques M, Boxus P (1987). *Vitrification: review of literature*. Acta Hortic. 212:155–166

Park S Y, Ahn J K, Lee W Y, Murthy H N, Paek K Y (2005). Mass production of Eleutherococcus koreanum plantlets via somatic embryogenesis from root cultures and accumulation of eleutherosides in regenerants. Plant Sci. 168(5):1221-1225

Pavlov A, Bley T (2006). Betalains biosynthesis by Beta vulgaris L. hairy root culture in a temporary immersion cultivation system. Process Biochem. 41(4):848-852

Pavlov A I, Georgiev M I, Ilieva M P (2005). Production of rosmarinic acid by Lavandula vera MM cell suspension in bioreactor: effect of dissolved oxygen concentration and agitation. World J Microbiol Biotechnol. 21(4):389-392

Peña-Ramirez Y J, Juárez-Gómez J, Gómez-Lopéz L, Jerónimo-Pérez J L, García-Sheseña I, González-Rodríguez J A, Robert M L (2010). Multiple adventitious shoot formation in Spanish Red Cedar (Cedrela odorata L.) cultured in vitro using juvenile and mature tissues: an improved micropropagation protocol for a highly valuable tropical tree species. In vitro Cell Dev Biol- Plant. 46(2):149-160

Pépin M F, Chavarie C, Archambault J (1991). Growth and immpobilization of *Tripterygium wilfordii* cultured cells. Biotechnol Bioeng. 38(11):1285-1291

Perata P, Alpi A (1991). Ethanol-induced injuries to carrot cells- the role of acetaldehyde. Plant Physiol. 95(3):748-752

Pérez A, Nápoles L, Carvajal C, Hernandez M, Lorenzo J C (2004). Effect of sucrose, inorganic salts, inositol, and thiamine on protease excretion during pineapple culture in temporary immersion bioreactors. In vitro Cell Dev Biol- Plant. 40(3):311-316

Piehl G-W, Berlin J, Mollenschott C, Lehmann J (1988). Growth and alkaloid production of a cell suspension culture of *Thalictrum rugosum* in shake flasks and membrane-stirrer reactors with bubble free aeration. Appl Microbiol Biotechnol. 29:456-461

Pinto G, Loureiro J, Lopes T, Santos C (2004). Analysis of the genetic stability of Eucalyptus globulus Labill. somatic embryos by flow cytometry. Theor Appl Genet. 109:580-587

Prakash G, Srivastava A K (2006). Modeling of azadirachtin production Azadirachta indica and its use for feed forward optimization studies. Biochem Eng J. 29(1-2):62-68

Prakash G, Srivastava A K (2008). Statistical elicitor optimization studies for the enhancement of azadirachtin production in bioreactor Azadirachta indica cell cultivation. Biochem Eng J. 40(2):218-226

Preil W, Florek P, Wix U, Beck A (1988). Towards mass propagation by use of bioreactors. Acta Hortic. 226:99-106

Preil W (1991). Application of bioreactors in plant micropropagation. In: Debergh P C, Zimmerman R H (Eds). Micropropagation, technology and application. Dordrecht, Netherlands: Kluwer Academic Publishers, 425-455

Qian Z G, Zhao Z J, Xu Y F, Qian X H, Zhong J J (2005). Highly efficient strategy for enhancing taxoid production by repeated elicitation with a newly synthesized jasmonate in fed-batch cultivation of Taxus chinensis cells. Biotechnol Bioeng. 90(4):516-521

Quiroz-Figueroa F R, Rojas-Herrera R, Galaz-Avalos R M, Loyola-Vargas V M (2006). Embryo production through somatic embryogenesis can be used to study cell differentiation in plants. Plant Cell Tissue Organ Cult. 86:285-301

Rathore K S, Sunilkumar G, Campbell L M. (2006). Cotton (Gossypium hirsutum L.). In: ed. Wang K, Methods in Molecular Biology: Agrobacterium Protocols. Humana Press Inc. Totowa, NJ. 343: 267- 279

Rosensweig R E (1979). Fluidization: Hydrodynamic stabilization with a magnetic field. Science. 204(6):57-60

Rout G R, Samantaray S, Das P (2000). In vitro manipulation and propagation of medicinal plants. Biotechnol Adv. 18(2):91-120

Rout G R, Mohapatra A, Jain S M (2006). Tissue culture of ornamental pot plant: A critical review on present scenario and future prospects. Biotechnol Adv. 24(6):531-560

Sajc L, Vunjak-Novakovic G, Grubisic D, Kovačević N, Vuković D, Bugarski B (1995). Production of anthraquinones by immobilized *Frangula alnus* Mill. plant cells in a four-phase air-lift bioreactor. Appl Microbiol Biotechnol. 43:416-423

Sánchez M J, Jimenez-Aparicio A, Lopez G G, Tapia G T, Rodriguez-Monroy M (2002). Broth rheology of Beta vulgaris cultures growing in an air lift bioreactor. Biochem Eng J. 12(1):37-41

Schlatmann J E, Moreno P R H, Vinke J L, Tenhoopen H J G, Verpoorte R, Heijnen J J (1994). Effect of oxygen and nutrient limitation on ajmalicine production and related enzyme activities in high density cultures of Catharanthus reseus. Biotechnol Bioeng. 44(4):461-468

Schlatmann J E, Nuutila A M, van Gulik W M, ten Hoopen H J G, Verpoorte R, Heijnen J J (1993). Scaleup of ajmalicine production by plant cell cultures of *Catharanthus roseus*. Biotechnol Bioeng. 41:253-262

Schmidt E D L, Guzzo F, Toonen M A J, de Vries S C (1997). A leucine-rich repeat containing receptor-like kinase marks somatic plant cells competent to form embryos. Development. 124(10): 2049-2062

Schubert S, Schubert E, Mengel K (1990). Effect of low pH of the root medium on proton release, growth, and nutrient uptake of field beans (*Vicia faba*). Plant Soil. 124:239-244

Scragg A H (1992). Large-scale plant cell culture: methods, applications and products. Curr Opin Biotechnol. 3:105–109

Scragg A H (1995). The problems associated with high biomass levels in plant cell suspensions. Plant Cell, Tissue Organ Cult. 43:163-170

Seki M, Ohzora C, Takeda M, Furusaki S (1997). Taxol (paclitaxel) production using free and immobilized cells of *Taxus cuspidate*. Biotechnol Bioeng. 53(2):214-219

Seydel P, Christian W, Heike D (2009). Scale-up of Oldenlandia affinis suspension cultures in photobioreactors for cyclotide production. Eng Life Sci. 9(3):219-226

Shi Z D, Yuan Y J, Wu J C, Shang G M (2003). Biological responses of suspension cultures of *Taxus chinensis* var. mairei to shear stresses in the short term. Appl Biochem Biotechnol. 110: 61-74

Shin K-S, Chakrabarty D, Ko J-Y, Han S-S, K-Y P (2003). Sucrose utilization and mineral nutrient uptake during hairy root growth of red beet (*Beta vulgaris* L.) in liquid culture. Plant Growth Regulation. 39:187-193

Shohael A M, Chakrabarty D, Yu K W, Hahn E, Paek K Y (2005). Application of bioreactor system for large-scale production of Eleutherococcus sessiliflorus somatic embryos in an air-lift bioreactor and production of eleutherosides. J Biotechnol. 120(2):228-236

Siegrist H, Gujer W (1985). Mass transfer mechanisms in a heterotrophic biofilm. Water Res. 19(11):1369-1378

Sim S J, Chang H N (1993). Increased shikonin production by hairy roots of Lithospermum erythrorhizon in 2 phase bubble column reactor. Biotechnol Lett. 15(2):145-150

Singh V (1999). Disposable bioreactor for cell culture using wave-induced agitation. Cytotechnology. 30:149-158

Slattery J C (1967). Flow of viscoelastic fluids through porous media. AIChE Journal. 13(6):1066-1071

Small J G, Potgiether G P, Botha F C (1989). Anoxic seed germination of *Erythrina caffra*: Ethanol fermentation and response to metabolic inhibitors. J Exp Bot. 40(3):375-381

Smart N J, Fowler M W (1984). Mass cultivation of *Catharanthus roseus* cells using a nonmechanically agitated bioreactor. Appl Biochem Biotechnol. 9:209-216

Snyman S J, Meyer G M, Richards J R, Ramgareeb S, Banasiak M, Huckett B (2007). Use of the temporary immersion RITA (R) bioreactor system for micropropagation of sugarcane. S Afr J Bot. 73(2):336-337

Srinivasan V, Pestchanker L, Moser S, Hirasuna T J, Taticek R A, Shuler M L (1995). Taxol production in bioreactors- kinetics of biomass accumulation, nutrient-uptake, and taxol production by cell suspensions of Taxus baccata. Biotechnol Bioeng. 47(6):666-676

Stewart P S (2003). Diffusion in biofilms. J Bacteriol. 185(5):1485-1491 .

Stitt M, Lilley R M, Gerhardt R, Heldt H W (1989). Metabolite levels in specific cells and subcellular compartments of plant leaves. Methods in Enzymology. 174:518-552

Stoner M R, Humphrey C A, Coutts D J, Shih N J R, McDonald K A, Jackman A P (1997). Kinetics of growth and ribosome-inactivating protein production from *Trichosanthes kirilowii* plant cell cultures in a 5-L bioreactor. Biotechnol Prog. 13(6):799-804

Suehara K-I, Nagamori E, Honda H, Uozumi N, Kobayashi T (1998). Development of rotating-mesh basket type bioreactor for carrot embryo production in immobilized callus system. J. Chem Eng Jpn. 31(4): 613-617

Su W W, Arias R (2003). Continuous plant cell perfusion culture: bioreactor characterization and secreted enzyme production. J Biosci Bioeng. 95(1):13-20

Su W W, He B J, Liang H, Sun S (1996). A perfusion air-lift bioreactor for high density plant cell cultivation and secreted protein production. J Biotechnol. 50(2-3):225-233

Su W W, Lei F, Kao N P (1995). High density cultivation of Anchusa officinalis in a stirred-tank bioreactor with in situ filtration. Appl Microbiol Biotechnol. 44(3-4):293-299

Sun H (2010). The effect of hydrodynamic stress on plant embryo development. Ph.D. thesis, Georgia Institute of Technology, Atlanta, GA.

Sun X, Linden J C (1999). Shear stress effects on plant cell suspension cultures in a rotating wall vessel bioreactor. J Ind Microbiol Biotechnol. 22(1):44-47

Takayama S (1991). Mass propagation of plants through shake and bioreactor culture techniques. In: Bajaj Y P S (ed.), Biotechnology in agriculture and forestry: Hightech and micropropagation. Springer-Verlag, Berlin. 17:1–46.

Takayama S, Akita M (1994). The types of bioreactors used for shoots and embryos. Plant Cell Tissue Organ Cult. 39:147–156

Tallarida R J, Murray R B (1987). Duncan Multiple Range Test. Manual of Pharmacologic Calculations with Computer Programs. 125-127

Tanaka H, Nishijima F, Suwa M, Iwamoto T (1983). Rotating drum fermentor for plant cell suspension cultures. Biotechnol Bioeng. 25:2359-2370

Taticek R A, Moo-Young M, Legge R L (1990). Effect of bioreactor configuration on substrate uptake by cell suspension cultures of the plant *Eschscholtzia calfornica*. Appl Microbiol Biotechnol. 33:280-286

Teng W-L, Liu Y-J, Tsai Y-C, Soong T-S (1994). Somatic embryogenesis of carrot in bioreactor culture systems. HortScience. 29(11):1349–1352

Terashima M, Ejirim Y, Hashikawa N, Yoshida H (2000). Effects of sugar concentration on recombinant human alpha(1)-antitrypsin production by genetically engineered rice cell. Biochem Eng J. 6(3):201-205

Terrier B, Courtois D, Henault N, Cuvier A, Bastin M, Aknin A, Dubreuil J, Petiard V (2007). Two new disposable bioreactors for plant cell culture: the wave and undertow bioreactor and the slug bubble bioreactor. Biotechnol Bioeng. 96(5):914-923

Thanh N T, Murthy H N, Yu K W, Jeong C S, Hahn E J, Paek K Y (2006a). Effect of oxygen supply on cell growth and saponin production in bioreactor cultures of Panax ginseng. J Plant Physiol. 163(12):1337-1341

Thanh N T, Murthy H N, Pandey D M, Yu K W, Hahn E J, Paek K Y (2006b). Effect of carbon dioxide on cell gwowth and saponin production in suspension cultures of Panax ginseng. Biol Plant. 50(4):752-754

Tikhomiroff C, Allais S, Klvana M, Hisiger S, Jolicoeur M (2002). Continuous selective extraction of secondary metabolites from Catharanthus roseus hairy roots with silicon oil in a two-liquid-phase bioreactor. Biotechnol Prog. 18: 1003-1009

Tisserat B, Vandercook C E (1985). Development of an automated plant culture system. Plant Cell, Tissue Organ Cult. 5:107-117

Thomas D S, Murashige T (1979). Volatile emissions of plant tissue cultures. I. Identification of the major components. In Vitro. 15(9):654-658

Thorpe T A, Harry I S, Yeung E C. (2006). Clonal propagation of softwoods. In: Loyala-Vargs V M, Vázquez-Flota F (eds), Methods in Molecular Biology: Plant Cell Culture Protocols. Humana Press Inc., Totowa, NJ. 318:187-197

Tikhomiroff C, Allais S, Klvana M, Hisiger S, Jolicoeur M (2002). Continuous selective extraction of secondary metabolites from Catharanthus roseus hairy roots with silicon oil in a two-liquid-phase bioreactor. Biotechnol Prog. 18: 1003-1009

Tisserat B, Murashige T (1977). Effects of ethephon, ethylene, and 2,4-Dichlorophenoxyacetic acid on asexual embryogenesis in vitro. Plant Physiol. 60(3):437-439

Tisserat B, Vandercook CE (1985). Development of an automated plant culture system. Plant Cell, Tissue Organ Cult. 5:107-117

Tokashiki M, Arai T, Hamamoto K, Ishimaru K (1990). High density culture of hybridoma cells using a perfusion culture vessel with an external centrifuge. Cytotechnology. 3(3):239-244

Tonon G, Berardi G, Rossi C, Bagnaresi U (2001). Synchronized somatic embryo development in embryogenic suspensions of *Fraxinus angustifolia*. In Vitro Cell. Dev. Biol.- Plant. 37: 462-465

Townsley P M, Webster F, Kutney J P, Salisbury P, Hewitt G, Kawamura N, Choi L, Kurihara T (1983). The recycling air lift transfer fermenter for plant cell. Biotechnol Lett. 5(1):13-18

Treat W J, Engler C R, Soltes E J (1989). Culture of photomixotrophic soybean and pine in a modified fermenter using a novel impeller. Biotechnol Bioeng. 34(9):1191-1202

Trejo-Tapia G, Cerda-Garcia-Rojas C M, Rodriguez-Monroy M, Ramos-Valdivia A C (2005). Monoterpenoid oxindole alkaloid production by Uncaria tomentosa (Willd) D. C. cell suspension cultures in a stirred tank bioreactor. Biotechnol Prog. 21(3):786-792

Trejo-Tapia G, Jimenez-Aparicio A, Villarreal L, Rodriguez-Monroy M (2001). Broth rheology and morphological analysis of Solanum chrysotrichum cultivated in a stirred tank. Biotechnol Lett. 23(23):1943-1946

Trexler M M, McDonald K A, Jackman A P (2002). Bioreactor production of human α1-antitrypsin using metabolically regulated plant cell cultures. Biotechnol Prog. 18:501-508

Valluri J V, Treat W J, Soltes E J (1991). Bioreactor culture of heterotrophic sandalwood (*Santalum album* L.) cell-suspensions utilizing a cell-lift impeller. Plant Cell Rep. 10(6-7):366-370

van Gulik W M, ten Hoopen H J, Heijen J J (1993). A structured model describing carbon and phosphate limited growth of Catharanthus roseus plant cell suspensios in batch and chemostat culture. Biotechnol Bioeng. 41:771-780

Vinocur B, Carmi T, Altman A, Ziv M (2000). Enhanced bud regeneration in aspen (Populus tremula L.) roots cultured in liquid media. Plant Cell Rep. 19(12):1146-1154

von Arnold S, Clapham D (2008). Spruce embryogenesis. In: Suárez M F, Bozhkov P V (eds), Plant embryogenesis: methods in molecular biology. Human Press, Totowa, NJ, 427: 31-47

von Arnold S, Bozhkov P, Clapham D, Dyachok J, Filonova L, Högberg K A, Ingouff M, Wiweger M (2005). Propagation of Norway spruce via somatic embryogenesis. Plant Cell, Tissue Organ Cult. 81:323-329

von Arnold S, Eriksson T (1981). *In vitro* studies of adventitious shoot formation in *Pinus contorta*. Can J Bot. 59:870-874.

Wang G R, Qi N M, Wang Z M (2010). Application of stir-tank bioreactor for perfusion culture and continuous harvest of *Glycyrrhiza inflate* suspension cells. Afr J Biotechnol. 9(3):347-351

Wang S-J, Zhong J-J (1996). A novel centrifugal impeller bioreactor I. Fluid circulation, mixing, and liquid velocity profiles. Biotechnol Bioeng. 51:511-519

Wang W, Zhang Z Y, Zhong J J (2005). Enhancement of ginsenoside biosynthesis in high-density cultivation of Panax notoginseng cells by various strategies of methyl jasmonate elicitation. Appl Microbiol Biotechnol. 67(6):752-758

Wang Z Y, Zhong J J (2002). Combination of conditioned medium and elicitation enhances taxoid production in bioreactor cultures of Taxus chinensis cells. Biochem Eng J. 12(2):93-97

Wann S R, Veazey R L, Kaphammer J (1997). Activated charcoal does not catalyze sucrose hydrolysis in tissue culture media during autoclaving. Plant Cell Tissue Organ Cult. 50: 221-224.

Whitaker S (1967). Diffusion and dispersion in porous media. AIChE Journal. 13 (3): 420-427

Williams R D, Chauret N, Bédard C, Archambault J (1992). Effect of polymeric adsorbents on the production of sanguinarine by *Papaver somniferum* cell-cultures. Biotechnol Bioeng. 40:971-977

Wongsamuth R, Doran P M (1997). The filtration properties of *Atropa belladonna* plant cell suspensions; effects of hydrodynamic shear and elevated carbon dioxide levels on culture and filtration parameters. J Chem Technol Biotechnol. 69:15-26

Woragidbumrung K O, Sae-Tang P, Yao H, Han J, Chauvatcharin S, Zhong J J (2001). Impact of conditioned medium on cell cultures of Panax notoginseng in an airlift bioreactor. Process Biochem. 37(2):209-213

Xu J F, Shapak E, Gu T Y, Moo-Young M. Kieliszewski M (2005). Production of recombinant plant gum with tobacco cell culture in bioreactor and gum characterization. Biotechnol Bioeng. 90(5):578-588

Yang R Y K, Bayraktar O, Pu H T (2003). Plant-cell bioreactors with simultaneous electropermeabilization and electrophoresis. J Biotechnol. 100(1):13-22

Yuan X F, Zhao B, Wang Y C (2004). Cell culture of Saussurea medusa in a periodically submerge air-lift bioreactor. Biochem Eng J. 21(3):235-239

Zhang Z Y, Zhong J J (2004). Scale-up of centrifugal impeller bioreactor for hyperproduction of ginseng saponin and polysaccharide by high-density cultivation of Panax notoginseng cells. Biotechnol Prog. 20(4):1076-1081

Zhong C, Yuan Y J (2009). Responses of *Taxus cuspidata* to hydrodynamics in bubble column bioreactors with different sparging nozzle sizes. Biochem Eng J. 45:100-106

Zhong J J, Chen F, Hu W W (1999). High density cultivation of Panax notoginseng cells in stirred bioreactors for the production of ginseng biomass and ginseng saponin. Process Biochem. 35(5):491-496

Zhong J J, Fujiyama K, Seki T, Yoshida T (1994). A quantitative analysis of shear effects on cell suspension and cell culture of *Perilla frutescens* in bioreactors. Biotechnol Bioeng. 44:649-654

Zhong J J, Pan Z W, Wang Z Y, Wu J Y, Chen F, Takagi M, Yoshida T (2002). Effect of mixing time on taxoid production using suspension cultures of Taxus chinensis in a centrifugal impeller bioreactor. J Biosci Bioeng. 94(3):244-250

Zhong J J, Seki T, Kinoshita S, Yoshida T (1991). Effect of light irradiation on anthocyanin production by suspended culture of Perilla frutescens. Biotechnol Bioeng. 38(6):653-658

Zhu L H, Li X Y, Welander M (2005). Optimisation of growing conditions for the apple rootstock M26 grown in RITA containers using temporary immersion principle. Plant Cell, Tissue Organ Cult. 81(3):313-318

Ziv M (1991). Vitrification: Morphological and physiological disorders of in vitro plants. In: Debergh P G, Zimmerman R H, (Eds). Micorpropagation: Technology and Application. Dordrecht, The Netherlands: Kluwer Academic Publishers, 45-69

Ziv M (2005). Simple bioreactors for mass propagation of plants. Plant Cell, Tissue Organ Cult. 81(3):277-285

Ziv M, Ronen G, Raviv M (1998). Proliferation of meristematic clusters in disposable presterilized plastic bioreactors for large-scale micropropagation of plants. In vitro Cell Dev Biol- Plant. 34:152-158

Zobayed S M A, Murch S J, Rupasinghe H P V, Saxena P K (2003). Elevated carbon supply altered hypericin and hyperforin contents of St. John's wort (Hypericum perforatum) grown in bioreactors. Plant Cell, Tissue Organ Cult. 75(2):143-149

Zobayed S M A, Saxena P K (2003). In vitro-grown roots: a superior explant for prolific shoot regeneration of St. John's wort (Hypericum perforatum L. cv 'New Stem') in a temporary immersion bioreactor. Plant Sci. 165(3):463-470